10306 Eaton Place, Suite 340
Fairfax, VA 22030
Tel 703-385-6000

MEMORANDUM

To:	U.S. EPA, Washington Ecology, Washington Department of Health
From:	Sen Bai and Aileen Molloy, Tetra Tech
Date:	June 16, 2023
Subject:	Lower Yakima Valley Groundwater Management Area – Generating Maps for Groundwater Level and Nitrate Concentrations

1.0 INTRODUCTION

To aid in the targeting of nonpoint source pollution reduction measures, this project supports the development of a groundwater contour mapping modeling tool in the Lower Yakima Valley, utilizing existing ambient groundwater data collected from July 2021 through June 2022 by the Washington State Department of Ecology (Ecology). Groundwater contour mapping increases the visible connection between land use practices on the surface and groundwater recharge, including nitrate contamination, and allows growers to observe the potential radius of their fields' influence and for stakeholders to identify influences that are up-gradient of the wells. Developing a model for mapping groundwater elevations and nitrate concentrations provides partners with a valuable tool for tracking changes in nitrate concentrations in relation to management measures used. This methodology document summarizes the available data sources and the methodology for developing the groundwater contour mapping tool.

2.0 DATA

To develop the maps of groundwater table and the nitrate concentrations in the Lower Yakima Valley, the following data were used:

1. Locations of monitoring wells and domestic water supply and irrigation wells (supply wells).
2. Observed water table elevation data from monitoring wells.

Groundwater Level and Nitrate Map Generations

3. Digital elevation model (DEM) data to estimate the water levels in the Yakima River and observed water level data at USGS flow gages.
4. Observed nitrate concentrations from monitoring wells and supply wells.

Well data were downloaded from Ecology's Environmental Information Management (EIM) database (https://apps.ecology.wa.gov/eim). The locations (latitude and longitude) of Lower Yakima Valley monitoring wells were extracted from the data file and loaded into ArcMap. The locations of these wells are shown in Figure 2-1.

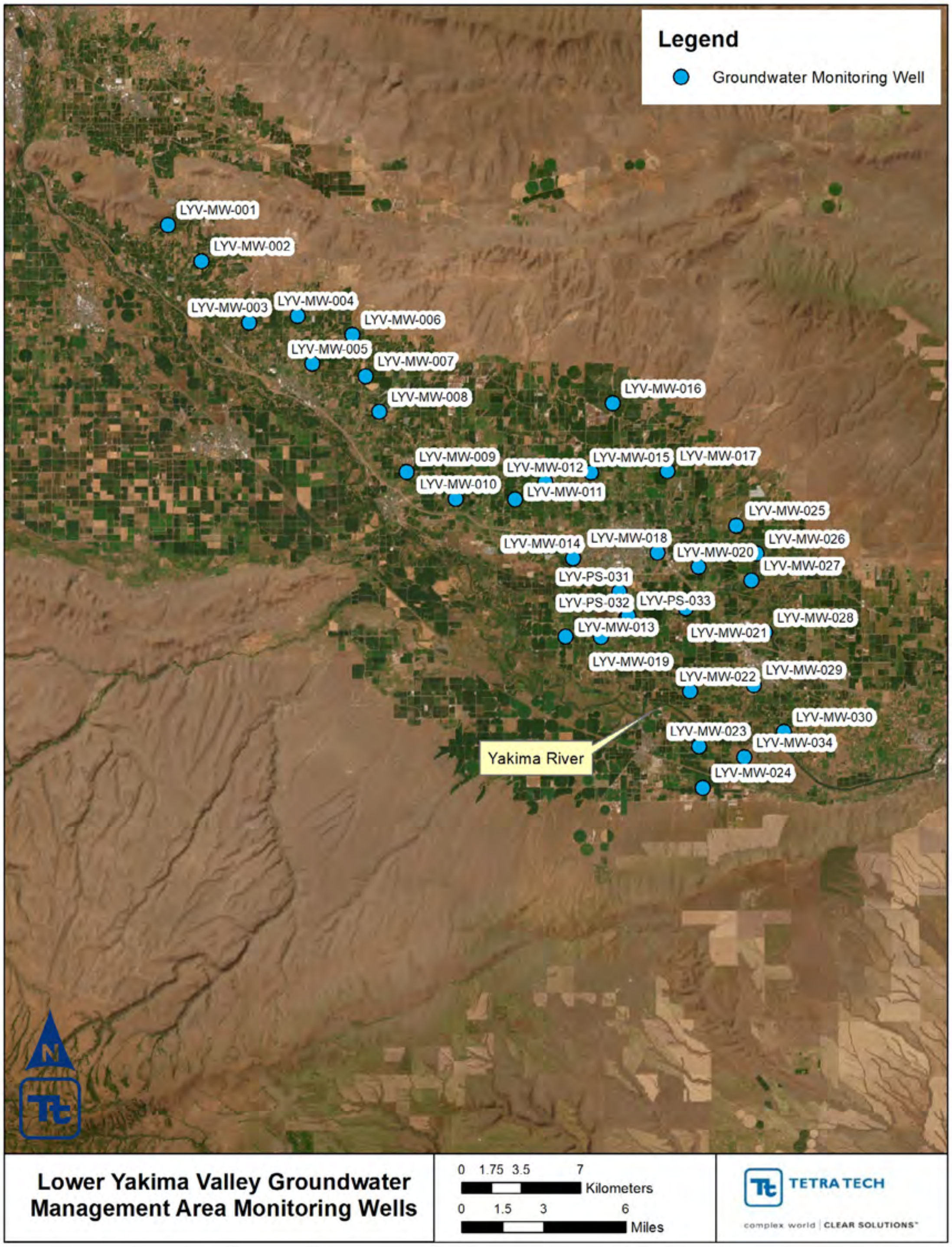

Figure 2-1. Monitoring Well Locations

Groundwater Level and Nitrate Map Generations

Data from a total of 34 monitoring wells were available. Thirty of these wells are randomly located, spatially distributed throughout the Lower Yakima Valley Groundwater Management Area (LYV GWMA). The remaining four wells are not randomly located, and belong to the Port of Sunnyside and Grandview, Washington. Out of the 34 wells, 3 wells are on the south side of the Yakima River. Data including water depth from top of casing and nitrate concentrations were both available. In addition to the monitoring wells, there are 139 domestic water supply wells and one irrigation well (total 140 supply wells) that have nitrate sampling data. The nitrate samples were taken at the surface of the water table for the monitoring wells and at deeper locations for the supply wells. All wells are within the unconfined aquifer. These wells represent Ecology's Ambient Groundwater Monitoring Network. The design of this network assumes that the wells will produce groundwater nitrate concentrations which are representative of the uppermost surficial aquifer conditions. The design also assumes that the distribution and number of wells will provide adequate coverage across the GWMA. Water quality data were analyzed and reported as nitrate-nitrite. It is assumed that the majority is nitrate, and the remainder of this report will refer to the water quality mapping as nitrate concentration mapping.

Data were collected on different days and months for the wells, and data are complete within a three-month period (i.e., for each three-month interval, there is at least one groundwater level and nitrate-nitrite sample from each well). Therefore, the data were grouped every three months (January-March, April-June, July-September, and October-December). The water levels were calculated from the measured depth data.

Groundwater flows following the gradient of hydraulic head, and the water level in the Yakima River represents part of the hydraulic head. The water levels in the Yakima River were coarsely estimated from the DEM data. The U.S. Geological Survey (USGS) DEM data with 1/3 arc second (30ft) resolution is available from the USGS website. The Washington Department of Natural Resources (WDNR) 12ft LiDAR data were also downloaded. The USGS DEM data is called "DEM", and the WDNR LiDAR data is called "LiDAR" here. The elevations within the Yakima River were extracted from the USGS DEM data. Water levels from USGS flow gages including the gages at Yakima at Union Gap (12503000), Yakima near Emerald (12507573), and Yakima at Mabton (12508990) were also downloaded to verify the water level estimated from the DEM data.

Figure 2-2 shows the locations in the Yakima River where the water levels were extracted from the DEM and LiDAR data as well as the extracted water levels along the Lower Yakima River. Figure 2-3 shows the longitudinal water level profiles extracted from the DEM and the LiDAR data. Figure 2-4 shows the comparison of the water levels extracted from the DEM and LiDAR data, and the maximum, mean, and minimum water levels from the USGS gages. The water levels from the WNDR 12ft LiDAR data show better agreement with the ranges of water levels from the USGS gages than those from the USGS 1/3arc DEM data. Therefore, the water levels in Lower Yakima River based on the WNDR 12ft LiDAR data were used for the water level map generations.

Groundwater Level and Nitrate Map Generations

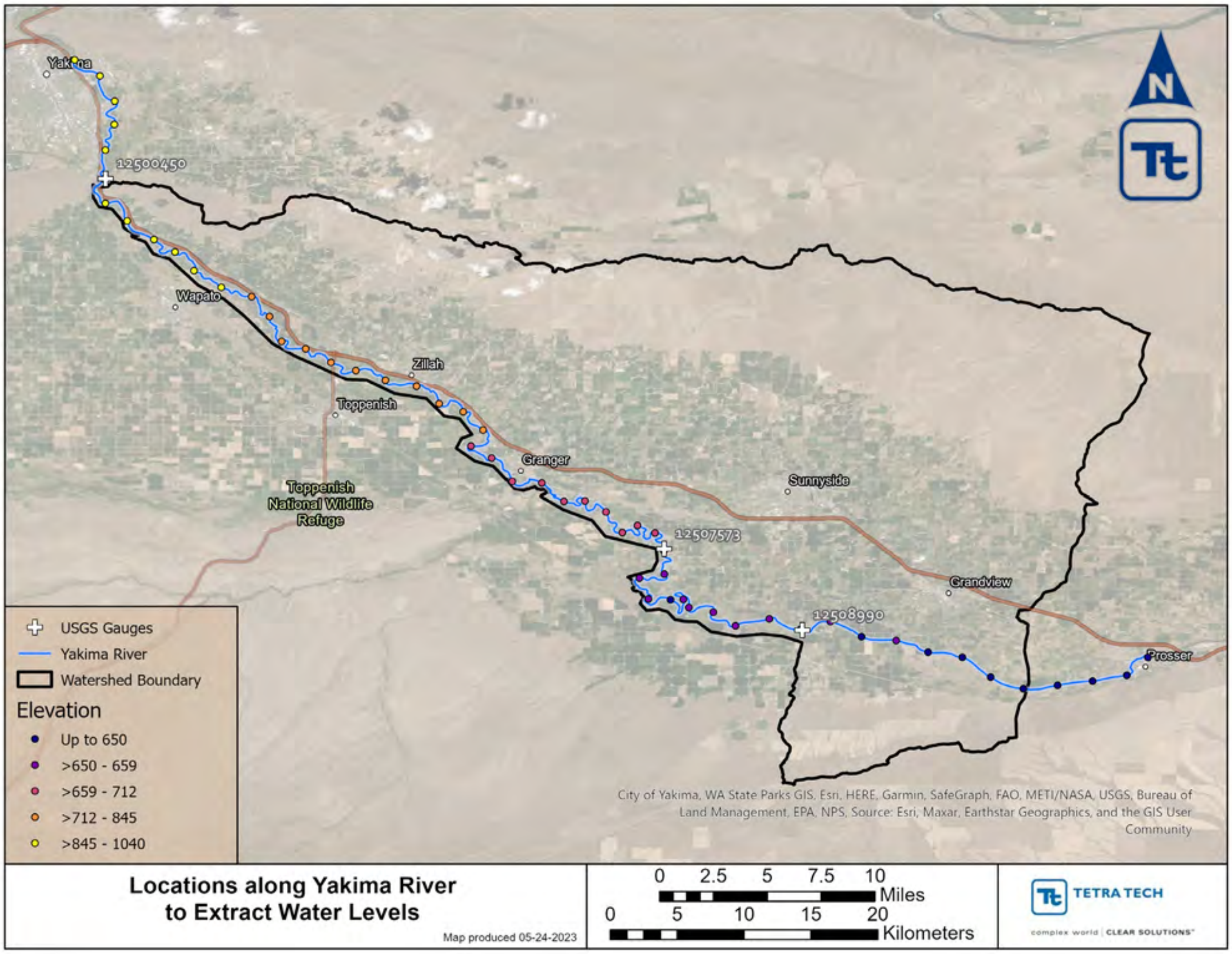

Figure 2-2. Water Level Locations and Water Levels Extracted from DEM and LiDAR data and USGS Gages along the Lower Yakima River

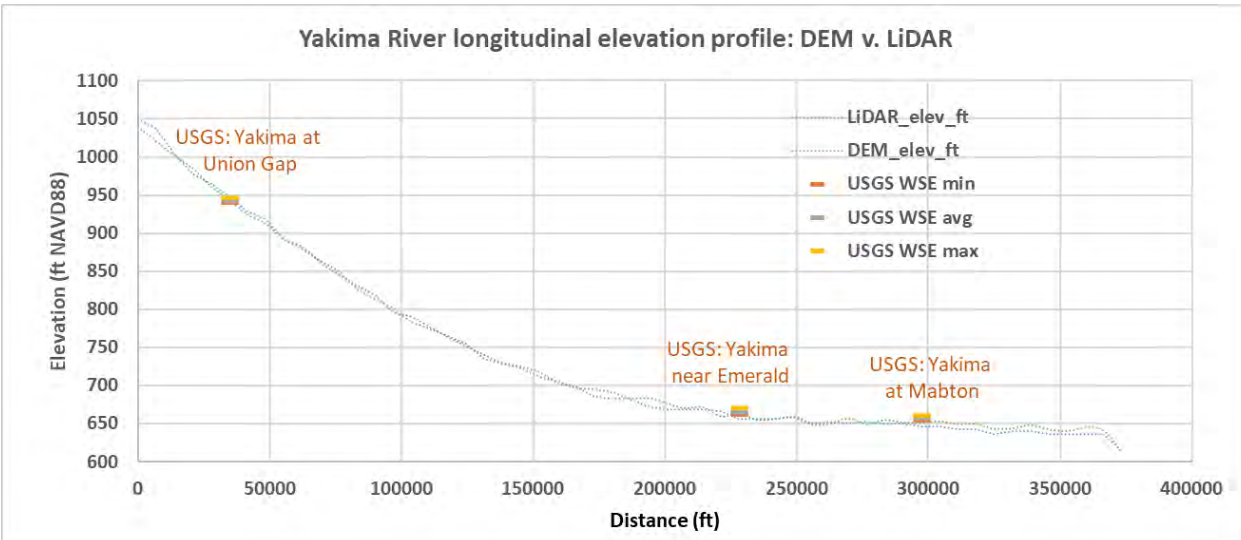

Figure 2-3. Extracted Water Level from DEM and LiDAR Data

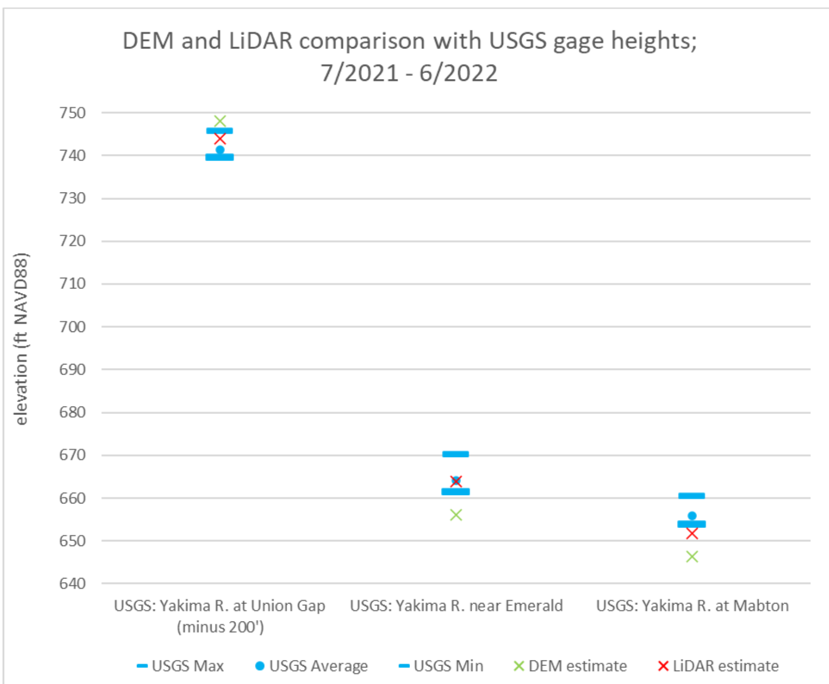

Figure 2-4. Comparisons of Water Level Extracted from DEM and LiDAR Data and USGS Gages

Groundwater Level and Nitrate Map Generations

While water levels in the river change depending on the flow rates, the DEM and LiDAR data can only capture one moment when the data were taken. Only one river elevation data set was available, which provides water levels for a snapshot in time, rather than representing actual river fluctuation throughout the year. However, the water levels vary less than 10 feet as shown by the USGS data in Figure 2-4, and such variation is not significant compared to the overall water level change in the river and in the wells. The water levels from the LiDAR data were combined with the water levels from the monitoring wells for map generation.

The nitrate data are taken from both the monitoring wells and supply wells. Since the sampling depth is different for the monitoring wells and the supply wells, the measured nitrate concentrations represent different vertical locations in the aquifer. The maps for nitrate concentrations are generated three different ways, using monitoring wells only, supply wells only, and combined monitoring and supply wells.

In summary, four datasets representing four seasons are used for the water level maps, and 12 datasets are used for the nitrate maps, representing the combinations of well types and season.

3.0 METHOD

Many methods can be used to generate maps using observed data. For example, ArcMap provides Inverse distance weighting (IDW), Kriging, Spline, and Natural Neighbor methods to generate maps. Among these methods, Kriging is the only method that analyzes the spatial correlation and therefore, Kriging was chosen as the primary method for generating the maps for the water level and nitrate concentrations in the Lower Yakima Valley. The quality of maps depends on the number of data points and the trend that the data represents. Because Kriging does not guarantee a good quality map for all datasets, the IDW method was used in cases where Kriging did not produce logical results.

The Kriging Model

Kriging is a geostatistical approach to estimate values at unsampled locations considering spatial correlations from the values at nearby sampled locations. Instead of using a simple IDW scheme, the Kriging approach develops a variogram to estimate the weights from the nearby sample locations. The variogram describes the changes of variance as a function of distance. Equation 1 describes how the variance (semivariogram) over distance is calculated.

$$\text{Semivariogram}(\text{distance}_h) = 0.5 * \text{average}((\text{value}_i - \text{value}_j)^2) \quad \text{(Equation 1)}$$

Equation 1 involves calculating the difference squared between the values of the paired locations. Figure 3-1 shows an example of the pairing of one point (the central red point) with all other measured locations. This process continues for each measured point.

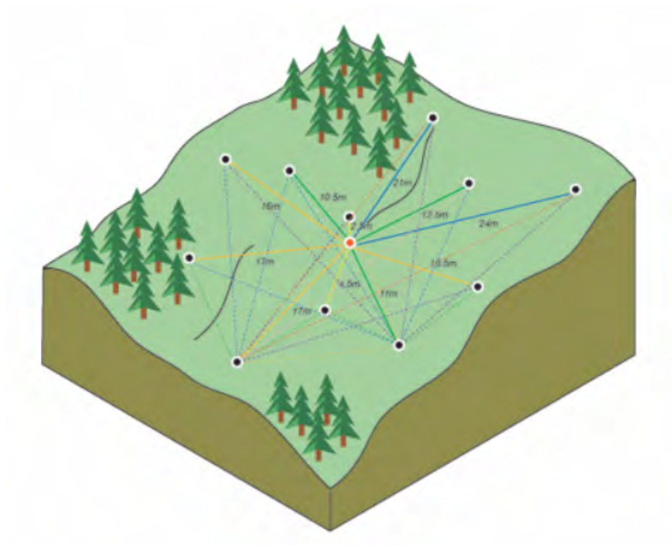

Figure 3-1. An Example of Paired Locations (From https://desktop.arcgis.com/en/arcmap/10.3/tools/3d-analyst-toolbox/how-kriging-works.htm)

Averages of semivariance for all pairs of points with similar distances are calculated, and plotted with the averaged semivariogram values on the y-axis and the distance on the x-axis (Figure 3-2).

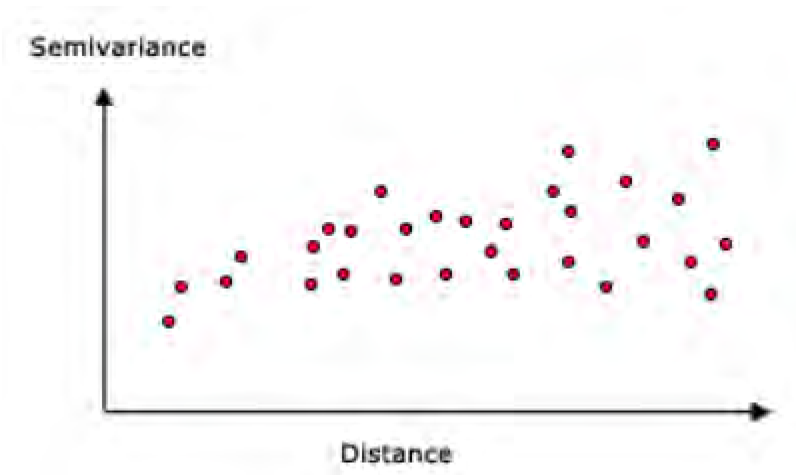

Figure 3-2. An Example of Calculated Semivariance (From https://desktop.arcgis.com/en/arcmap/10.3/tools/3d-analyst-toolbox/how-kriging-works.htm)

Different semivariograms models are available to fit the variance-distance data pairs calculated from observed data. Figure 3-3 shows an example of a variogram model curve. All the variogram models have three major parameters, which are sill, range, and nugget as shown in Figure 3-3. Range is the distance where the model first flattens out; Nugget is the intercept of the semivariogram model at the y-axis; Sill is the value that the semivariogram model attains at the range (the value on the y-axis); and the partial sill is the sill minus the nugget.

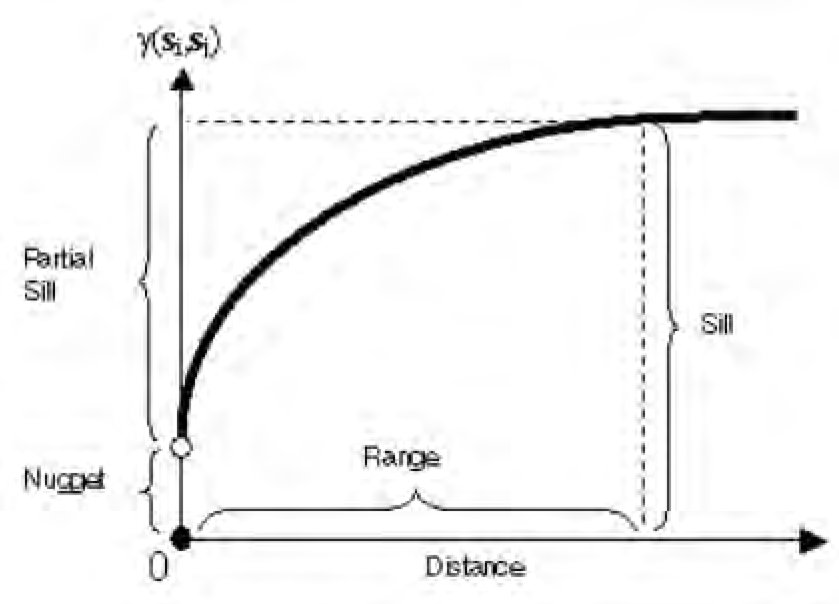

Figure 3-3. An Example of a Semivariogram Model (From https://desktop.arcgis.com/en/arcmap/latest/extensions/geostatistical-analyst/semivariogram-and-covariance-functions.htm)

Depending on the spatial trends of mean values such as the mean nitrate concentrations for a set of wells, and variances, different Kriging methods can be chosen. In theory, when both the mean values and variances-distance relationship do not vary in space, which is called stationary condition, the ordinary Kriging method can be applied. When the mean values show a strong spatial trend, but the variances-distance relationship does not change, the universal Kriging method can be applied, or the spatial trend can be removed first, and the ordinary Kriging method can then be applied to the updated data set after the trend is removed. The details of the stationary condition are available at https://desktop.arcgis.com/en/arcmap/latest/extensions/geostatistical-analyst/random-processes-with-dependence.htm#:~:text=In%20a%20spatial%20setting%2C%20the,and%20is%20independent%20of%20location. In this project, the available Kriging methods and models were tested using the observed data, and the models with the lowest model errors overall were selected for generating the maps. The Kriging methods and models are discussed below.

Kriging Method in ArcMap

ESRI's ArcMap provides two options to apply the Kriging method. One is through the Spatial Analyst where ArcMap either uses default values or user inputs for the parameters of selected semivariogram models. The other is the detailed analysis using the Geostatistical Analyst tool. In this project, the detailed analysis using the Geostatistical Analyst tool was used. The tool uses a point shapefile with both the location information of the wells and the data to be interpolated. A point shapefile was created to store all the water level and nitrate data. Variances between wells was then calculated and plotted for visual inspection. ArcMap provides multiple semivariogram models to fit the calculated variance – distance plot. For example, for the Ordinary Kriging method, ArcMap provides Spherical Model, Circular Model, Exponential Model, Gaussian Model, and Linear Model.

Groundwater Level and Nitrate Map Generations

In addition to the multiple Kriging methods and multiple semivariogram models for each Kriging method, the Geostatistical Analyst provides pre-processing of data to cluster certain data together with the Kernel Function for semivariogram model fitting, and options with or without anisotropy. It also provides options to apply different smoothing factors, and number of neighbors to use for map generation.

All the Kriging methods and models were tested first, and then errors were evaluated together with the maps generated for each model. The model with a combination of low error statistics and smooth gradient of value changes (i.e., minimized abrupt changes in groundwater levels or nitrate concentrations) was selected. Acceptable error levels were not pre-established because the data are inherently variable, and there is no option control or reduce errors in a specific model when all data are incorporated into the analysis.

4.0 MAP GENERATION FOR WATER LEVEL

For the water levels in Lower Yakima Valley, the data were loaded into ArcMap and the Geostatistical Analyst tool was activated for the testing of the different combinations of Kriging method, semivariogram models and options for map generation. The testing was conducted using the July-September 2021 dataset first to evaluate if applying the Kernel function reduces model errors. Six different kernel functions and no kernel were tested for both the Ordinary Kriging method and the Universal Kriging Method. For both methods, the Gaussian semivariogram model was selected after several initial testing runs with the different semivariogam models. For the kernel function testing, the no anisotropy option was used. Table 4-1 shows the model errors with the different kernel functions. The model errors are lowest when the kernel function is not activated (no kernel). When the kernel functions were used, the Universal Kriging method achieved slightly lower model errors than the Ordinary Kriging method for exponential, polynomial with 5, Gaussian, Epanechnikov, and quartic kernel functions, and almost same model errors for constant kernel function. When kernel function is not used, the model errors for the Ordinary and Universal Kriging methods are the same. The Ordinary Kriging method was selected for generating the maps of water levels. Error values represent the difference between the observed values and the model predicted values, so there is no pre-defined target error range that is considered optimal. Lower errors represent predicted values closer to the observed values.

Table 4-1. Testing Model Errors with Kernel Functions

			Kernel function (mean error)					
Method	Model	no kernel	exponential	polynomial5	Gaussian	Epanechnikov	quartic	constant
Ordinary	Gaussian- no anisotropy	-1.9631	-10.5048	-7.9521	-9.7088	-6.7127	-9.5418	-5.0606
Universal	Gaussian- no anisotropy	-1.9631	-9.1094	-6.7385	-8.4895	-5.8261	-8.4749	-5.0701

After the selection of the Ordinary Kriging method, all the semivariogram models available for the Ordinary Kriging method were tested for model errors. Table 4-2 lists the model errors for the semivariogram models including circular, spherical, exponential, Gaussian, and stable. This test also considered with and without anisotropy. The Gaussian semivariogram model achieved the lowest model error among the five semivariogram models. When anisotropy is considered, the model errors for Gaussian and stable models are the lowest, and the model errors are higher when anisotropy is not considered. Because the Gaussian semivariogram achieved the lowest model error for both the cases with and without anisotropy, the Gaussian semivariogram was selected for the generation of the water level maps.

Table 4-2. Testing Model Errors with Different Semivariogram Models

Method	Model	Mean error			
		JulSep21	OctDec21	JanMar22	AprJun22
Ordinary	circular	-2.3460	-2.3288	-2.3392	-2.2991
	spherical	-2.4825	-2.4700	-2.4897	-2.4634
	exponential	-2.8395	-2.8312	-2.8924	-2.8889
	Gaussian	-1.9631	-1.9291	-1.9146	-1.9083
	stable	-2.5887	-2.5724	-2.5651	-2.5417
Ordinary w/anisotropy	circular	-2.1136	-2.1084	-2.1258	-2.1197
	spherical	-2.2889	-2.2829	-2.3200	-2.3297
	exponential	-2.7924	-2.7909	-2.8389	-2.8358
	Gaussian	0.2886	0.2886	0.2139	0.2420
	stable	0.2886	0.2886	0.2139	0.2420

The Ordinary Kriging method with Gaussian model considering the anisotropy was selected to generate the maps. The parameters of the Gaussian model are listed in Table 4-3.

Table 4-3. Parameter Values for the Gaussian Semivariogram Models

Parameters	Data Set			
	July-September 2021	October-December 2021	January-March 2022	April-June 2022
Nugget (ft^2)	16.53	16.59	15.73	15.31
Range (Degree)	0.052	0.052	0.050	0.049
Partial Sill (ft^2)	16528.72	16590.67	15725.71	15312.91

The Geostatistical tool was used to generate raster files based on the Gaussian model results. The generated raster files were clipped using a boundary GIS file, which follows the Yakima River and the watershed boundary. The resulting groundwater level maps for each season are shown from Figure 4-1 to Figure 4-4.

The water level maps do not consider the three monitoring wells south of the Yakima River. Due to the paucity of data on the southern side of the river, excessive statistical noise was generating unrealistic results, and the decision was made, in consultation with Washington Departments of Ecology and Health to exclude these wells from the analysis. Therefore, the maps only show the water levels north of the Yakima River. The maps show that the water levels did not change dramatically over the four periods over approximately a year and show a strong gradient in the direction of the river, as would be expected. It should be noted that the reliability of the water levels estimated on the map depends on the distance from the monitoring wells. For the areas beyond the area that is covered by the monitoring wells, the reliability of the water levels is reduced and should be interpreted carefully, i.e., results for areas along the northern and northeastern portions of the watershed are least reliable.

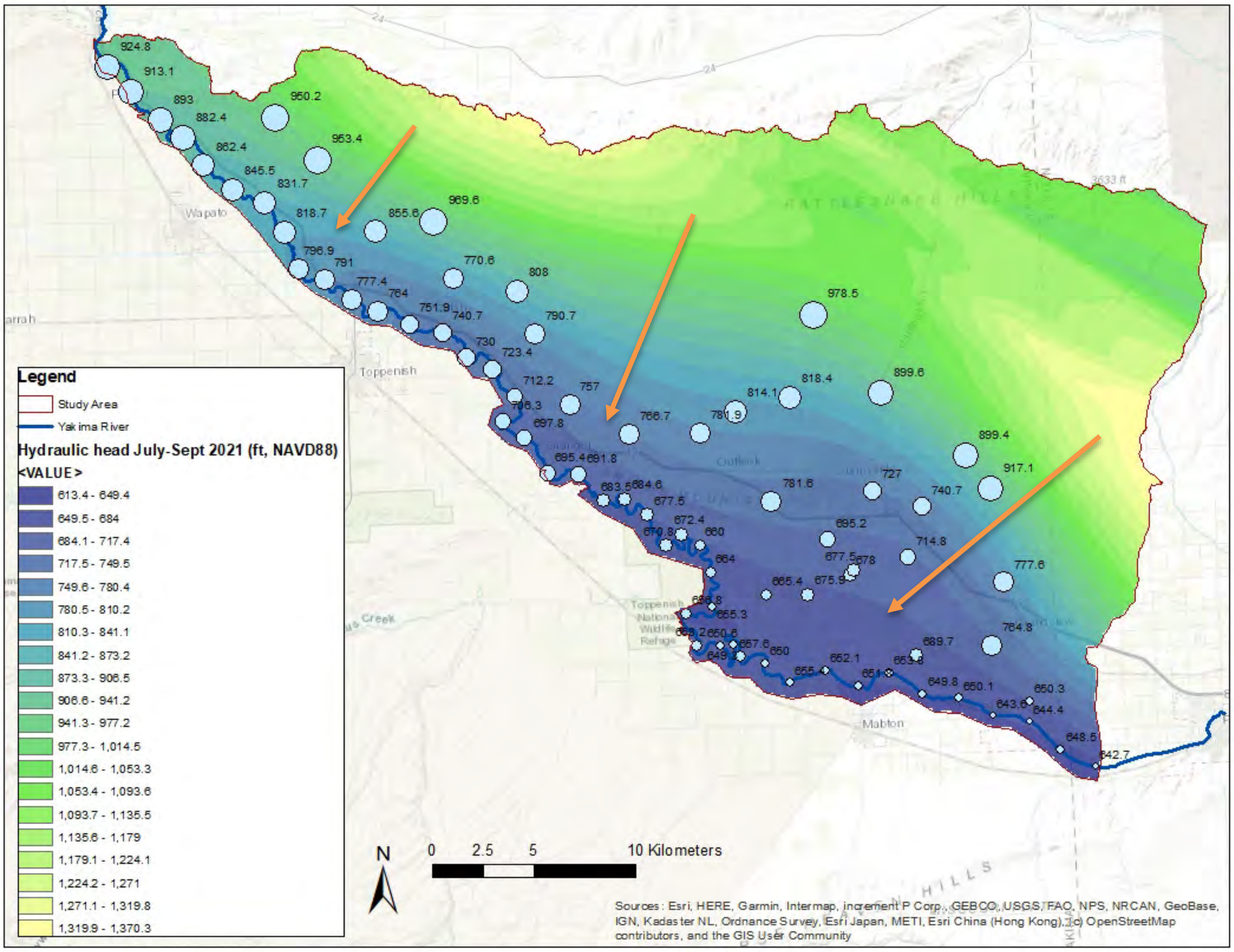

Figure 4-1. Water Level Map Generated for July-September 2021

Groundwater Level and Nitrate Map Generations

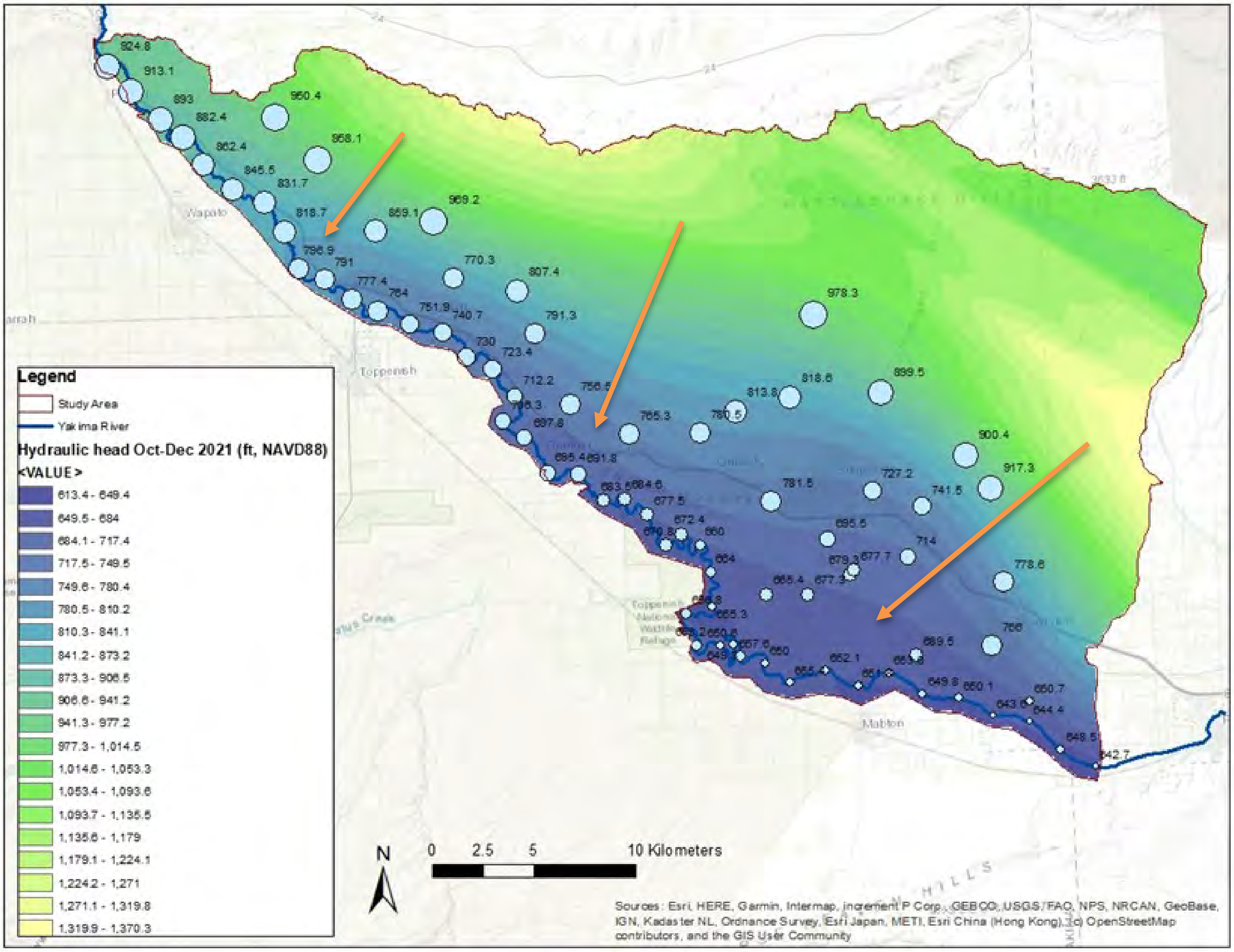

Figure 4-2. Water Level Map Generated for October-December 2021

Groundwater Level and Nitrate Map Generations

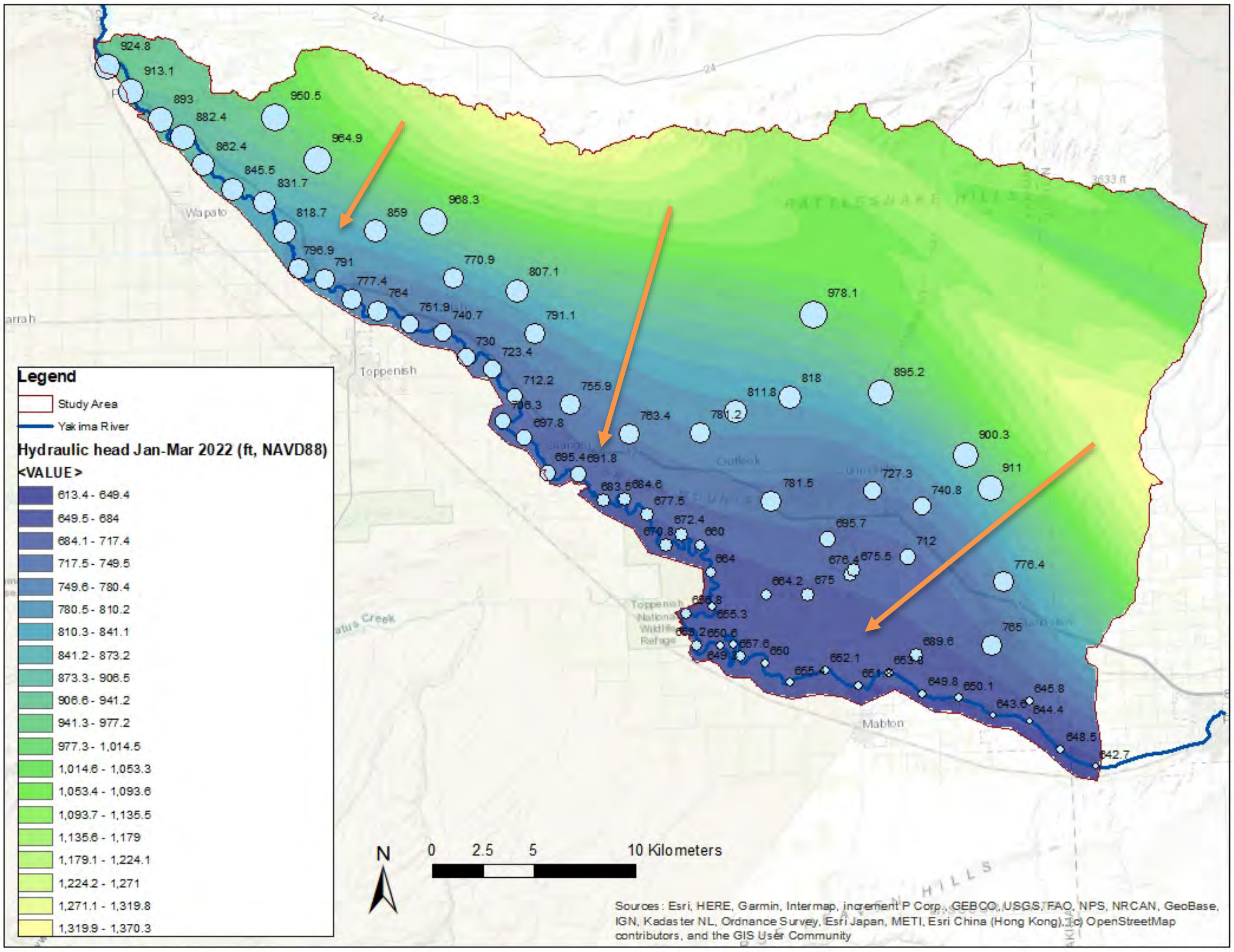

Figure 4-3. Water Level Map Generated for January-March 2022

Groundwater Level and Nitrate Map Generations

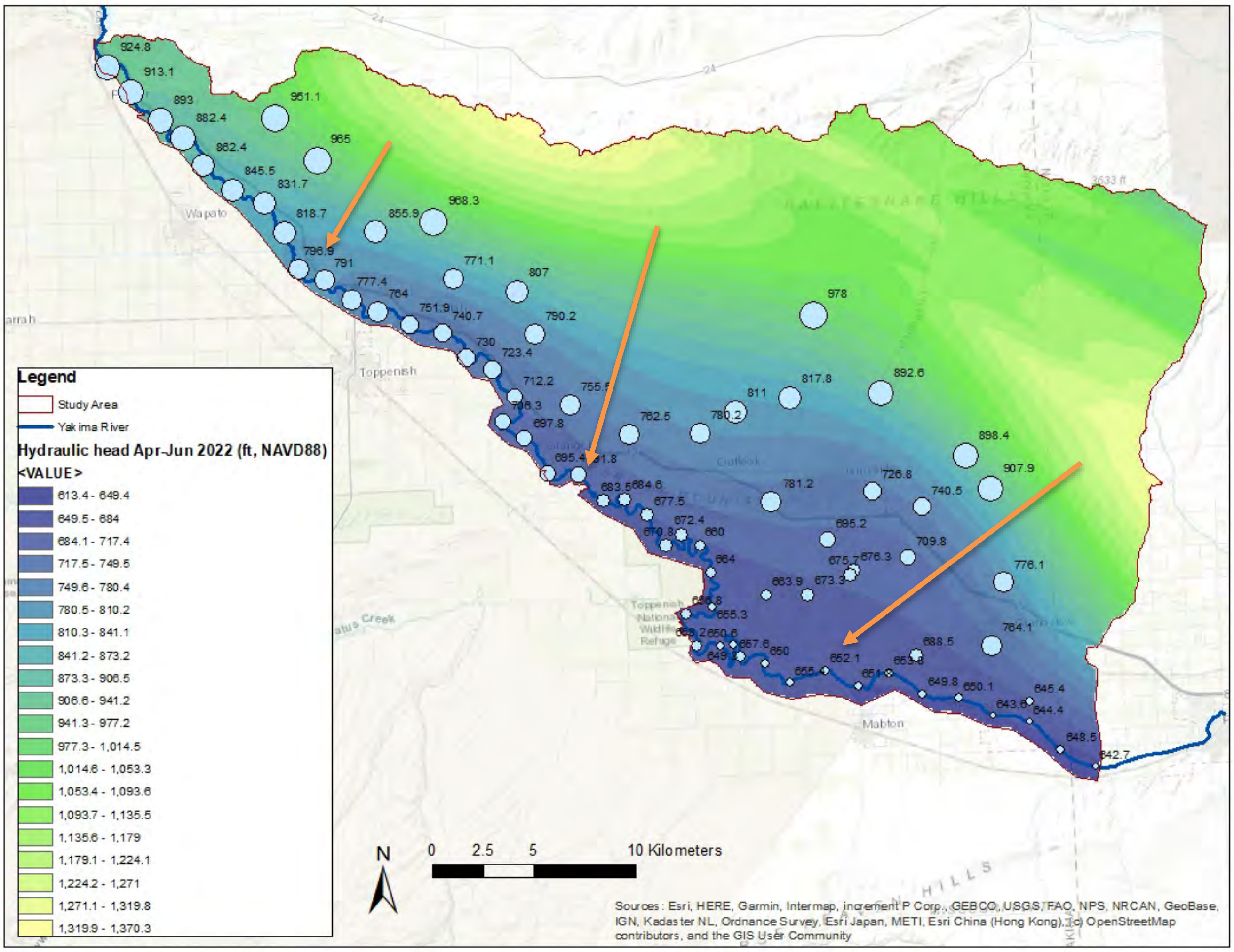

Figure 4-4. Water Level Map Generated for April-June 2022

5.0 MAP GENERATION FOR NITRATE

The locations of the wells used to generate nitrate concentration maps, including both the monitoring wells and supply wells, are shown in Figure 5-1. The first step for generating the nitrate maps is to evaluate the Kriging method and the kernel functions, which is similar to what was done for the water level maps. The testing was conducted using the July-September 2021 dataset first to evaluate if applying kernel function reduces model errors. Six different kernel functions and no kernel were tested for both the Ordinary Kriging method and the Universal Kriging Method. For both methods, the Gaussian semivariogram model was selected after several initial testing runs with the different semivariogam models. For the kernel function testing, the Gaussian semivariogram model without anisotropy option was used. Table 5-1 to Table 5-3 list the model errors with different kernel functions for all wells, monitoring wells only, and supply wells only.

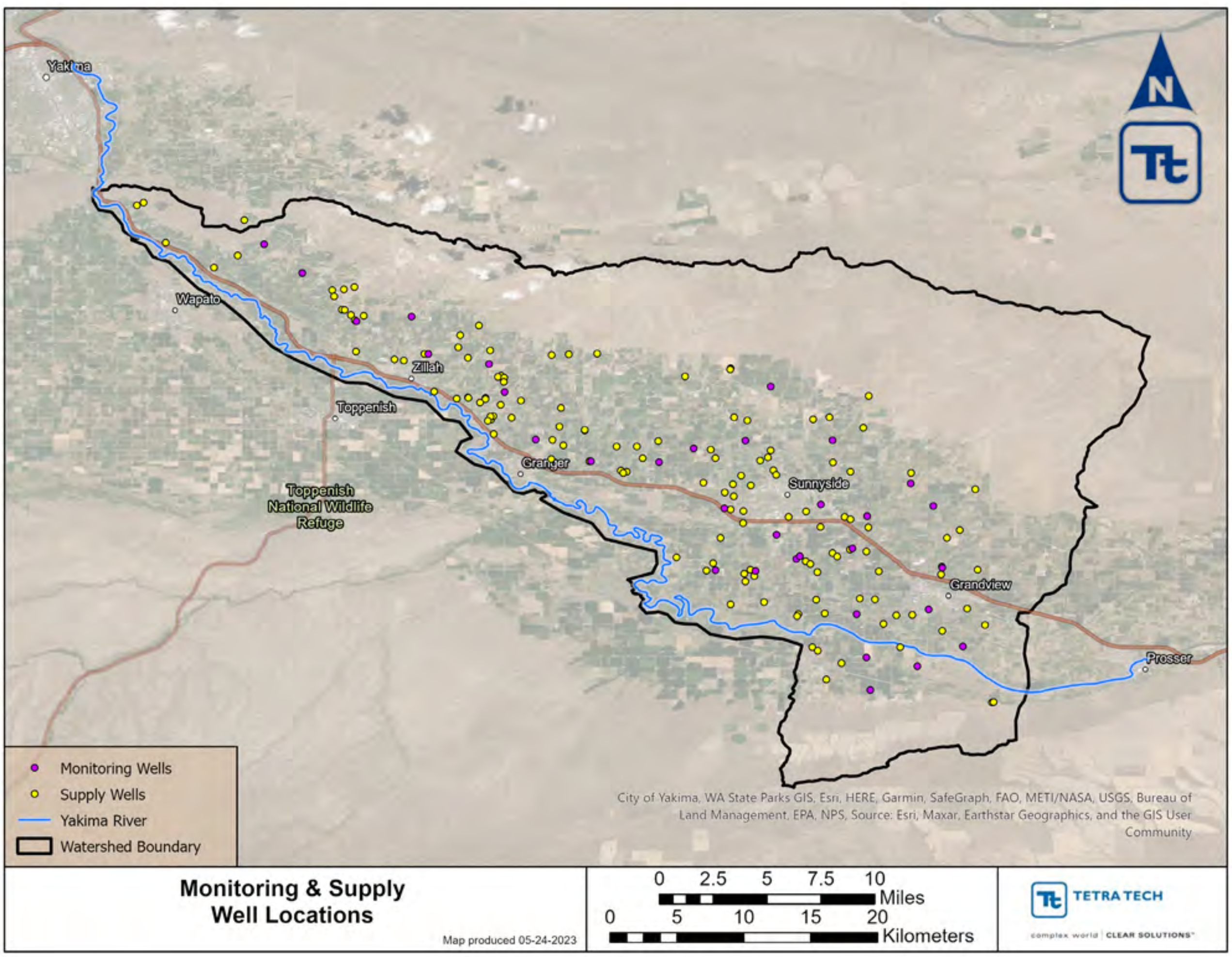

Figure 5-1. Locations of Wells for Nitrate Map Generations

Groundwater Level and Nitrate Map Generations

The kernel function with the lowest model errors for different Kriging methods and different datasets are not the same. For the nitrate data in lowest model errors occur with different kernel functions. For the nitrate dataset from all wells, the constant kernel function produced the lowest model error for the Ordinary Kriging method, while the no kernel option generated the lowest model error for the Universal Kriging method. For the nitrate dataset from monitoring wells, the Epanechnikov kernel option generated the lowest model error for both Ordinary and Universal Kriging methods. However, further evaluation revealed that the Kriging method does not work well for the monitoring wells when the maps were generated. A solution to this is discussed later in this report. Although a definitive reason that Kriging did not work well is unknown, a potential reason is that there were relatively few data points (wells), and there was no significant spatial correlation among these data points detectable by Kriging that would allow the algorithm to predict meaningful values in between these points.

For the nitrate dataset from supply wells, the exponential kernel function generated the lowest model errors. The model errors from the different kernel functions for data from all wells and data from supply wells are not dramatically different. The no kernel option does not necessarily achieve the lowest model errors, but there is a narrow range of error values among the seven kernel function options. Selecting the no kernel function simplifies the analysis for any new datasets. Otherwise, similar testing would need to be conducted to identify the appropriate kernel function option to use for each new dataset. Therefore, the no kernel option is used for the nitrate map generation. The errors for Ordinary and Universal Kriging methods are the same for the no kernel option, and the Ordinary Kriging method was selected.

Table 5-1. Testing Model Errors with Kernel Functions for All Wells

			Kernel function (mean error)					
Method	Model	no kernel	exponential	polynomial5	Gaussian	Epanechnikov	quartic	constant
Ordinary	Gaussian- no anisotropy	0.0359	0.0782	0.0377	0.0489	0.0345	0.0397	0.0191
Universal	Gaussian- no anisotropy	0.0359	0.0615	0.0411	0.0468	0.0417	0.0426	0.0406

Table 5-2. Testing Model Errors with Kernel Functions for Monitoring Wells Only

			Kernel function (mean error)					
Method	Model	no kernel	exponential	polynomial5	Gaussian	Epanechnikov	quartic	constant
Ordinary	Gaussian- no anisotropy	0.5911	0.1640	0.1250	0.1199	0.1189	0.1206	0.2693
Universal	Gaussian- no anisotropy	0.5911	0.0545	0.0545	0.0545	0.0545	0.0545	0.0545

Table 5-3. Testing Model Errors with Kernel Functions for Supply Wells Only

Method	Model		Kernel function (mean error)					
		no kernel	exponential	polynomial5	Gaussian	Epanechnikov	quartic	constant
Ordinary	Gaussian- no anisotropy	0.2499	-0.0949	0.4533	0.2112	0.3351	0.4362	0.1915
Universal	Gaussian- no anisotropy	0.2499	-0.1080	0.4352	0.1605	0.2899	0.4061	0.2251

After the selection of the Ordinary Kriging method, all the semivariogram models available for the Ordinary Kriging method were tested for model errors. Table 5-4 to Table 5-6 list the model errors for the semivariogram models including circular, spherical, exponential, Gaussian, and stable. This test also considered with and without anisotropy. The model errors for the monitoring wells are higher than the model errors for all wells and supply wells, and the model errors across all semivariogram models are identical. The model errors using the Gaussian semivariogram model without anisotropy option are lowest for the nitrate dataset for all wells. For the supply wells, the lowest model errors for different seasons are with different semivariogram models. The error differences among the different semivariogram models are relatively small therefore, for the purpose of simplicity and consistency, the Gaussian semivariogram model without anisotropy option is selected for generating all the nitrate maps. The parameters of the Gaussian model are listed in Table 5-7 to Table 5-9.

Table 5-4. Testing Model Errors with Different Semivariogram Models for All Wells

Method	Model	Mean error			
		JulSep21	OctDec21	JanMar22	AprJun22
Ordinary	circular	0.1671	0.0934	0.0805	0.1213
	spherical	0.1354	0.1261	0.1027	0.1352
	exponential	0.0737	0.0933	0.0824	0.0802
	Gaussian	0.0359	0.0661	0.0303	0.0615
	stable	0.0359	0.0661	0.0303	0.0615
Ordinary w/anistropy	circular	0.0438	0.1037	0.0883	0.0952
	spherical	0.0804	0.1516	0.0738	0.1444
	exponential	0.0737	0.2243	0.2190	0.2355
	Gaussian	0.0906	0.1733	-0.0603	-0.1222
	stable	0.0906	0.1733	-0.0603	-0.1222

Table 5-5. Testing Model Errors with Different Semivariogram Models for Monitoring Wells Only

Method	Model	Mean error			
		JulSep21	OctDec21	JanMar22	AprJun22
Ordinary	circular	0.5911	0.5372	0.5362	0.4799
	spherical	0.5911	0.5372	0.5362	0.4799
	exponential	0.5911	0.5372	0.5362	0.4799
	Gaussian	0.5911	0.5372	0.5362	0.4799
	stable	0.5911	0.5372	0.5362	0.4799
Ordinary w/anistropy	circular	0.5911	0.5372	0.5362	0.4799
	spherical	0.5911	0.5372	0.5362	0.4799
	exponential	0.5911	0.5372	0.5362	0.4799
	Gaussian	0.5911	0.5372	0.5362	0.4799
	stable	0.5911	0.5372	0.5362	0.4799

Table 5-6. Testing Model Errors with Different Semivariogram Models for Supply Wells Only

Method	Model	Mean error			
		JulSep21	OctDec21	JanMar22	AprJun22
Ordinary	circular	0.2056	0.2057	0.1844	0.1799
	spherical	0.2360	0.2004	0.2114	0.1739
	exponential	0.1910	0.2006	0.1837	0.1780
	Gaussian	0.2499	0.2330	0.2148	0.1937
	stable	0.2499	0.2330	0.2148	0.1937
Ordinary w/anistropy	circular	0.2241	0.2795	0.2612	0.2338
	spherical	0.1346	0.2240	0.2805	0.2812
	exponential	0.1268	0.0909	0.2444	0.1411
	Gaussian	0.1673	0.1186	0.1905	0.1241
	stable	0.1673	0.1186	0.1905	0.1241

Table 5-7. Parameter Values for the Gaussian Semivariogram Models for All Wells

	Data Set			
Parameters	July-September 2021	October-December 2021	January-March 2022	April-June 2022
Nugget (mg^2/L^2)	45.43	52.65	39.87	40.43
Range (Degree)	0.041	0.041	0.042	0.041
Partial Sill (mg2/L2)	134.33	115.37	92.35	108.13

Groundwater Level and Nitrate Map Generations

Table 5-8. Parameter Values for the Gaussian Semivariogram Models for Monitoring Wells

	Data Set			
Parameters	July-September 2021	October-December 2021	January-March 2022	April-June 2022
Nugget (mg^2/L^2)	354.72	331.42	242.21	281.90
Range (Degree)	0.557	0.557	0.557	0.557
Partial Sill (mg2/L2)	0.00	0.00	0.00	0.00

Table 5-9. Parameter Values for the Gaussian Semivariogram Models for Supply Wells

	Data Set			
Parameters	July-September 2021	October-December 2021	January-March 2022	April-June 2022
Nugget (mg^2/L^2)	10.57	12.33	13.48	10.30
Range (Degree)	0.023	0.023	0.024	0.022
Partial Sill (mg2/L2)	31.61	28.85	29.92	28.95

The values for the parameters for the monitoring wells are atypical. A zero partial sill value is meaningless. The distribution of nitrate on maps generated using the Kriging method for the monitoring wells are erratic (see Appendix A). Nitrate maps using other semivariogram models were also tested for the monitoring well only datasets. These maps also show erratic distribution of nitrate. Therefore, the IDW method was used for the nitrate maps using the monitoring wells only to produce more logical results. For the purposes of consistency and to demonstrate the erratic distribution, the maps generated with Kriging method for the monitoring wells only datasets are also included in Appendix A. IDW results for the monitoring wells are presented later in this report.

The Geostatistical tool was used to generate raster files based on the Gaussian model results. The generated raster files were clipped using a boundary GIS file. The boundary file for the nitrate map covers a larger area than the boundary file for the water level maps because of the more broadly distributed supply wells.

Two types of maps were generated for the nitrate concentrations. One is the raster map which uses color to represent the level of nitrate concentrations. The other is the contour map which uses lines to represent the level of nitrate concentrations. The raster maps are shown first in the order of all wells and then supply wells only from Figure 5-2 to Figure 5-9. As with the groundwater level, the results further away from the data used in the analysis are more unreliable and should be used with caution. This is illustrated in the “streaky” look of the results in the northeastern portion of the maps. For any statistical model, the prediction becomes less reliable as the distance from known data values increases, especially for the areas not covered by the data locations.

The raster and contour maps can be used to identify general spatial and seasonal trends in groundwater nitrate concentrations. For example, seasonal variations of the high nitrate concentrations can be visually inspected by comparing the maps. They are representative predicted values in the horizontal plane. No data on the depth from which the water samples were taken was available; therefore, these maps cannot be used to evaluate or predict variability in nitrate concentrations by depth. The data were also aggregated seasonally and may not capture finer time-scale changes in nitrate concentrations or patterns. The results represent seasonally averaged snapshots of nitrate concentrations. The maps are generated using only nitrate data and are not intended to address why the nitrate concentrations are distributed as they are. Sources of nitrate were not investigated as part of this analysis, so nitrate sources cannot be derived from these maps. However, they can be used in conjunction with other information on land uses or known potential sources to identify likely candidate sources of nitrate in the GWMA.

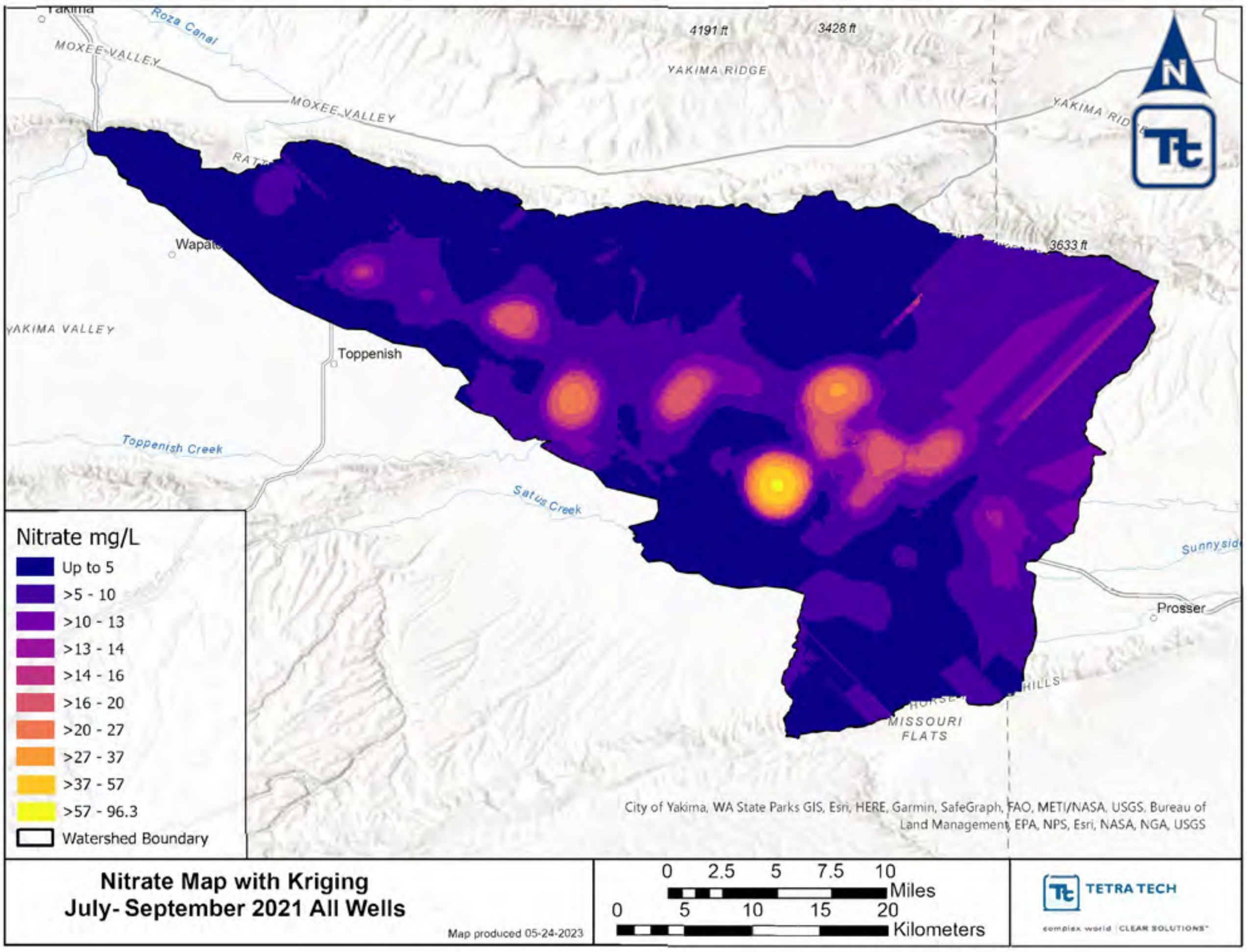

Figure 5-2. Nitrate Map with Kriging for the July-September 2021 Dataset for All Wells

Groundwater Level and Nitrate Map Generations

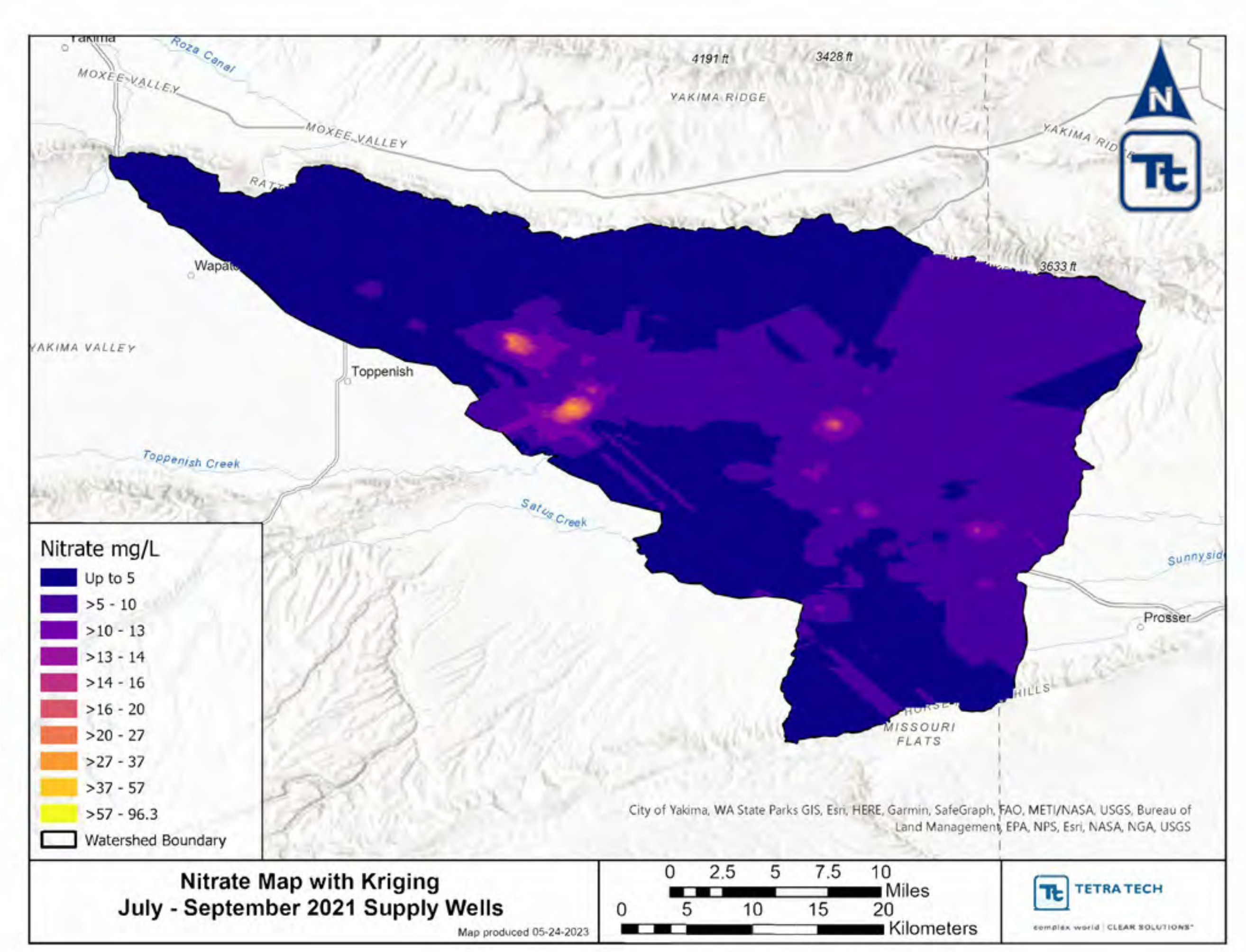

Figure 5-3. Nitrate Map with Kriging for the July-September 2021 Dataset for Supply Wells

Groundwater Level and Nitrate Map Generations

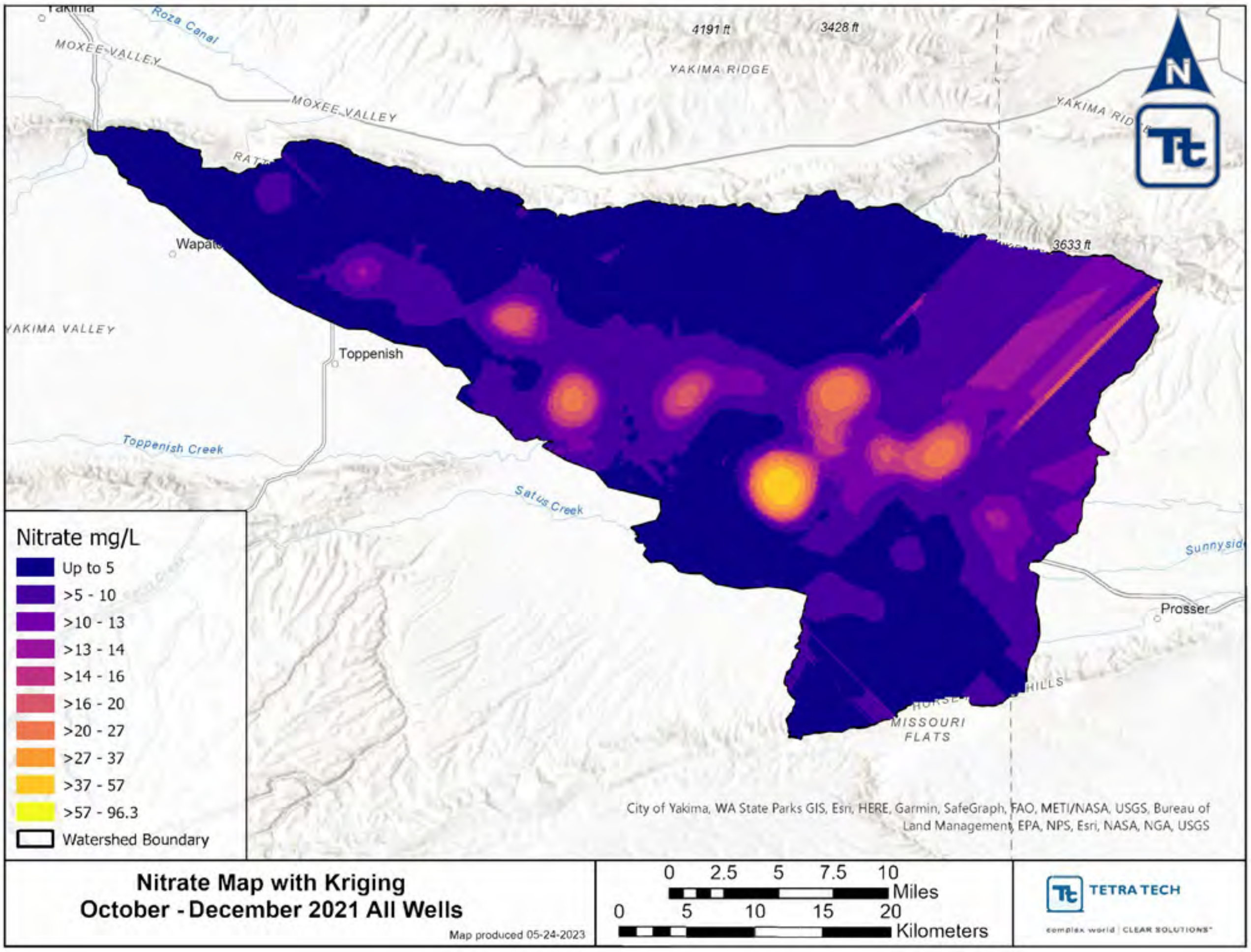

Figure 5-4. Nitrate Map with Kriging for the October-December 2021 Dataset for All Wells

Groundwater Level and Nitrate Map Generations

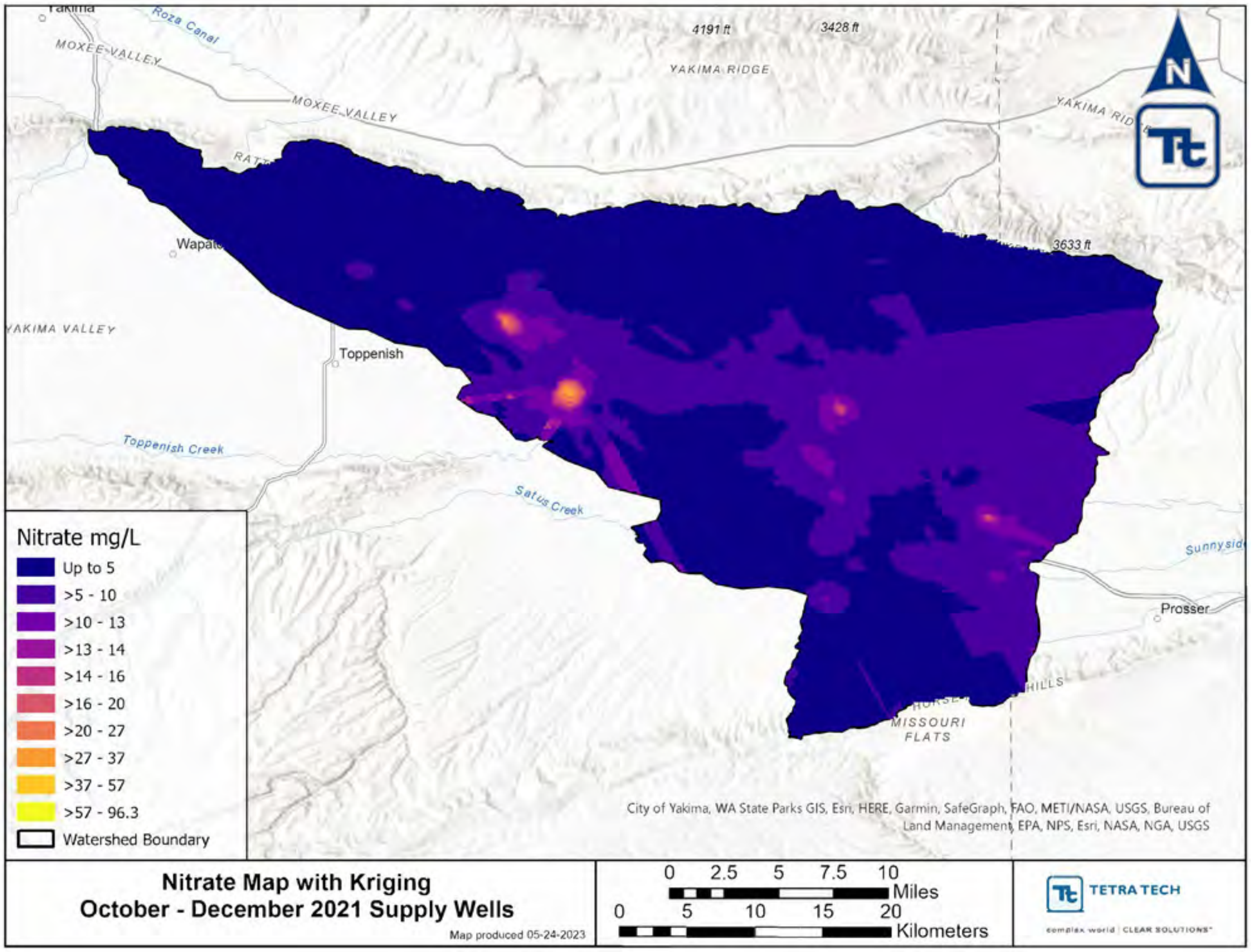

Figure 5-5. Nitrate Map with Kriging for the October-December 2021 Dataset for Supply Wells

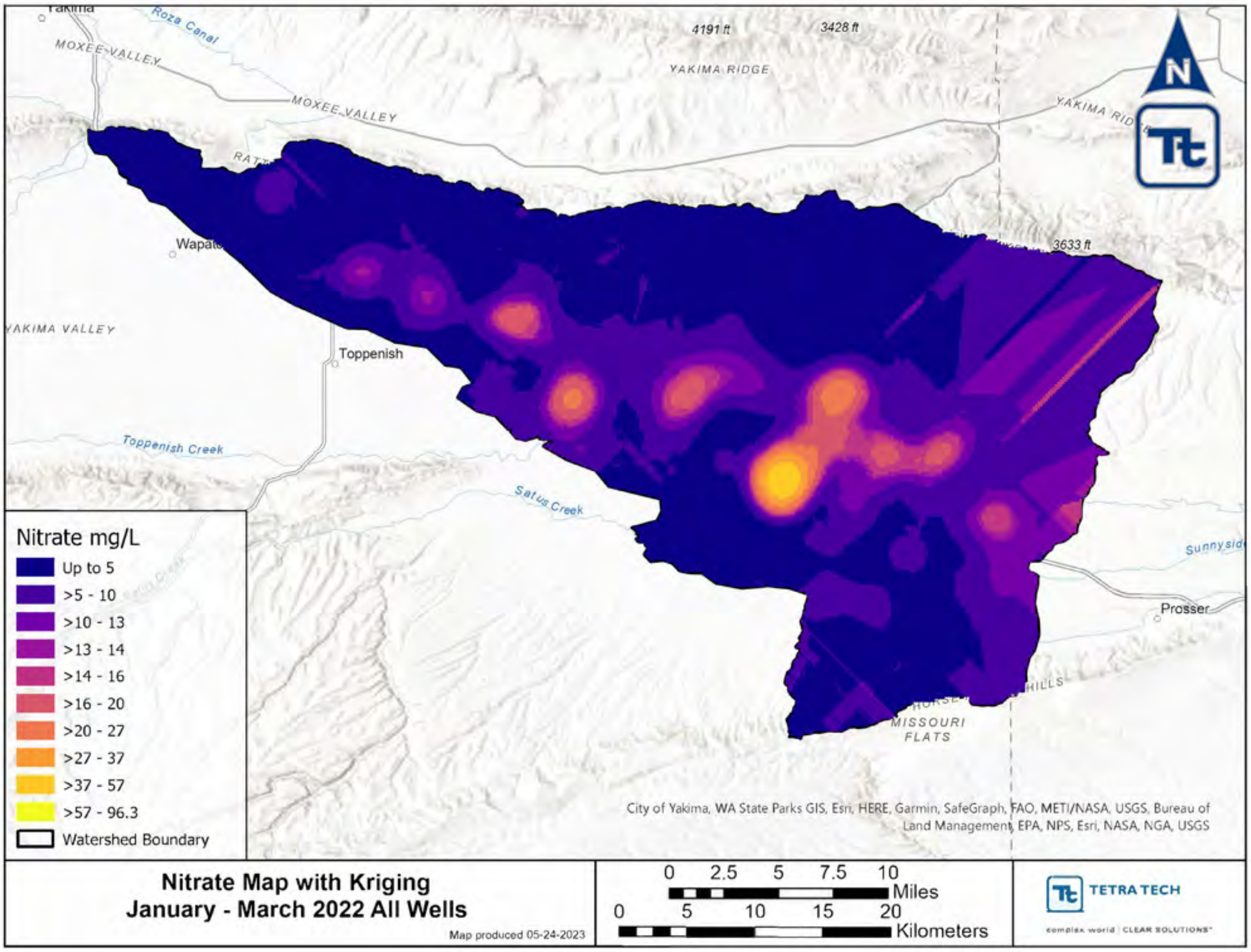

Figure 5-6. Nitrate Map with Kriging for the January-March 2022 Dataset for All Wells

Groundwater Level and Nitrate Map Generations

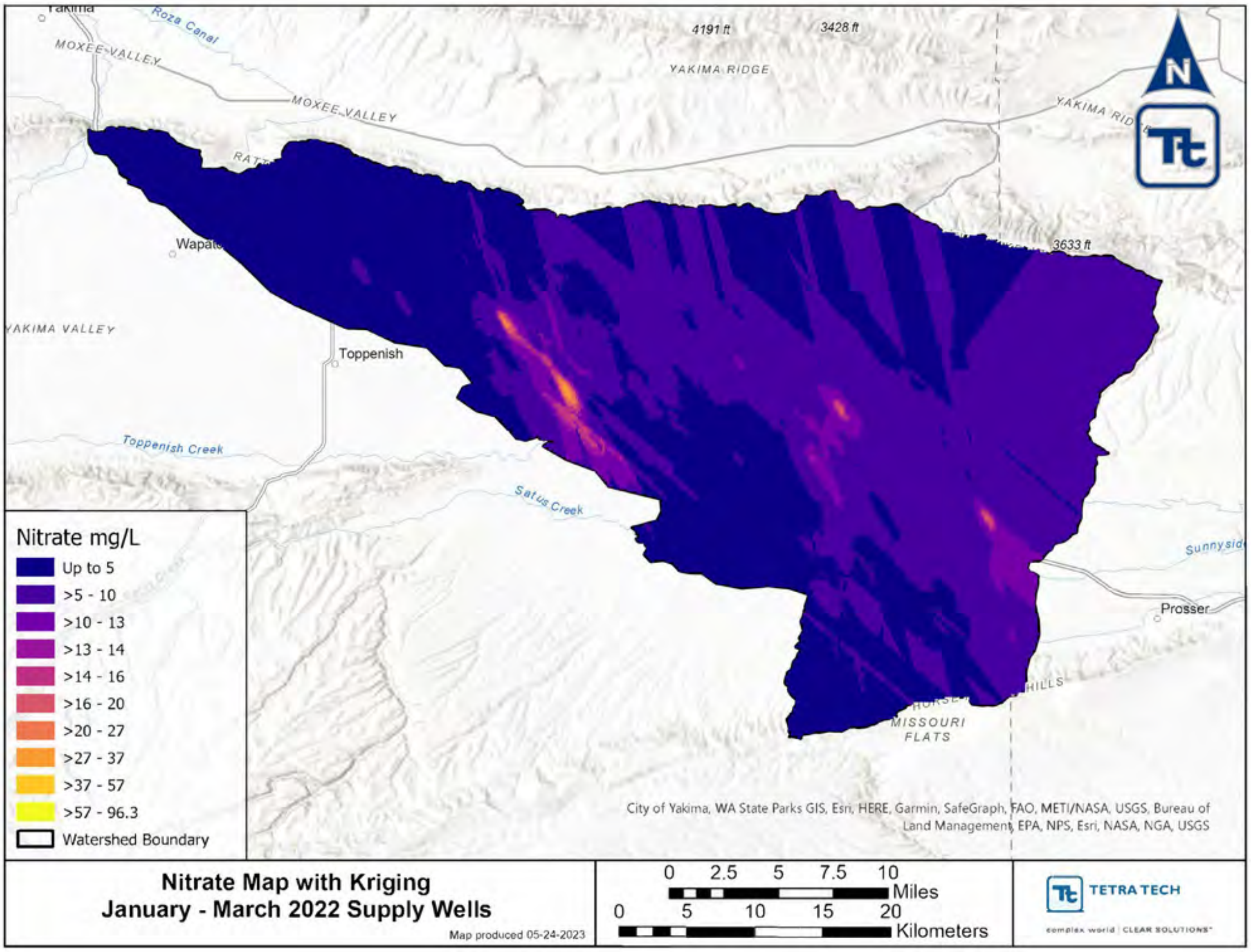

Figure 5-7. Nitrate Map with Kriging for the January-March 2022 Dataset for Supply Wells

Groundwater Level and Nitrate Map Generations

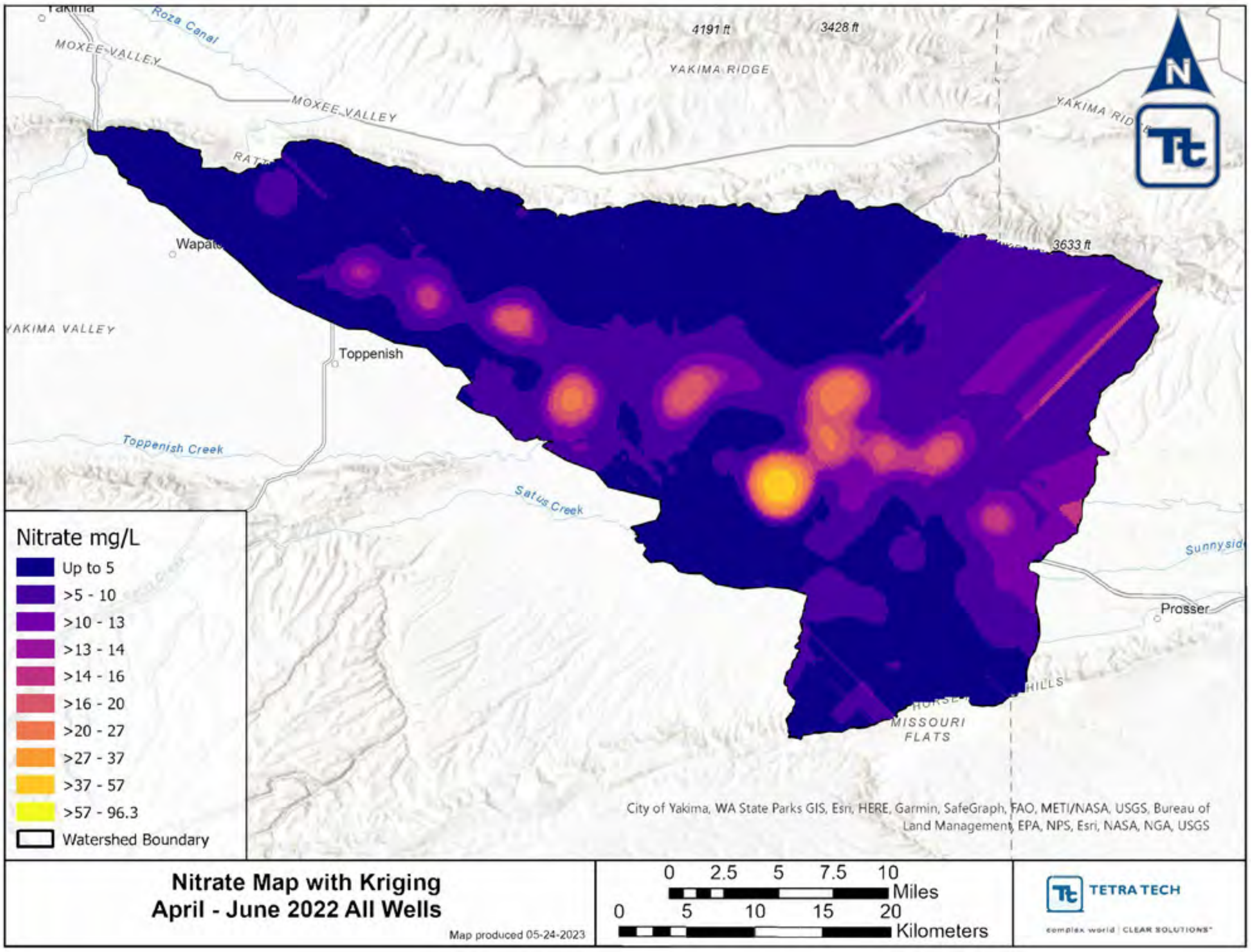

Figure 5-8. Nitrate Map with Kriging for the April-June 2022 Dataset for All Wells

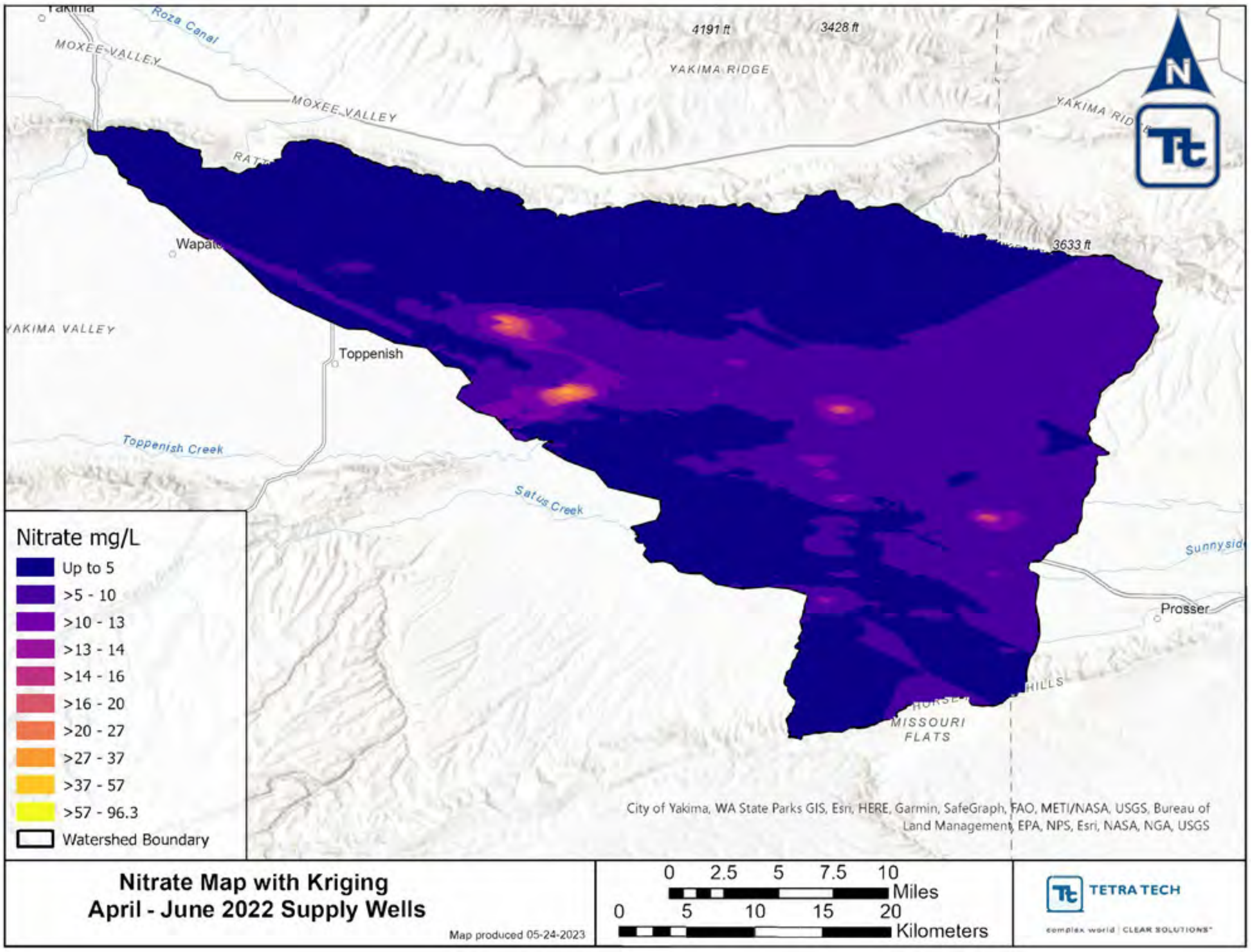

Figure 5-9. Nitrate Map with Kriging for the April-June 2022 Dataset for Supply Wells

Among the three datasets (all wells, monitoring wells, and supply wells), the maps using data from all the wells are smoothest. Maps using only the monitoring wells are erratic. The nitrate distribution using only the supply wells somewhat follows the trend of the maps using the data from all the wells. Based on a visual comparison of the maps across the four seasons using all wells, the nitrate distribution shifted slightly, but no distinct patterns were identified. The areas of high nitrate concentration remained distinct and consistent throughout the seasons. The nitrate concentrations in the more downstream portion (eastern part) vary slightly more than those in the upstream portion

The contour maps for the nitrate distributions using the Kriging method are shown from Figure 5-10 to Figure 5-17.

Groundwater Level and Nitrate Map Generations

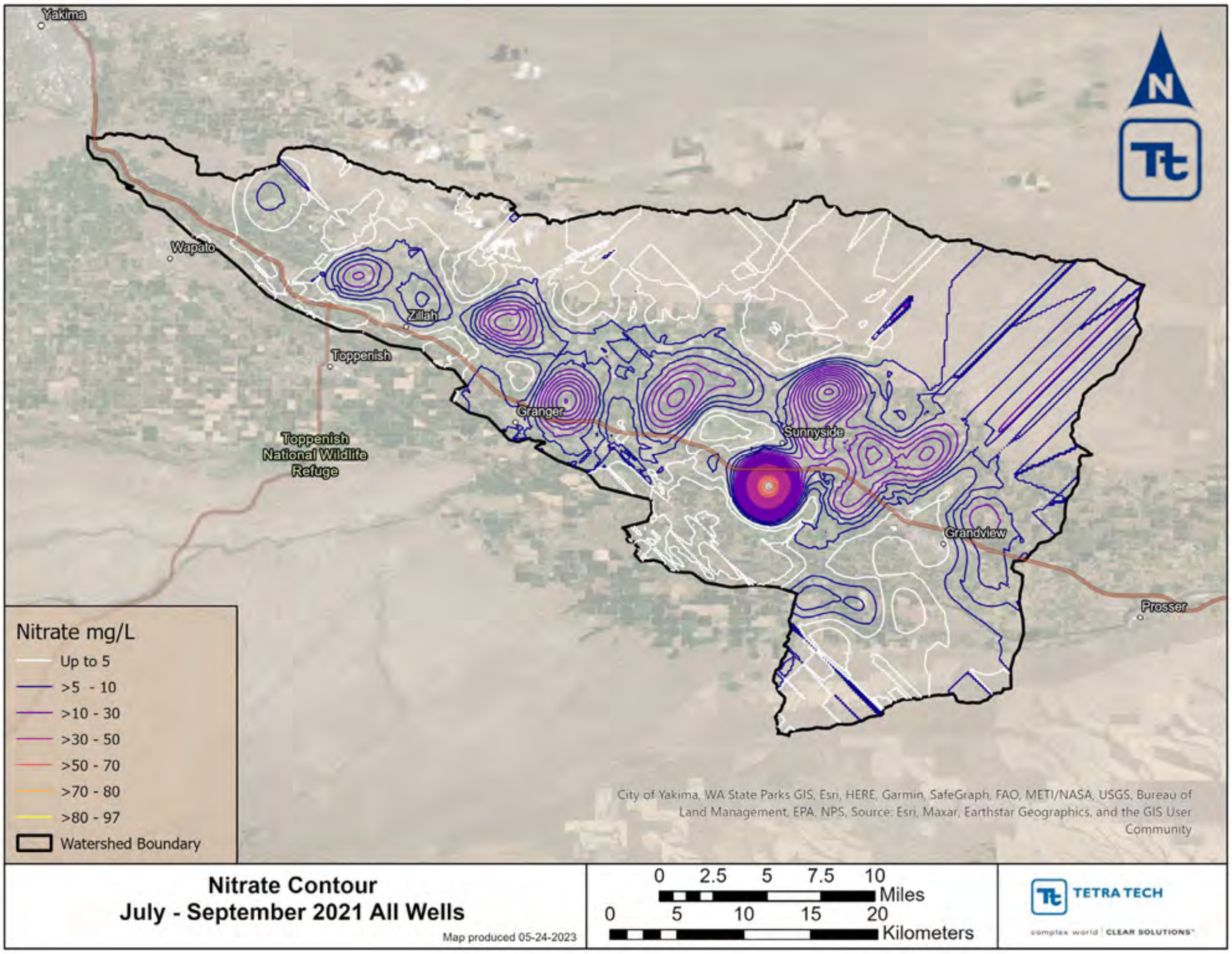

Figure 5-10. Nitrate Contour Map with Kriging for the July-September 2021 Dataset for All Wells

Groundwater Level and Nitrate Map Generations

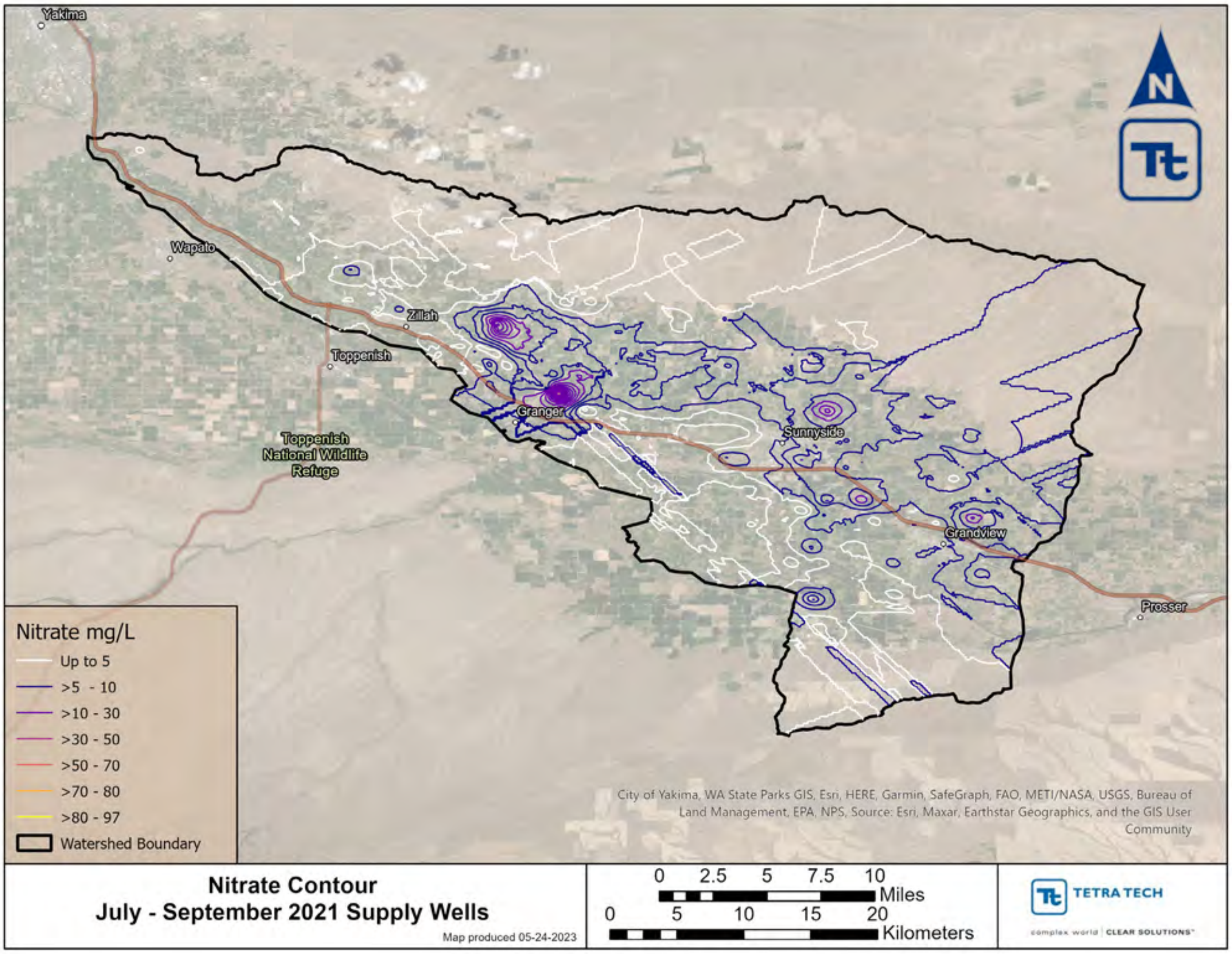

Figure 5-11. Nitrate Contour Map with Kriging for the July-September 2021 Dataset for Supply Wells

Groundwater Level and Nitrate Map Generations

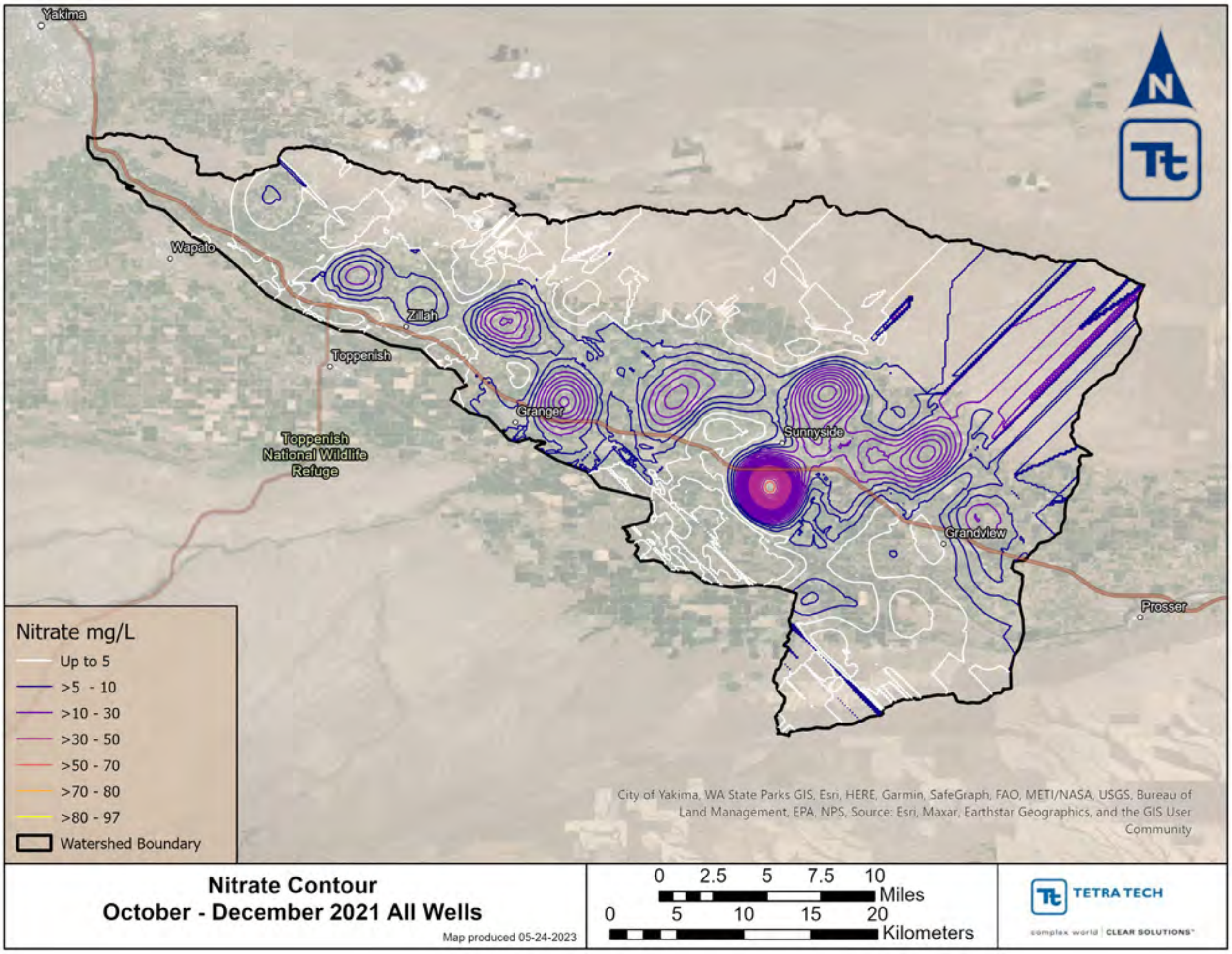

Figure 5-12. Nitrate Contour Map with Kriging for the October-December 2021 Dataset for All Wells

Groundwater Level and Nitrate Map Generations

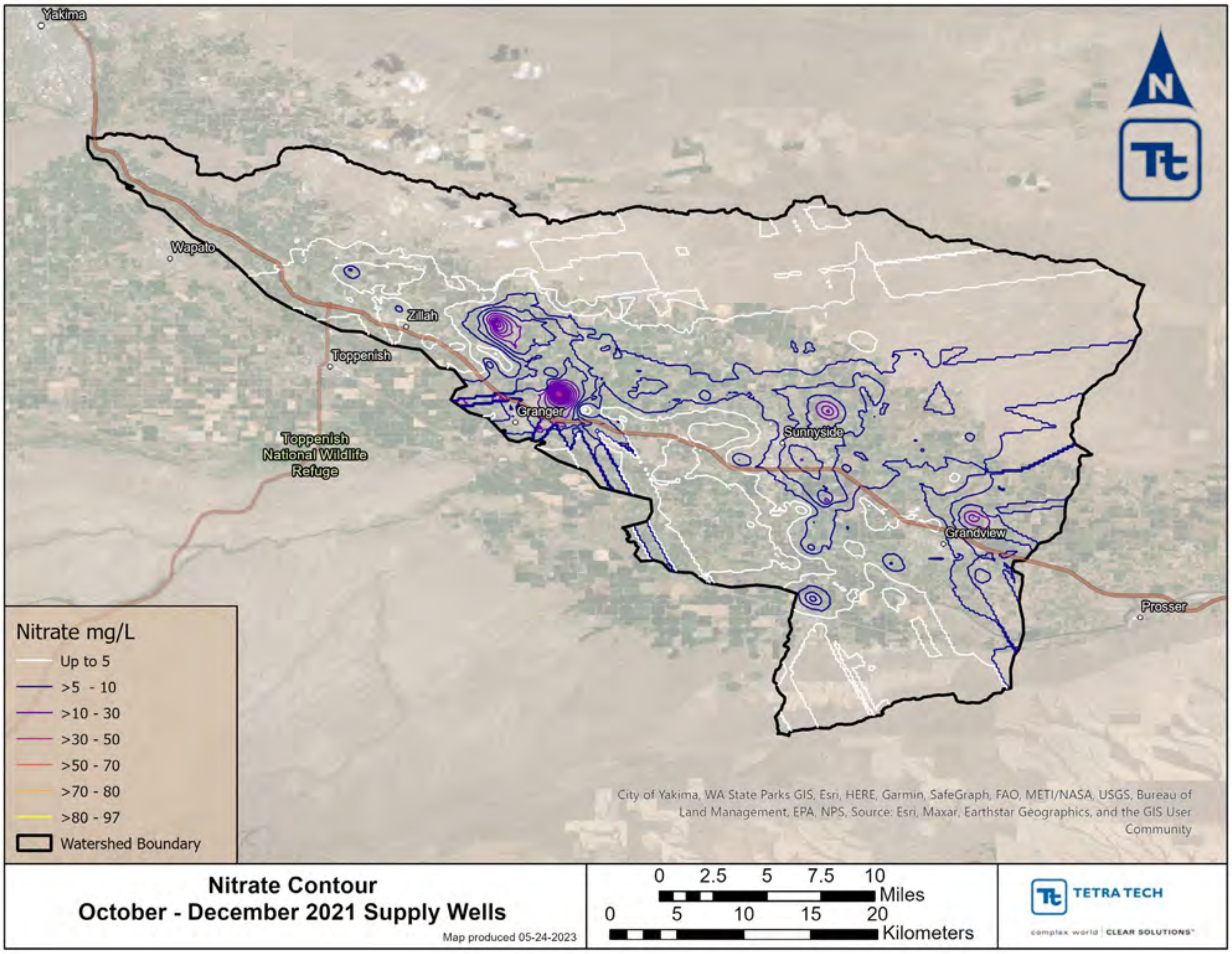

Figure 5-13. Nitrate Contour Map with Kriging for the October-December 2021 Dataset for Supply Wells

Groundwater Level and Nitrate Map Generations

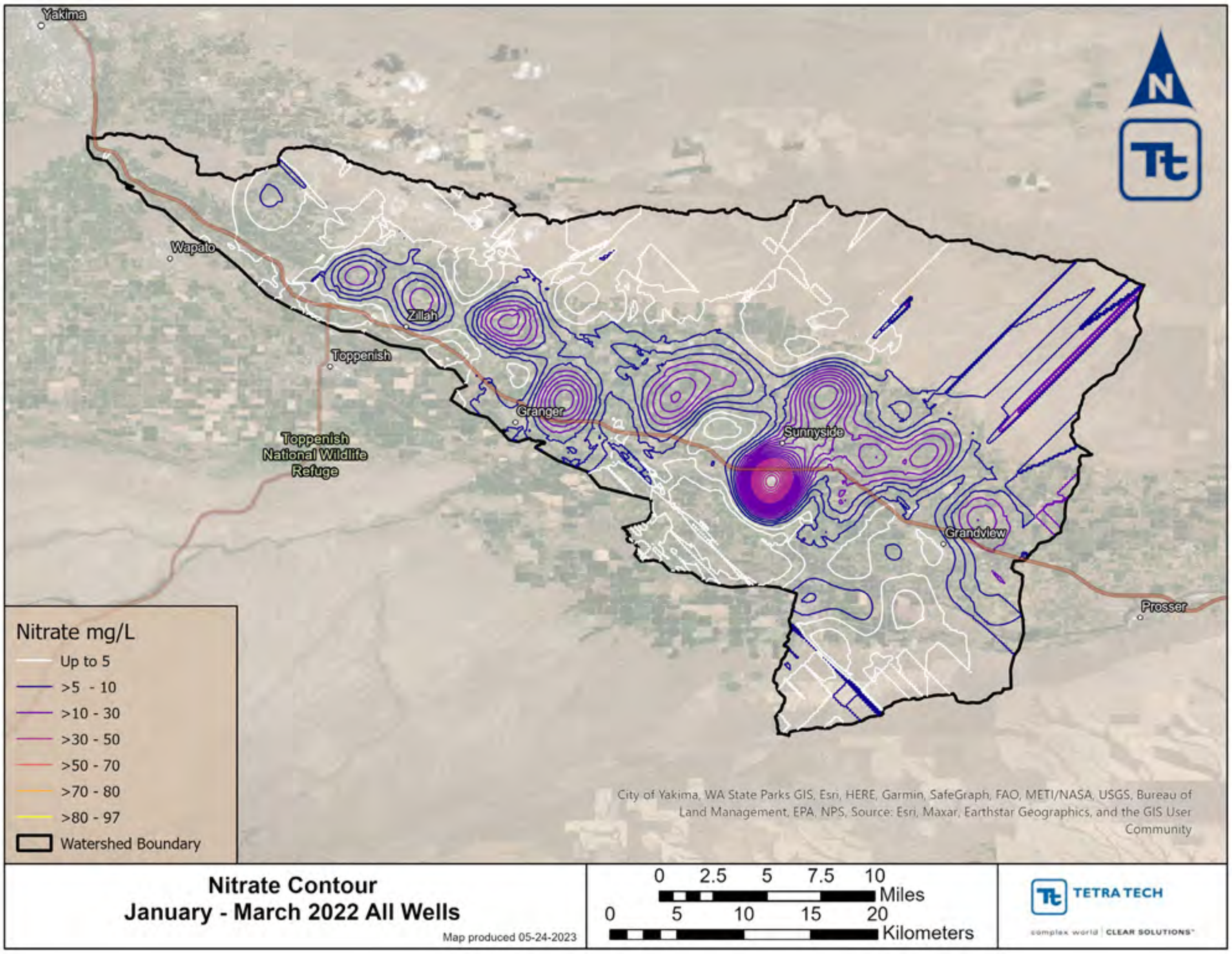

Figure 5-14. Nitrate Contour Map with Kriging for the January-March 2022 Dataset for All Wells

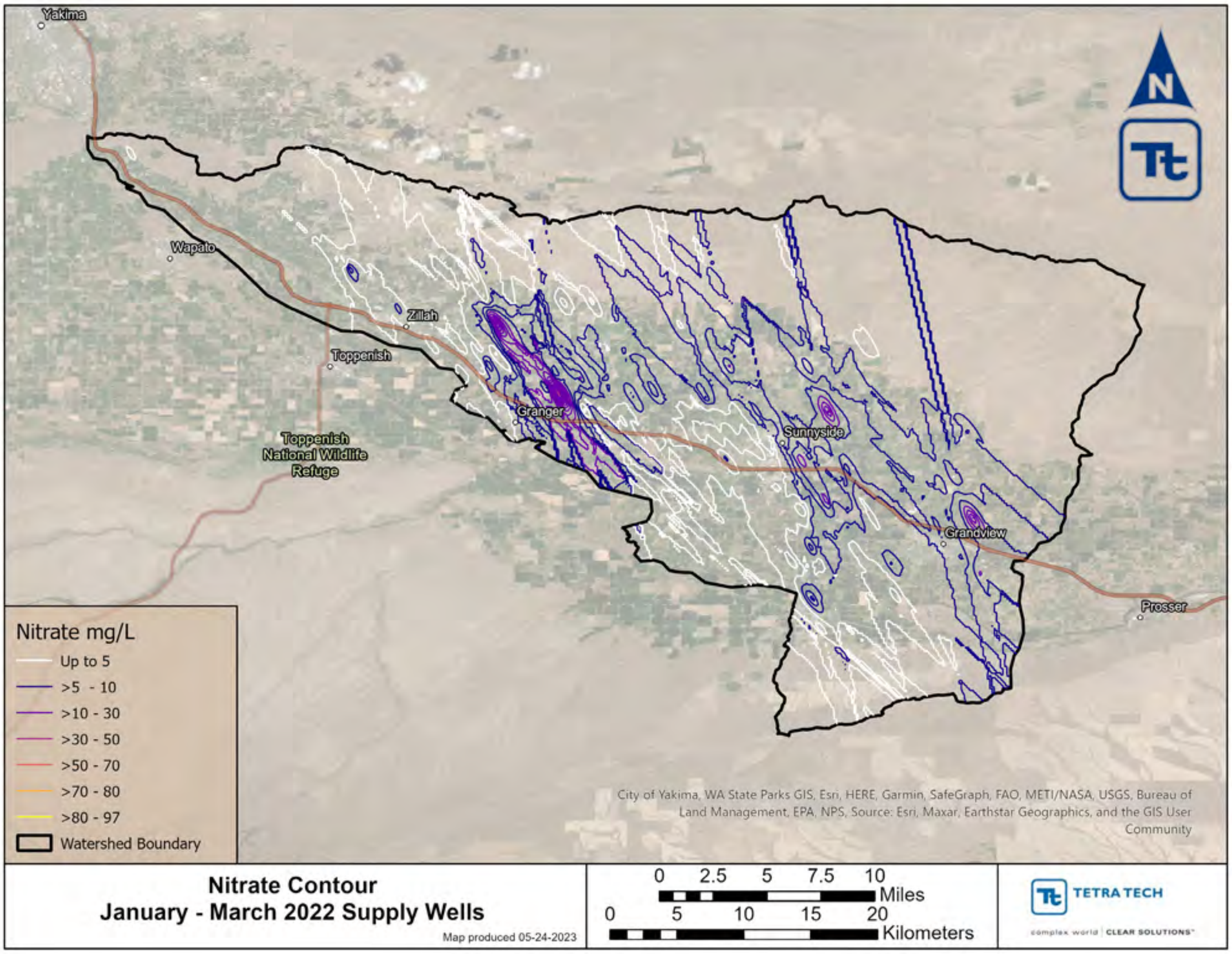

Figure 5-15. Nitrate Contour Map with Kriging for the January-March 2022 Dataset for Supply Wells

Groundwater Level and Nitrate Map Generations

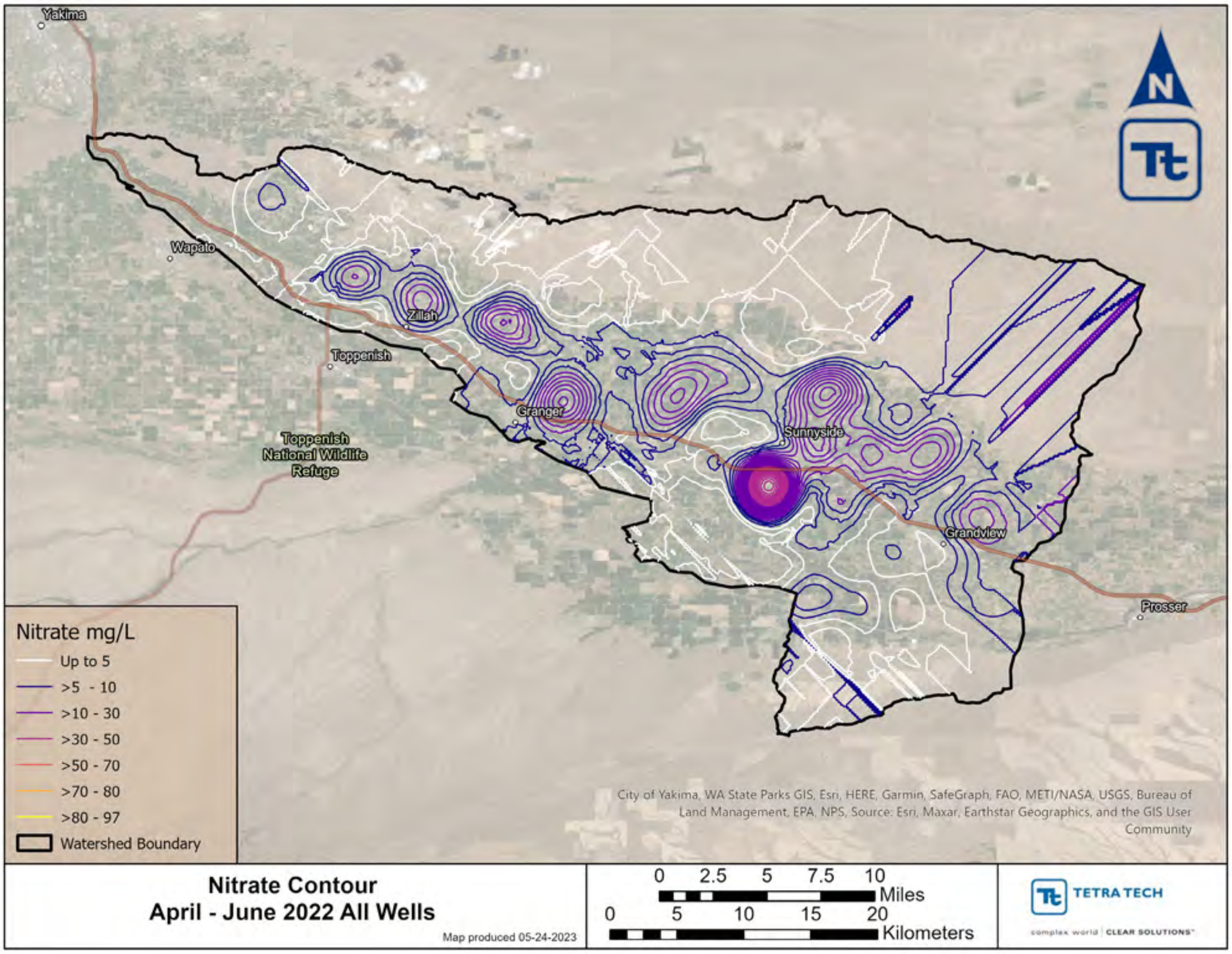

Figure 5-16. Nitrate Contour Map with Kriging for the April-June 2022 Dataset for All Wells

Groundwater Level and Nitrate Map Generations

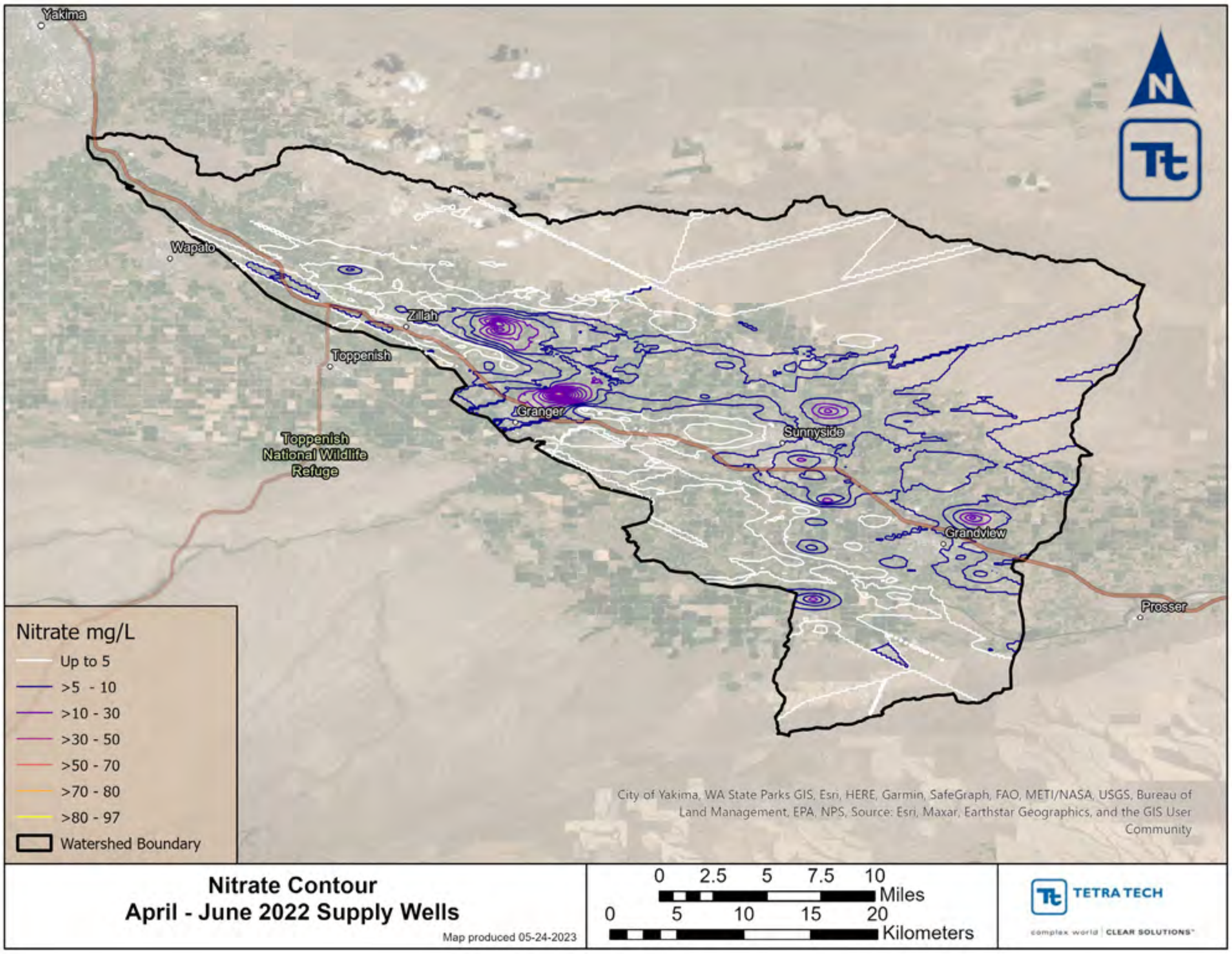

Figure 5-17. Nitrate Contour Map with Kriging for the April-June 2022 Dataset for Supply Wells

Groundwater Level and Nitrate Map Generations

As previously noted, the Kriging method does not work well for the data from only the monitoring wells. Therefore, the IDW method was used to generate the raster and contour maps for the datasets of the monitoring wells. The raster maps are shown from Figure 5-18 to Figure 5-21. The contour maps are shown from Figure 5-22 to Figure 5-25. One of the limitations of the IDW method is that it cannot extrapolate values beyond the farthest spatial extent of the data used in the analysis. Therefore, the IDW results are more limited within the watershed, using a polygon bounded by the wells at the farthest extent in the cardinal directions.

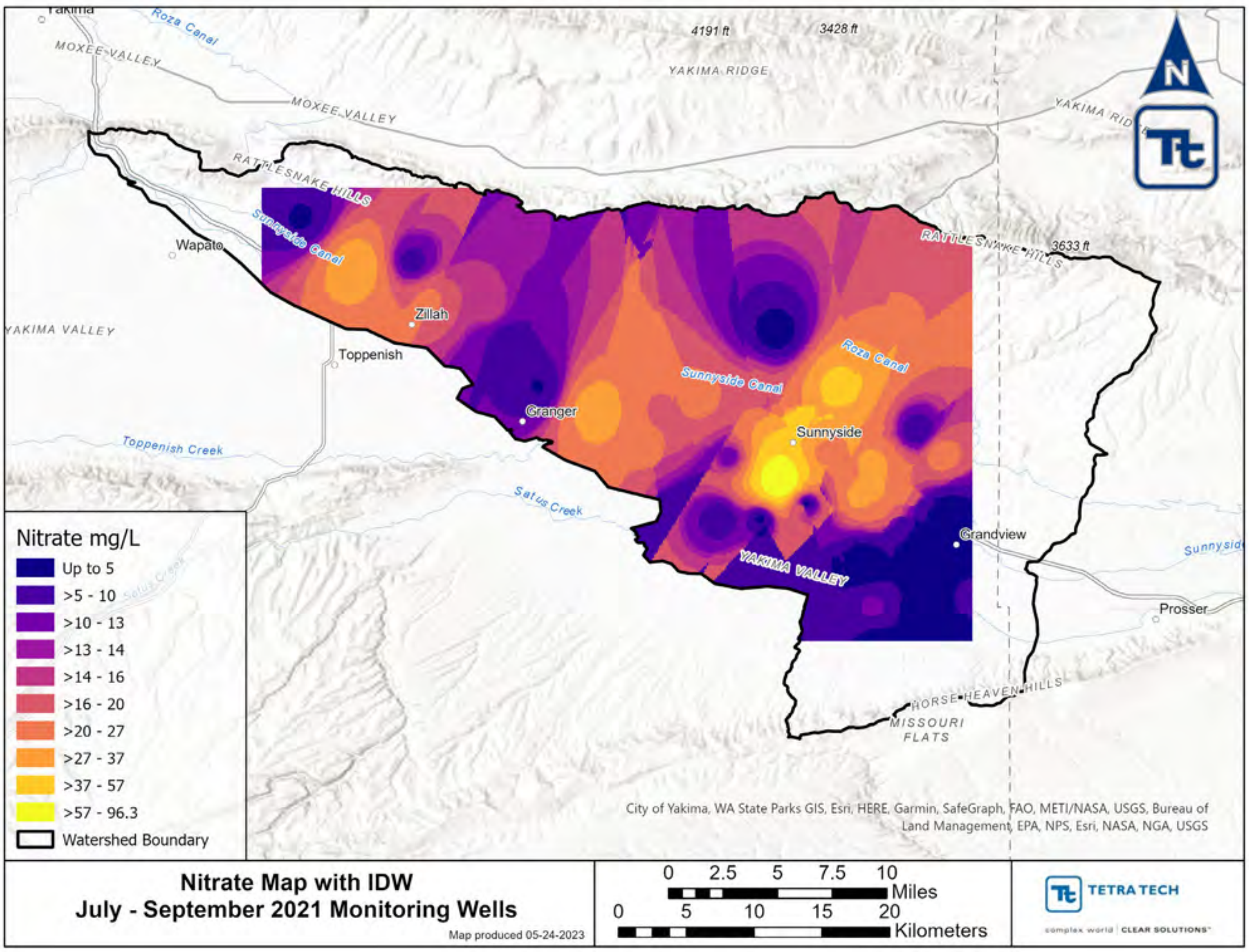

Figure 5-18. Nitrate Map with IDW for the July-September 2021 Dataset for Monitoring Wells

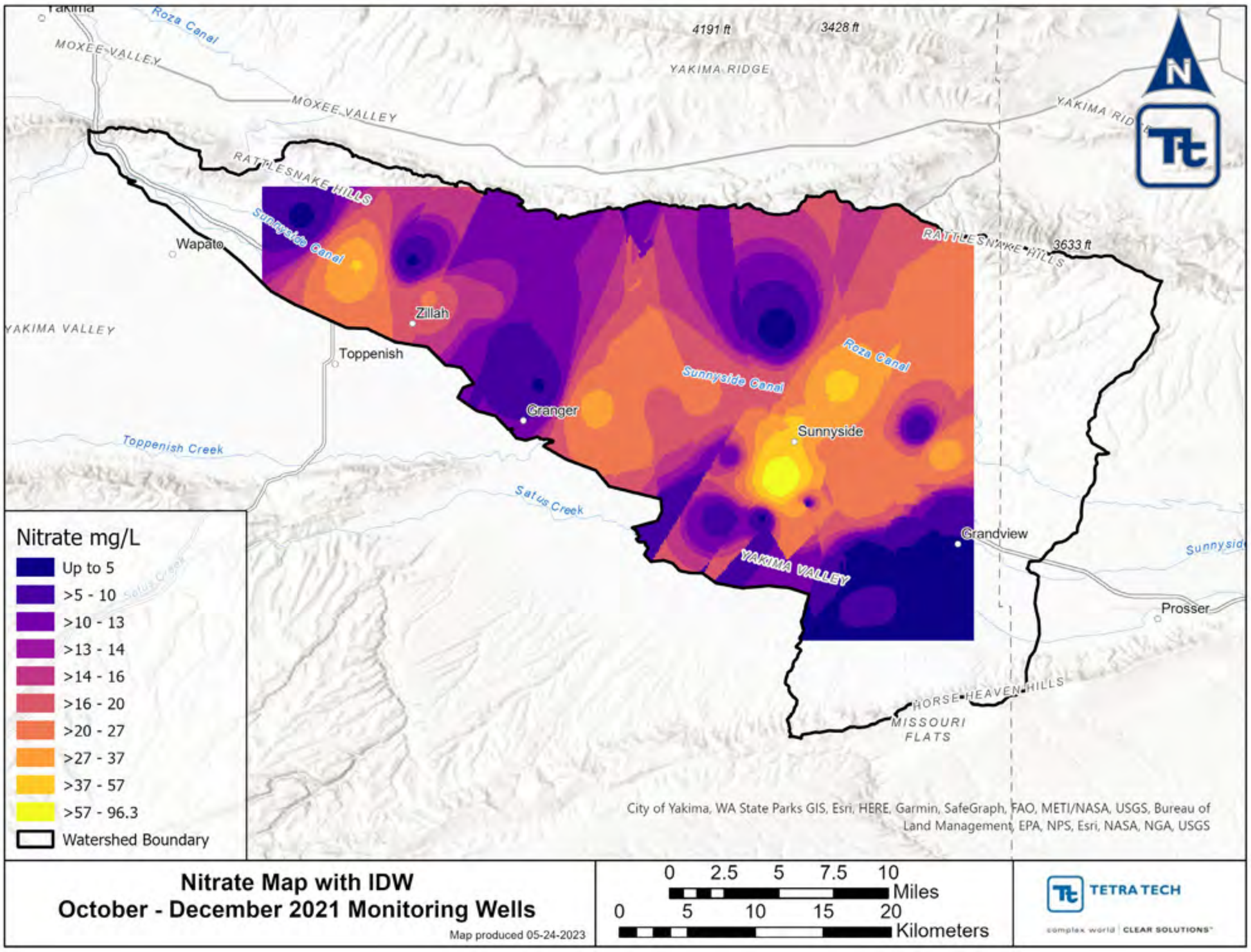

Figure 5-19. Nitrate Map with IDW for the October-December 2021 Dataset for Monitoring Wells

Groundwater Level and Nitrate Map Generations

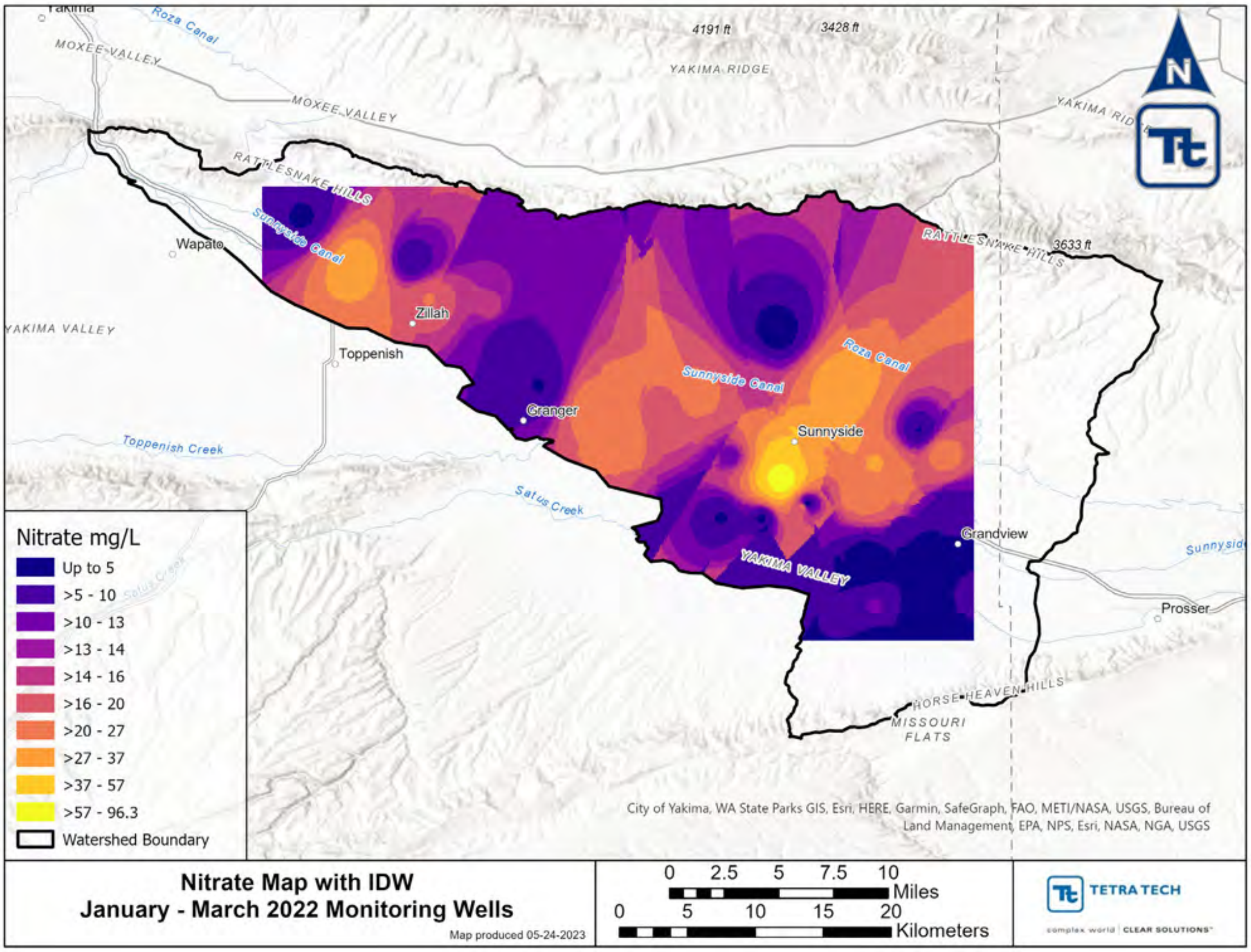

Figure 5-20. Nitrate Map with IDW for the January-March 2022 Dataset for Monitoring Wells

Groundwater Level and Nitrate Map Generations

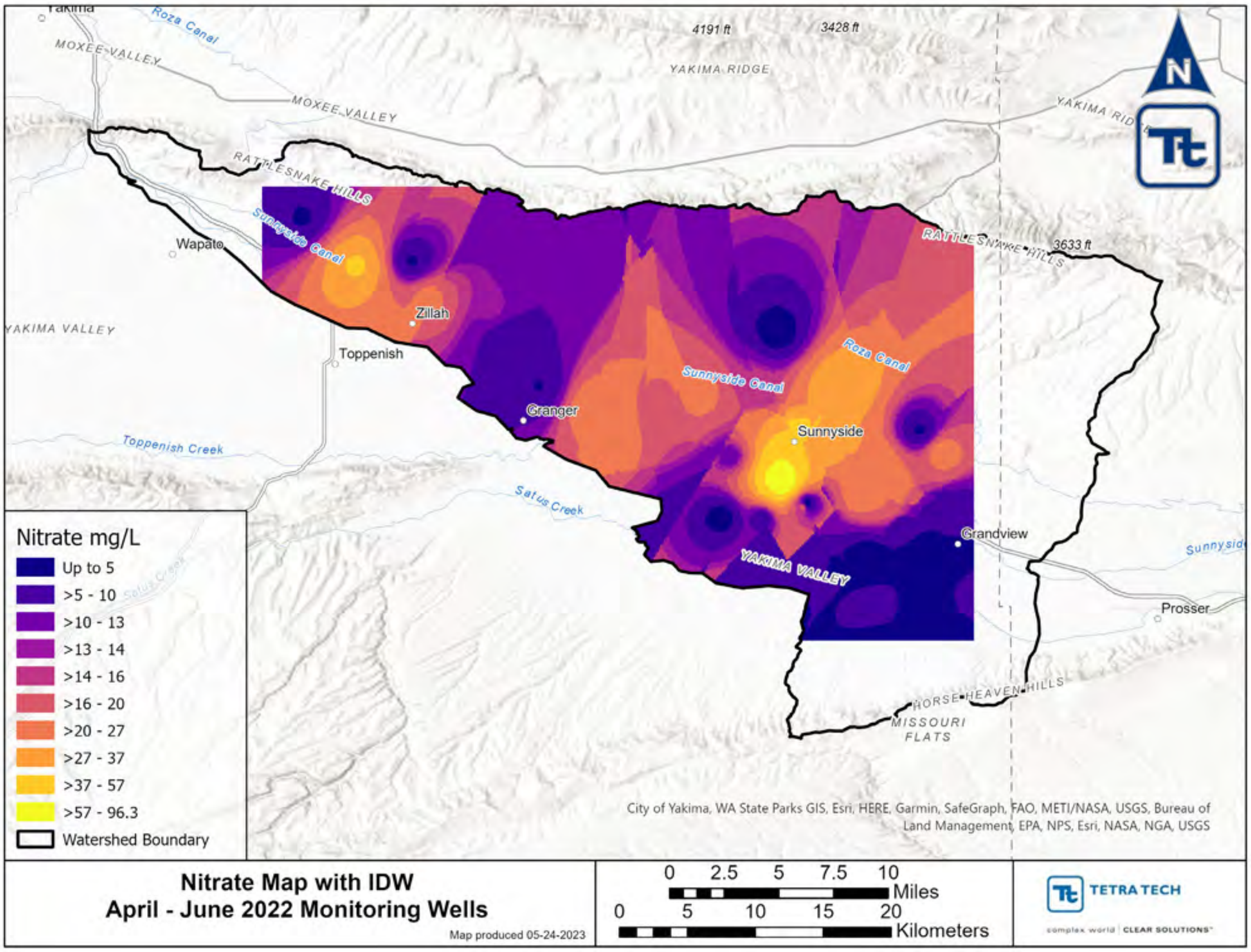

Figure 5-21. Nitrate Map with IDW for the April-June 2022 Dataset for Monitoring Wells

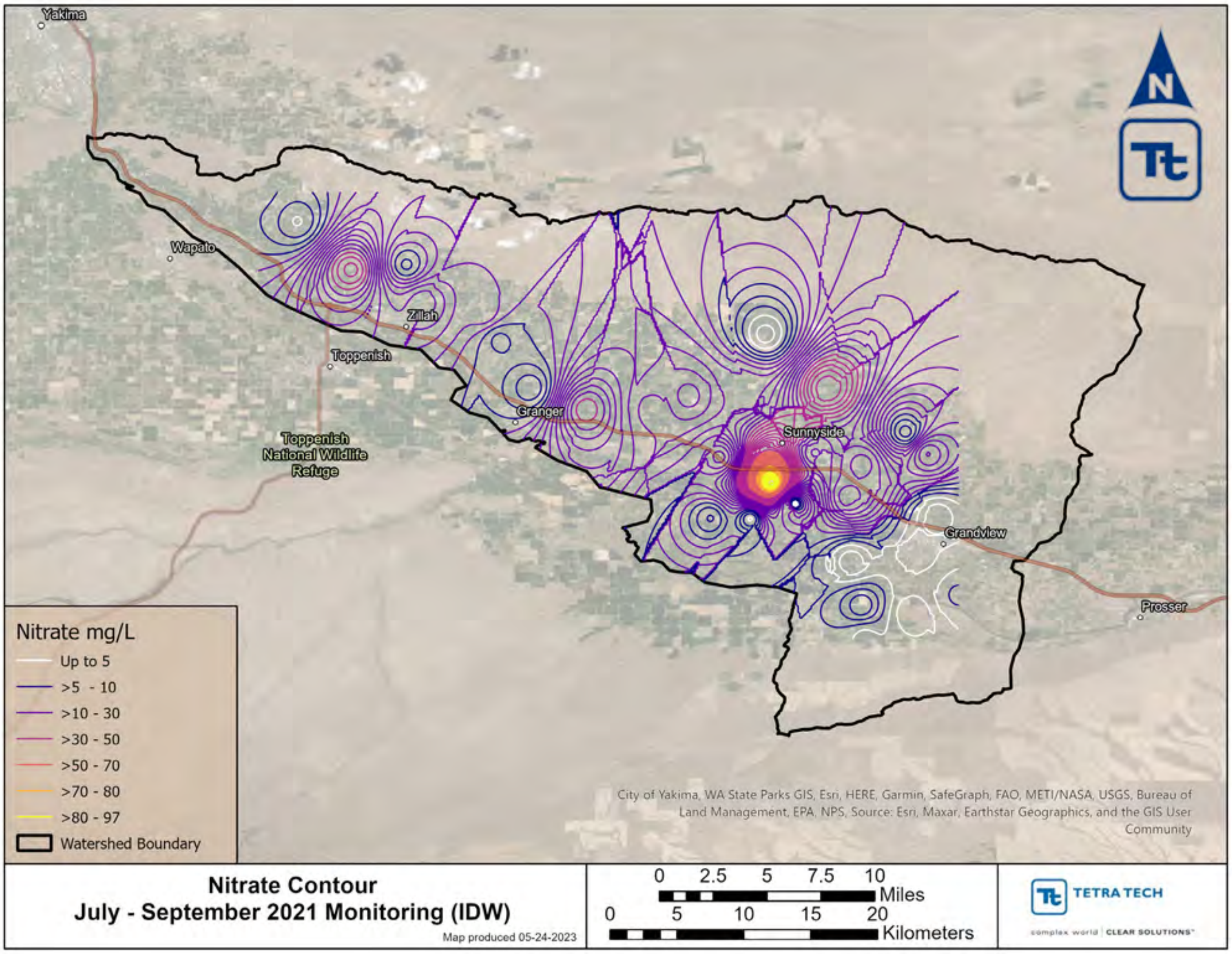

Figure 5-22. Nitrate Contour Map with IDW for the July-September 2021 Dataset for Monitoring Wells

Groundwater Level and Nitrate Map Generations

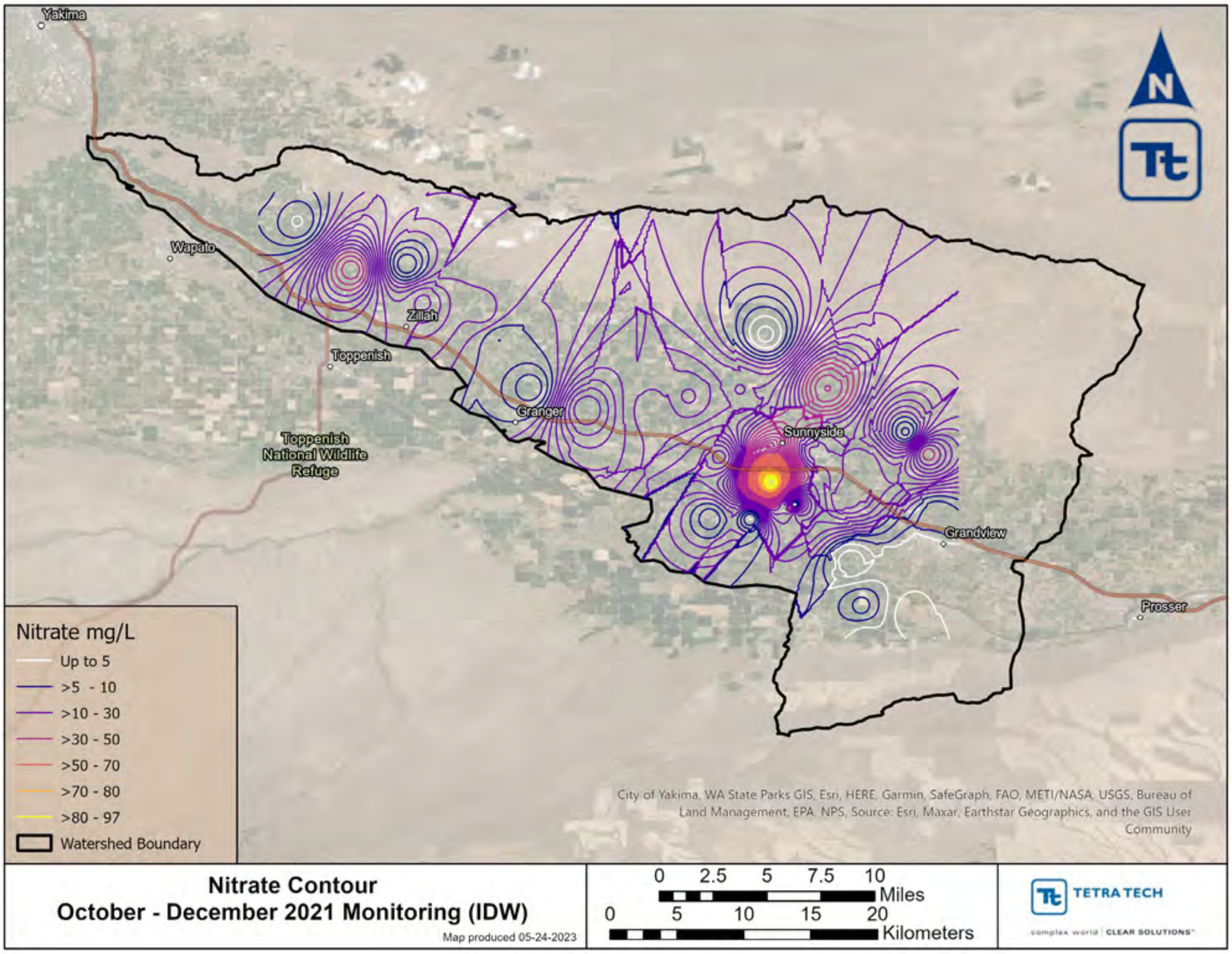

Figure 5-23. Nitrate Contour Map with IDW for the October-December 2021 Dataset for Monitoring Wells

Groundwater Level and Nitrate Map Generations

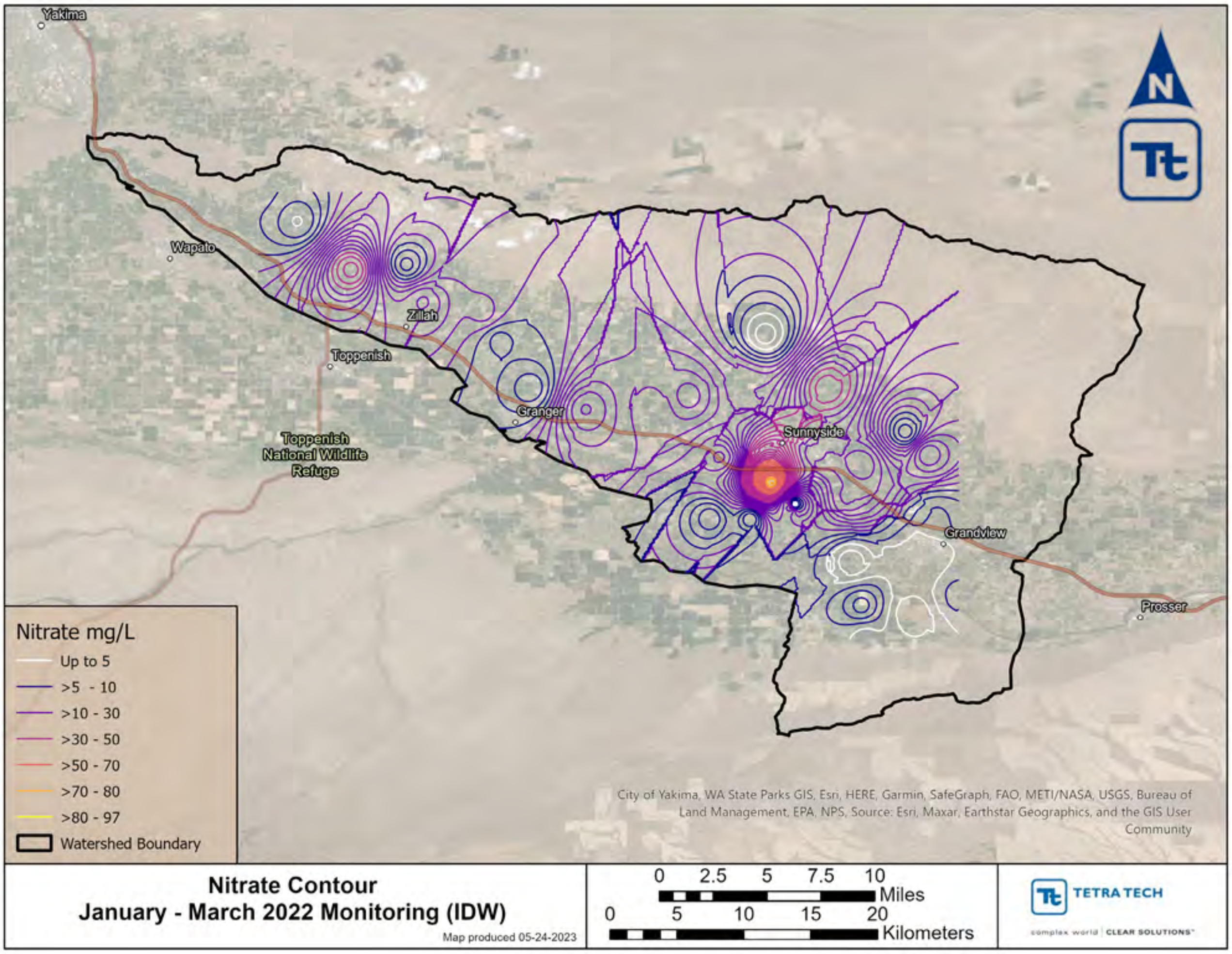

Figure 5-24. Nitrate Contour Map with IDW for the January-March 2022 Dataset for Monitoring Wells

Groundwater Level and Nitrate Map Generations

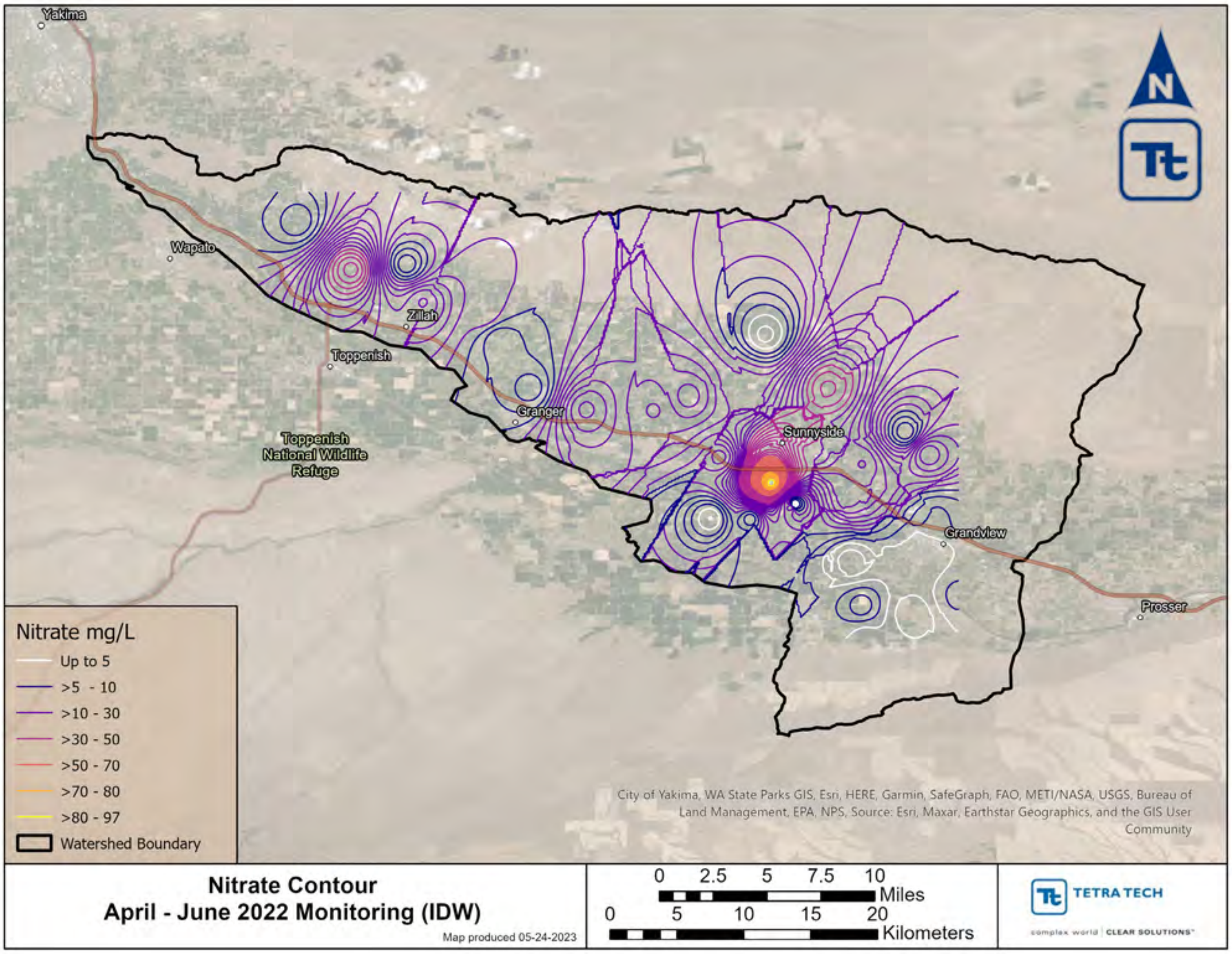

Figure 5-25. Nitrate Contour Map with IDW for the April-June 2022 Dataset for Monitoring Wells

Groundwater Level and Nitrate Map Generations

In addition to the raster maps and contour maps showing the full spectrum of nitrate concentrations with multiple concentration intervals, raster maps highlighting the areas with nitrate concentrations higher than 5 mg/L and higher than 10 mg/L were generated. For these maps, Kriging results are shown for all wells and supply wells only, while the IDW method for the monitoring wells is presented. These raster maps are shown from Figure 5-26 to Figure 5-37.

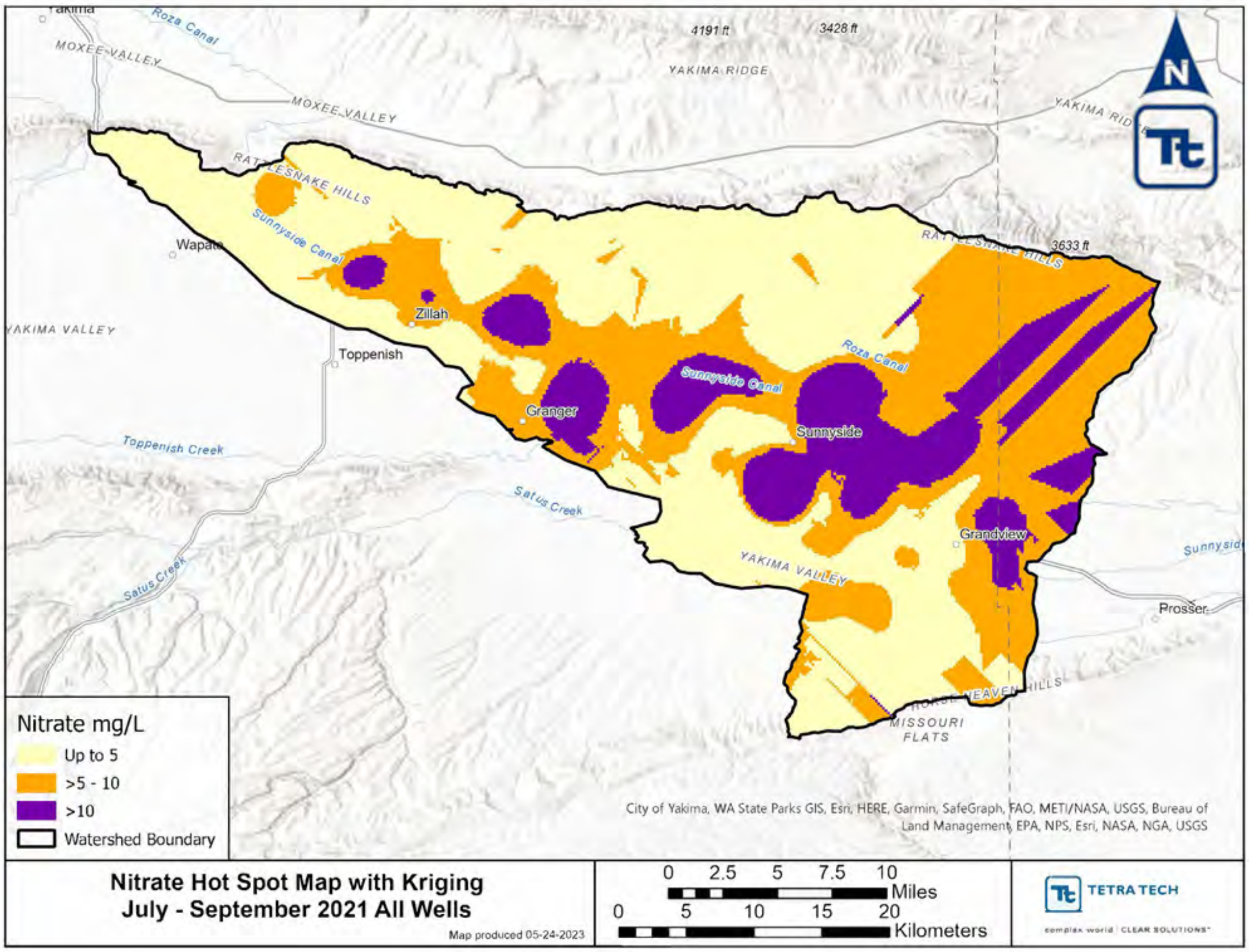

Figure 5-26. Nitrate Map of Highlighted Areas with Nitrate Concentrations Higher than 5mg/L and Higher than 10 mg/L for the July-September 2021 Dataset for All Wells

Groundwater Level and Nitrate Map Generations

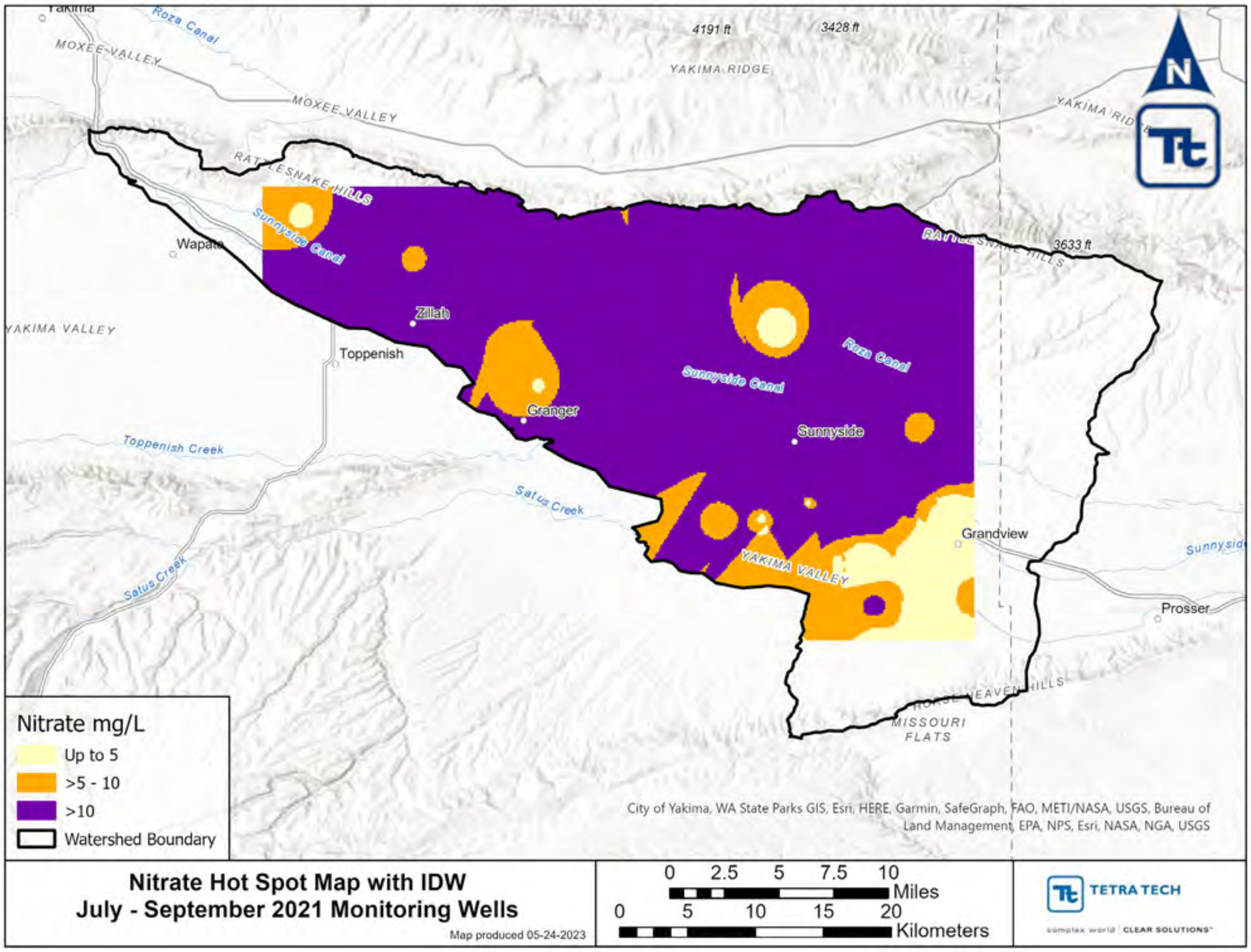

Figure 5-27. Nitrate Map of Highlighted Areas with Nitrate Concentrations Higher than 5mg/L and Higher than 10 mg/L for the July-September 2021 Dataset for Monitoring Wells

Groundwater Level and Nitrate Map Generations

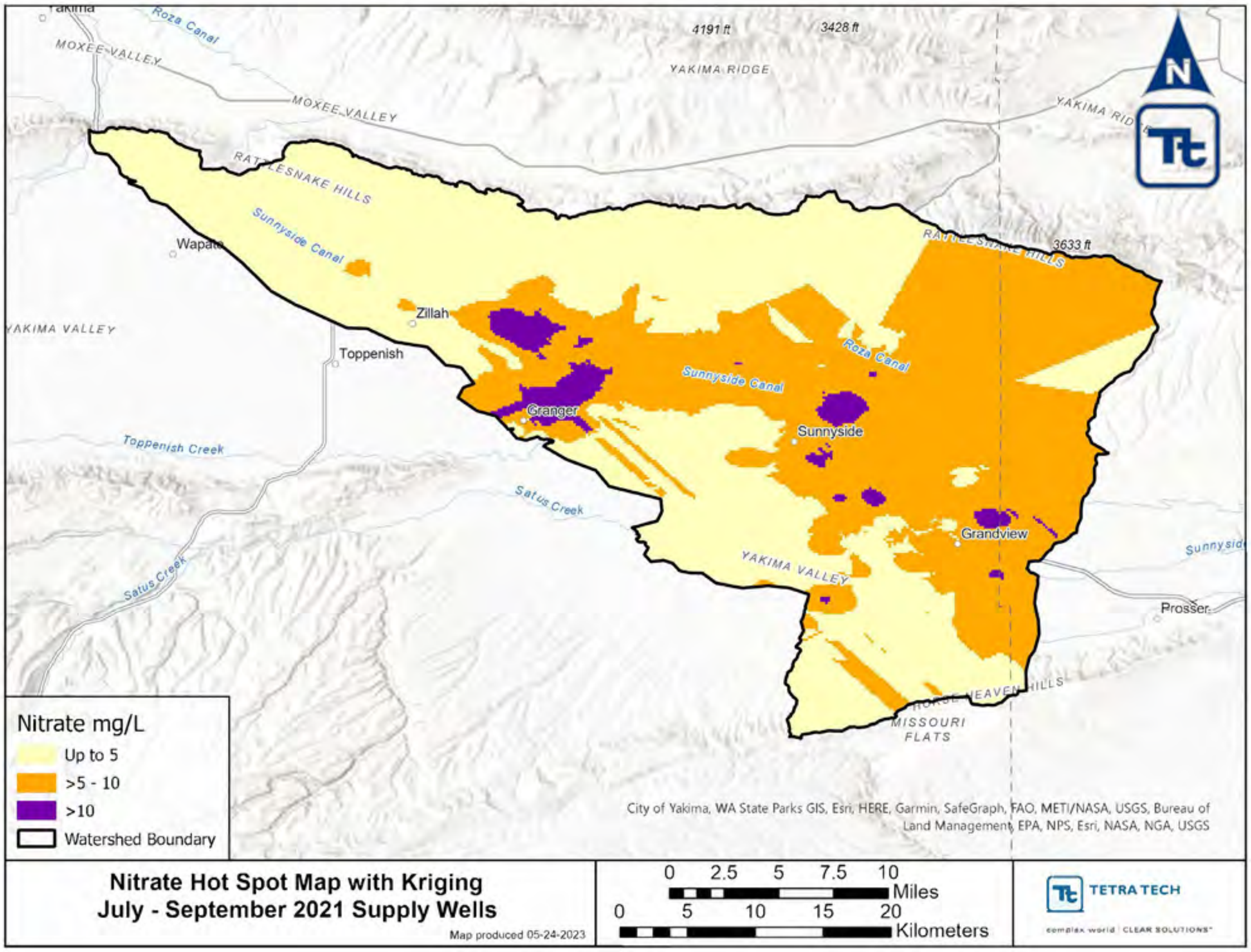

Figure 5-28. Nitrate Map of Highlighted Areas with Nitrate Concentrations Higher than 5mg/L and Higher than 10 mg/L for the July-September 2021 Dataset for Supply Wells

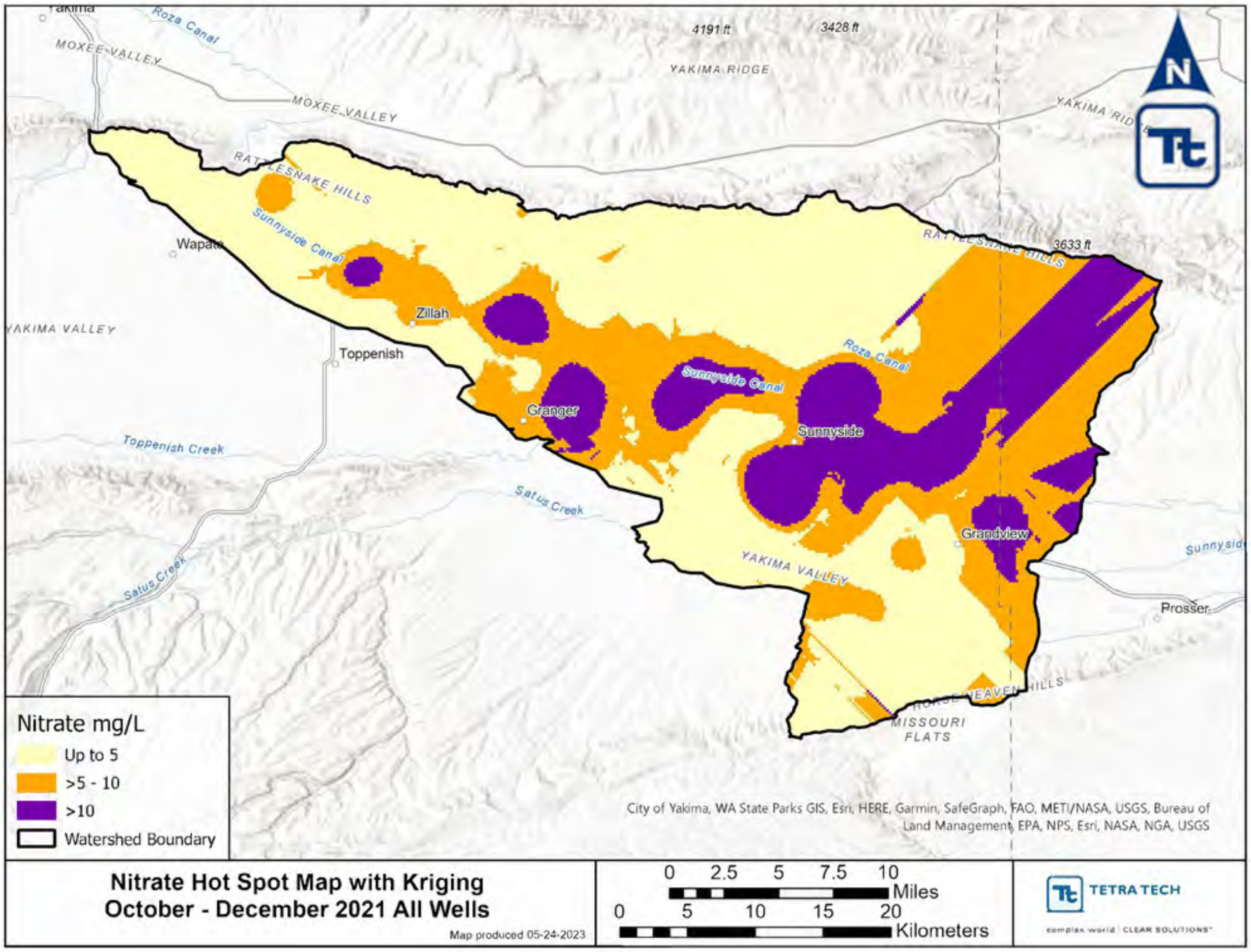

Figure 5-29. Nitrate Map of Highlighted Areas with Nitrate Concentrations Higher than 5mg/L and Higher than 10 mg/L for the October-December 2021 Dataset for All Wells

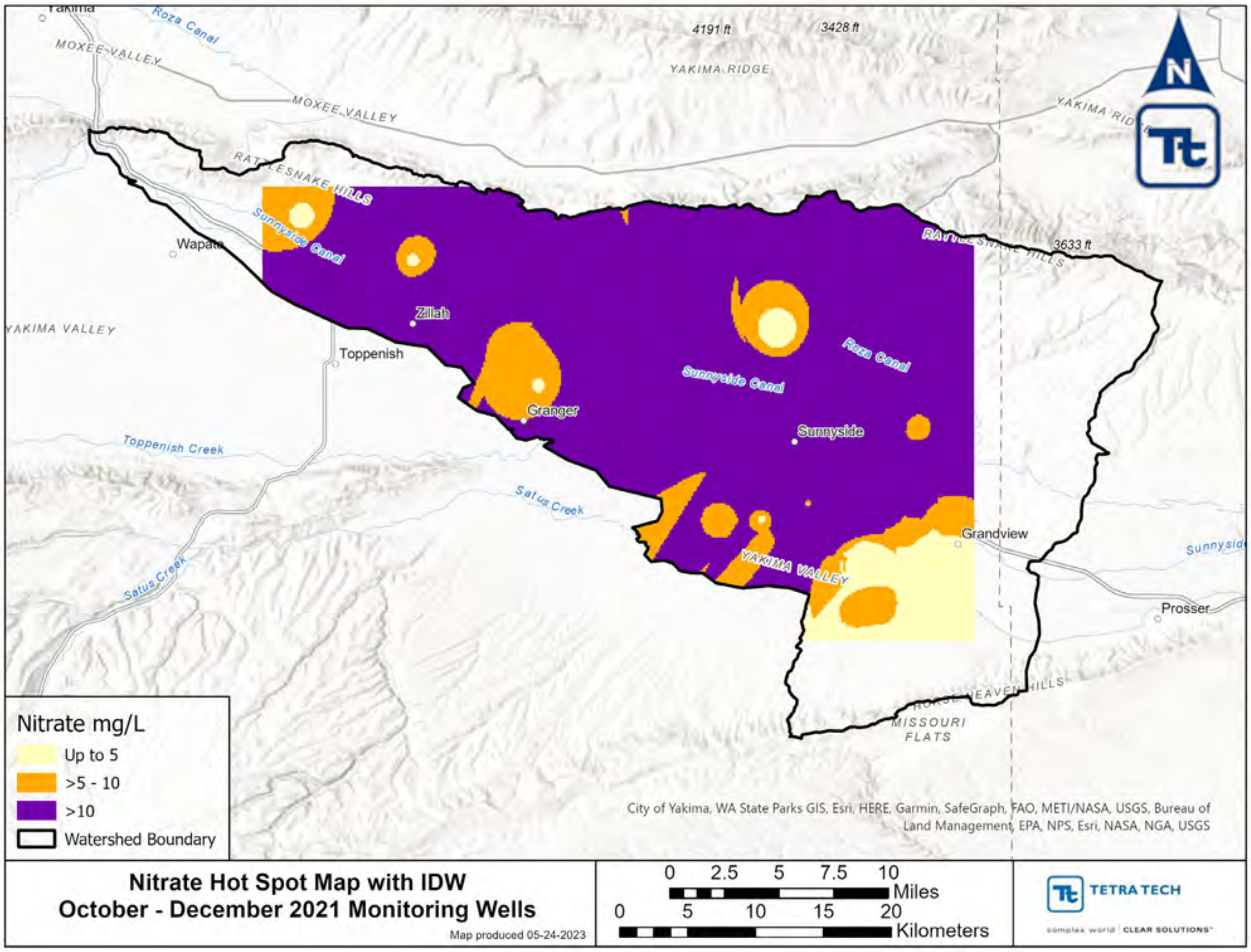

Figure 5-30. Nitrate Map of Highlighted Areas with Nitrate Concentrations Higher than 5mg/L and Higher than 10 mg/L for the October-December 2021 Dataset for Monitoring Wells

Groundwater Level and Nitrate Map Generations

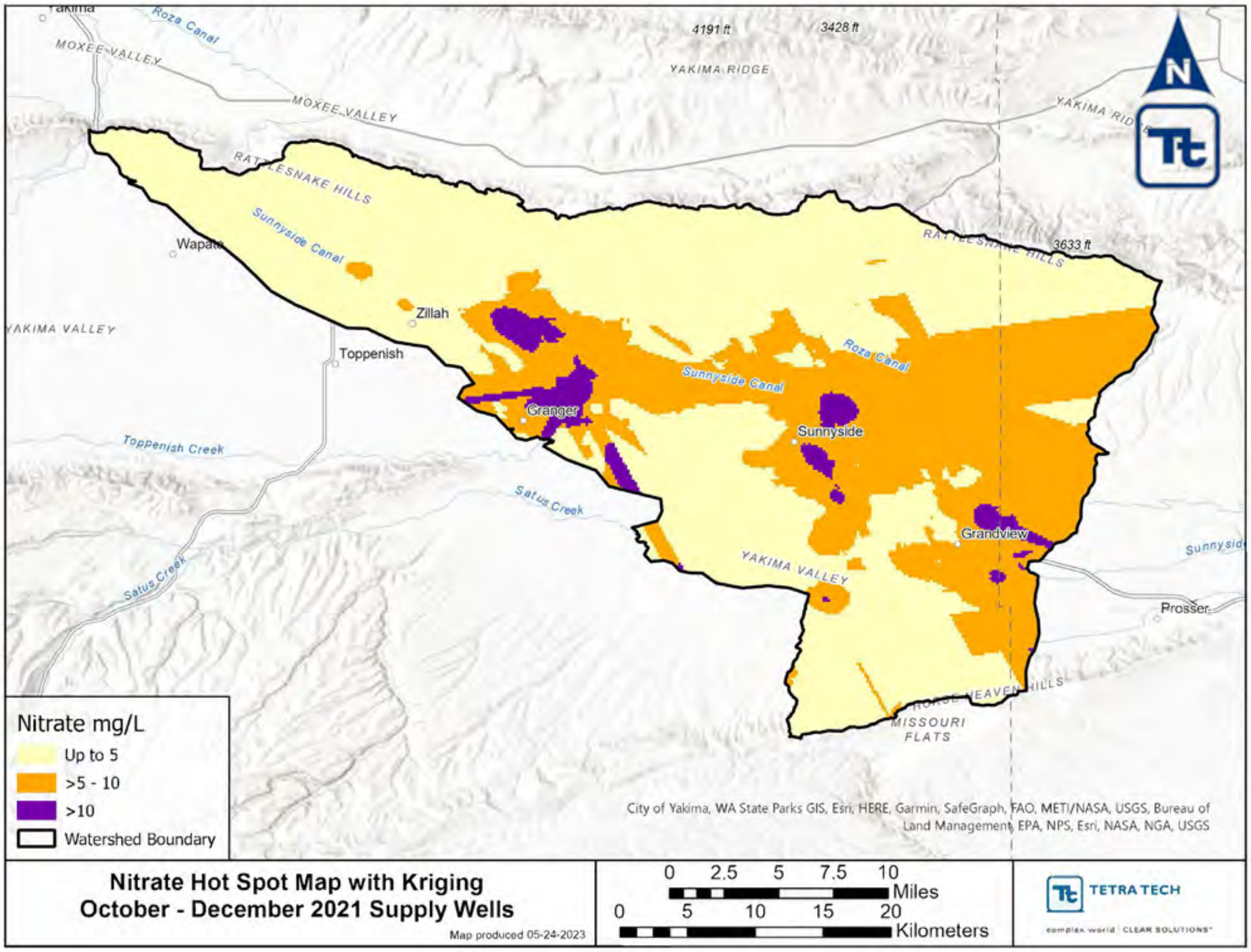

Figure 5-31. Nitrate Map of Highlighted Areas with Nitrate Concentrations Higher than 5mg/L and Higher than 10 mg/L for the October-December 2021 Dataset for Supply Wells

Groundwater Level and Nitrate Map Generations

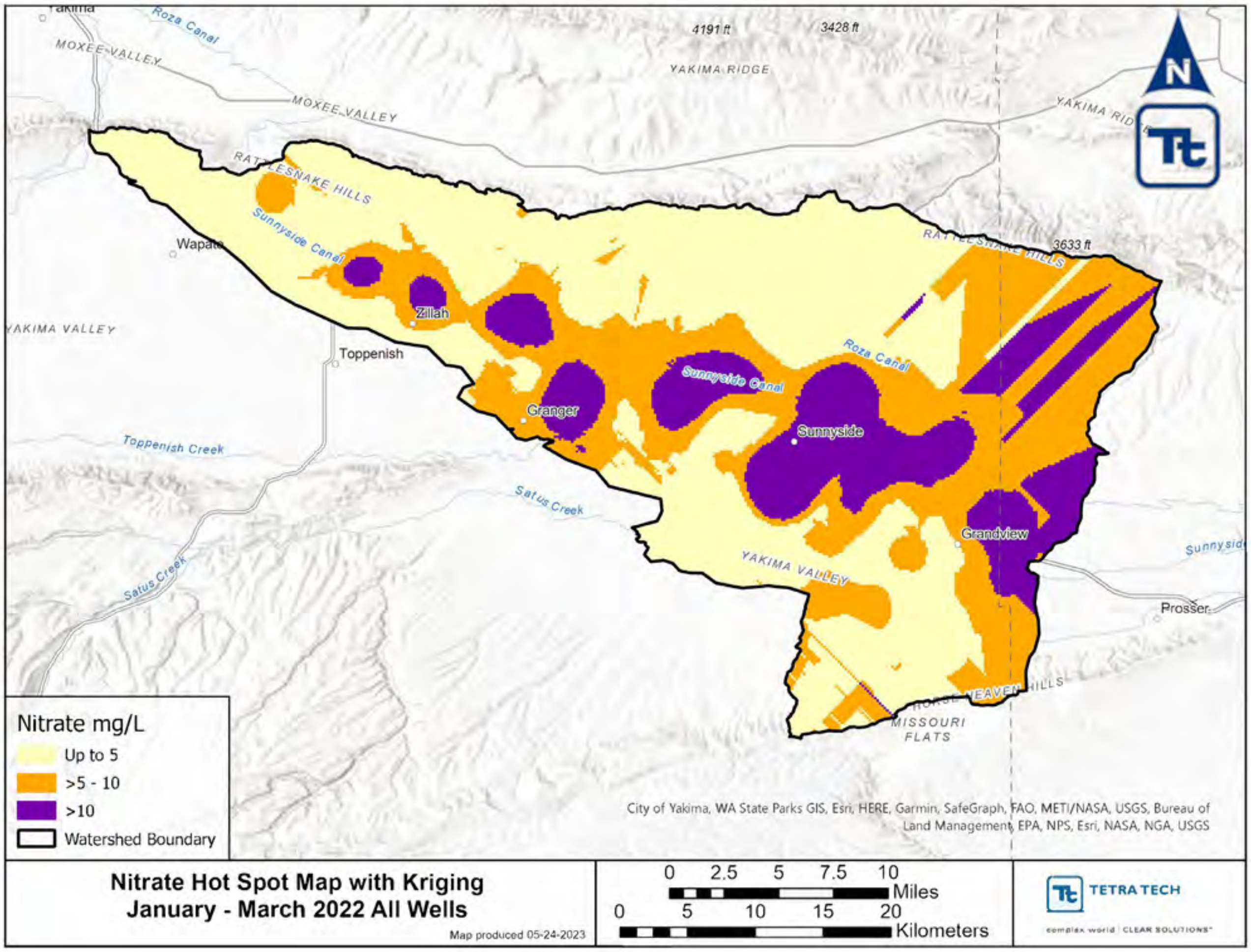

Figure 5-32. Nitrate Map of Highlighted Areas with Nitrate Concentrations Higher than 5mg/L and Higher than 10 mg/L for the January-March 2022 Dataset for All Wells

Groundwater Level and Nitrate Map Generations

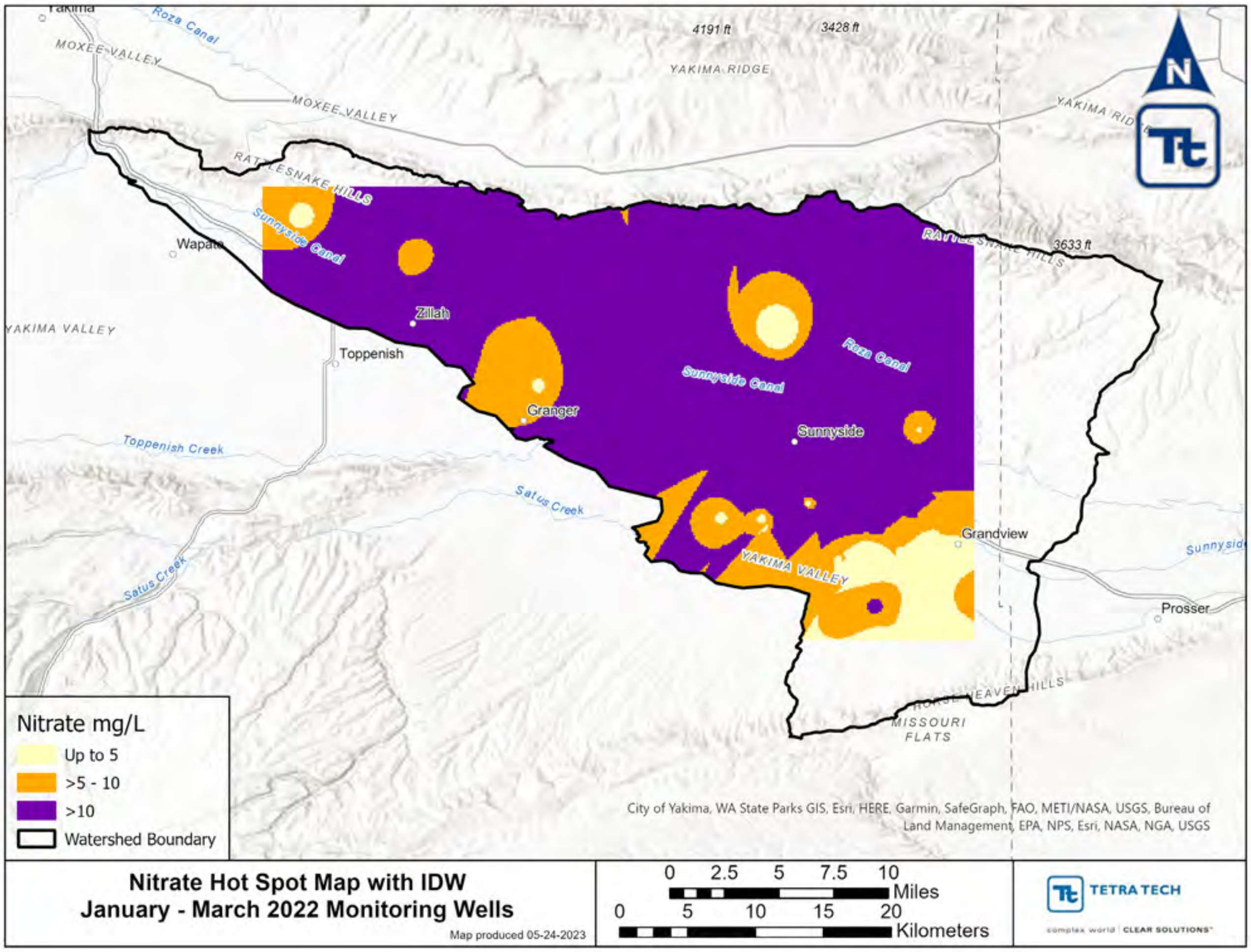

Figure 5-33. Nitrate Map of Highlighted Areas with Nitrate Concentrations Higher than 5mg/L and Higher than 10 mg/L for the January-March 2022 Dataset for Monitoring Wells

Groundwater Level and Nitrate Map Generations

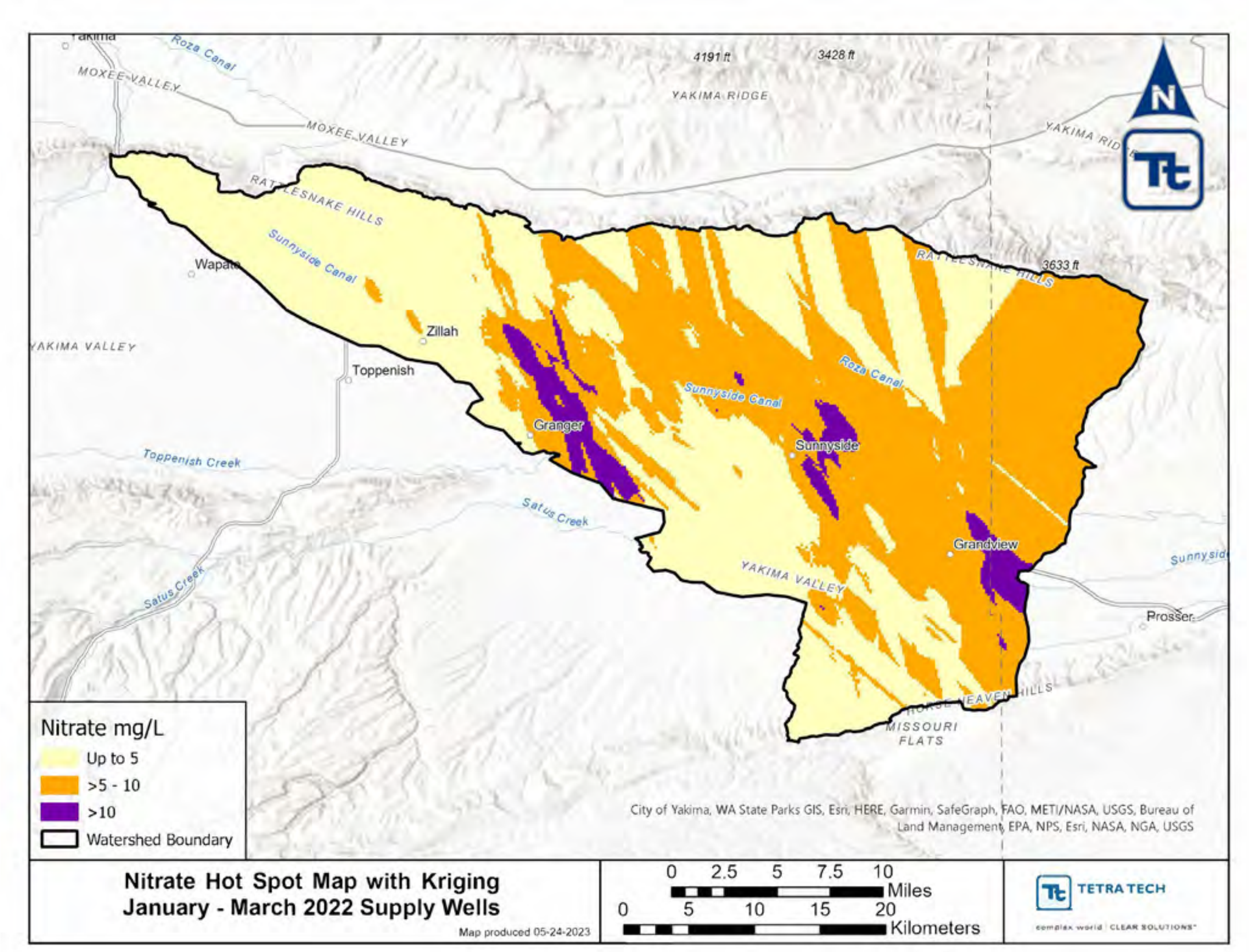

Figure 5-34. Nitrate Map of Highlighted Areas with Nitrate Concentrations Higher than 5mg/L and Higher than 10 mg/L for the January-March 2022 Dataset for Supply Wells

Groundwater Level and Nitrate Map Generations

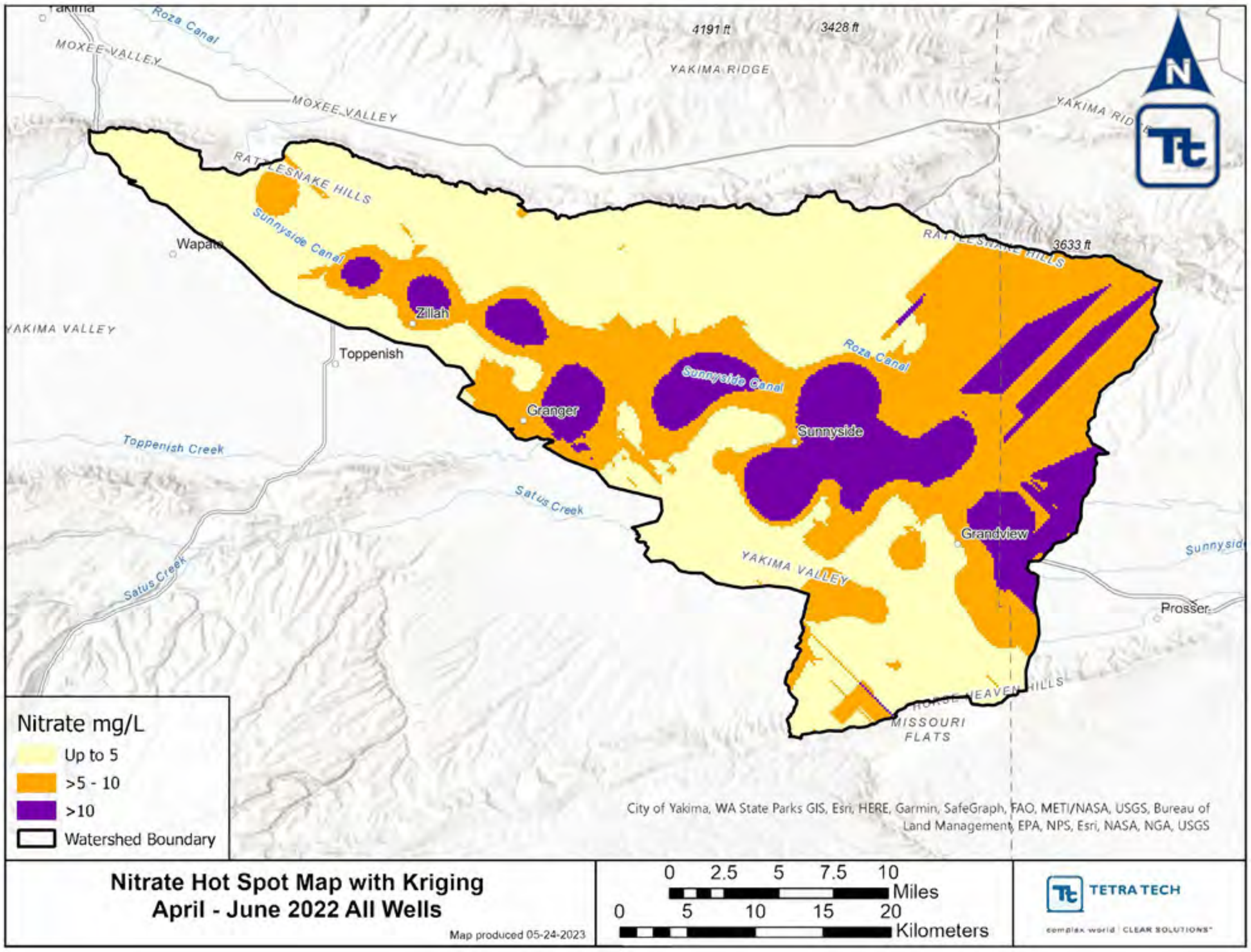

Figure 5-35. Nitrate Map of Highlighted Areas with Nitrate Concentrations Higher than 5mg/L and Higher than 10 mg/L for the April-June 2022 Dataset for All Wells

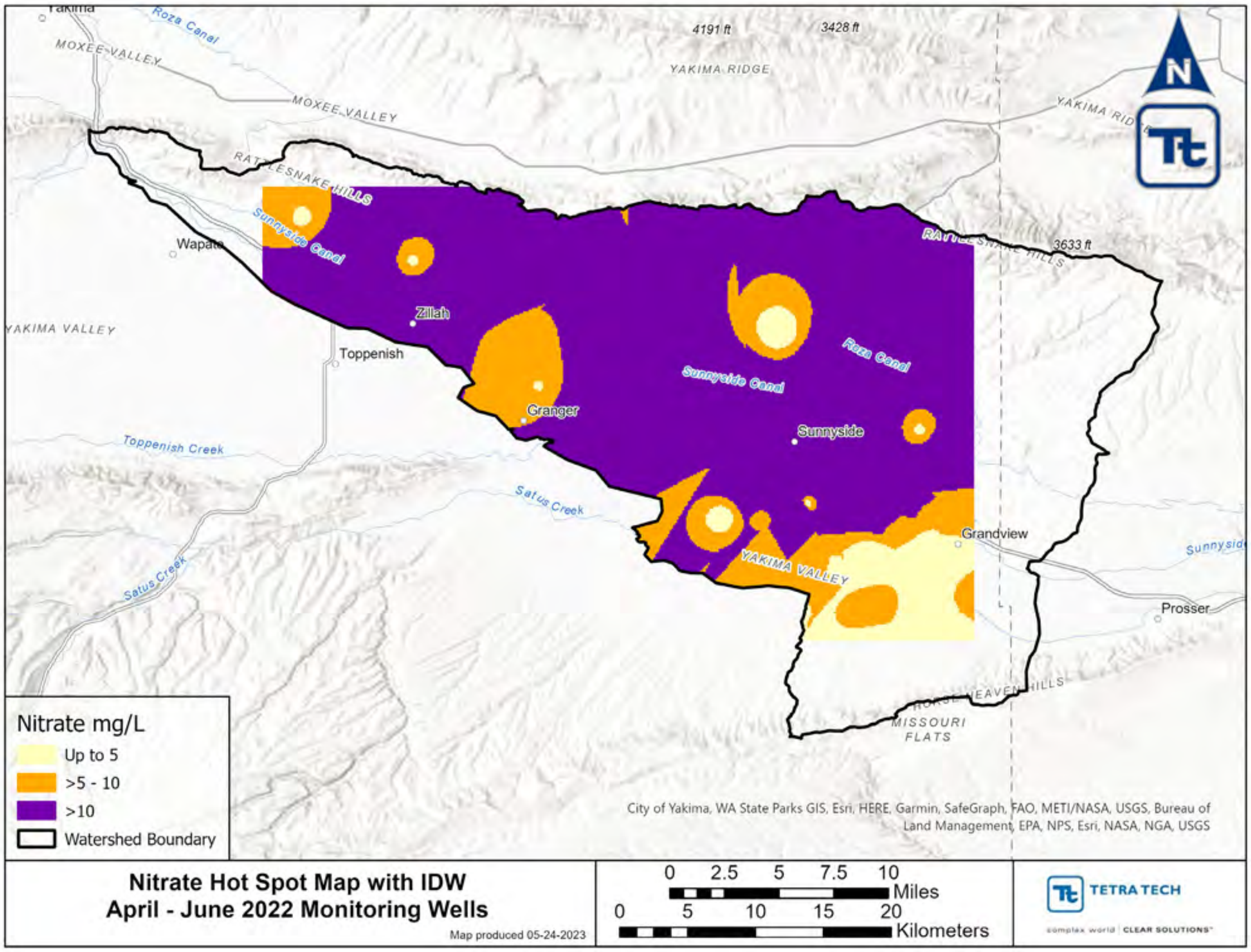

Figure 5-36. Nitrate Map of Highlighted Areas with Nitrate Concentrations Higher than 5mg/L and Higher than 10 mg/L for the April-June 2022 Dataset for Monitoring Wells

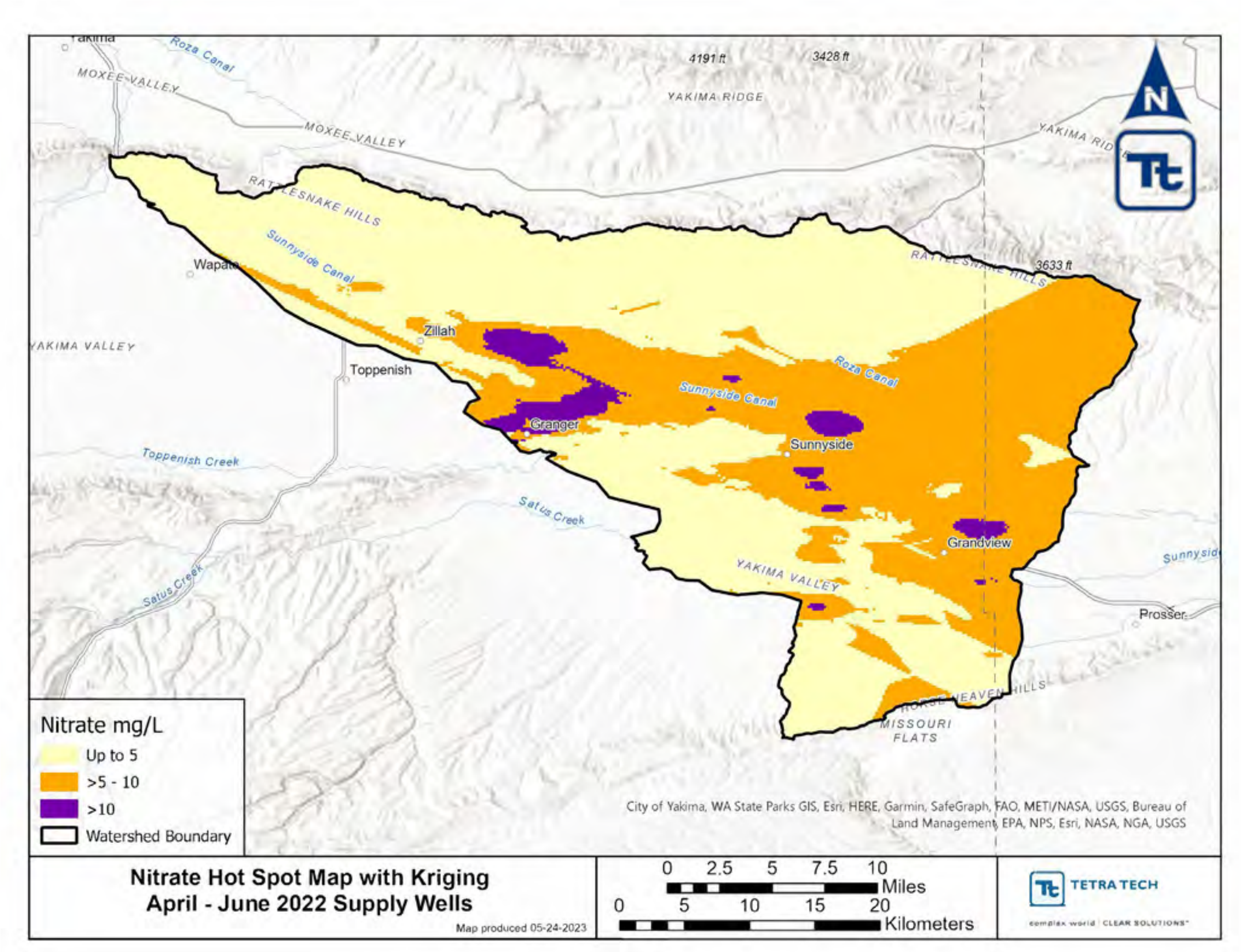

Figure 5-37. Nitrate Map of Highlighted Areas with Nitrate Concentrations Higher than 5mg/L and Higher than 10 mg/L for the April-June 2022 Dataset for Supply Wells

6.0 SUMMARY AND CONCLUSIONS

The Kriging method was used to support the generation of groundwater level and nitrate spatial distribution maps. Multiple combinations of the Kriging method with different semivariogram models and options for anisotropy, kernel functions were tested. The Ordinary Kriging method with the Gaussian semivariogram model was selected for both the water level and nitrate maps. The model errors with the no kernel option are the lowest for the water level dataset. For the nitrate data, different kernel function options achieved the lowest model errors for different datasets. However, the model errors associated with the no kernel option are still low. For the purposes of consistency and simplicity, the no kernel option is used for both the water level and nitrate map generation. The model errors with anisotropy for the water level data are lower than the model errors without anisotropy. Considering anisotropy does not improve the model errors much for the nitrate datasets, it is not used for the nitrate datasets. Water level maps were all generated using the Kriging method. For nitrate maps, the Kriging method does not work well when using the nitrate data from only the monitoring wells. In this case, the traditional IDW method was used. In addition to raster maps, contour maps were also generated for nitrate spatial distribution. When new water level data from the monitoring wells, and nitrate data from all wells are available, the selected Kriging method can be used the produce new raster and contour maps.

The nitrate maps clearly show the areas of high nitrate concentrations. These maps can also illustrate the seasonal changes in nitrate concentrations when the maps are compared with one another. Even though the maps do not directly answer questions on the causes of high nitrates, the maps can be layered with other information such as land uses, agricultural activities, and septic tank distributions to identify likely candidate sources of nitrate in the GWMA.

APPENDIX A – KRIGING RESULTS FOR MONITORING WELLS

Groundwater Level and Nitrate Map Generations

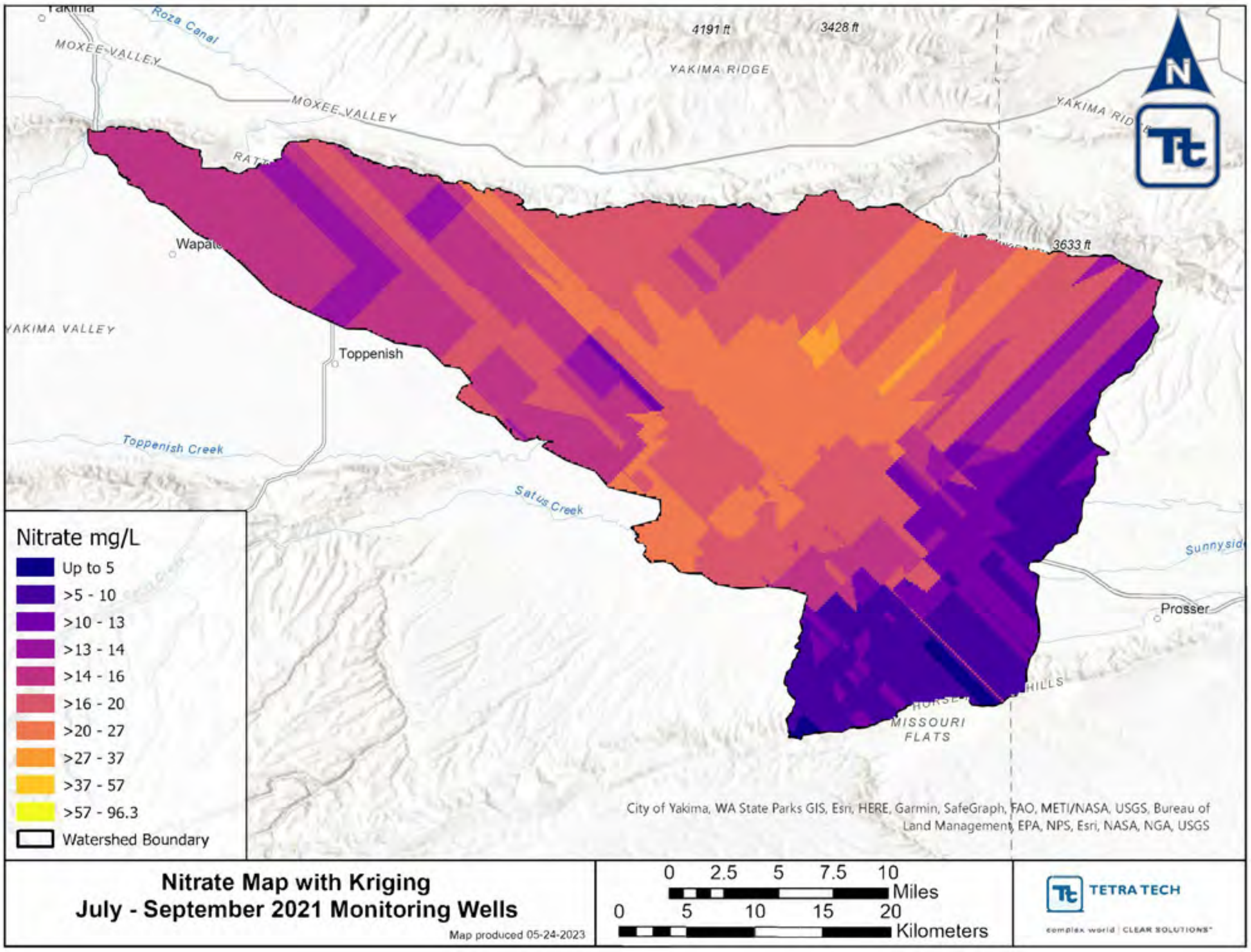

Figure 1. Nitrate Map with Kriging for the July-September 2021 Dataset for Monitoring Wells

Groundwater Level and Nitrate Map Generations

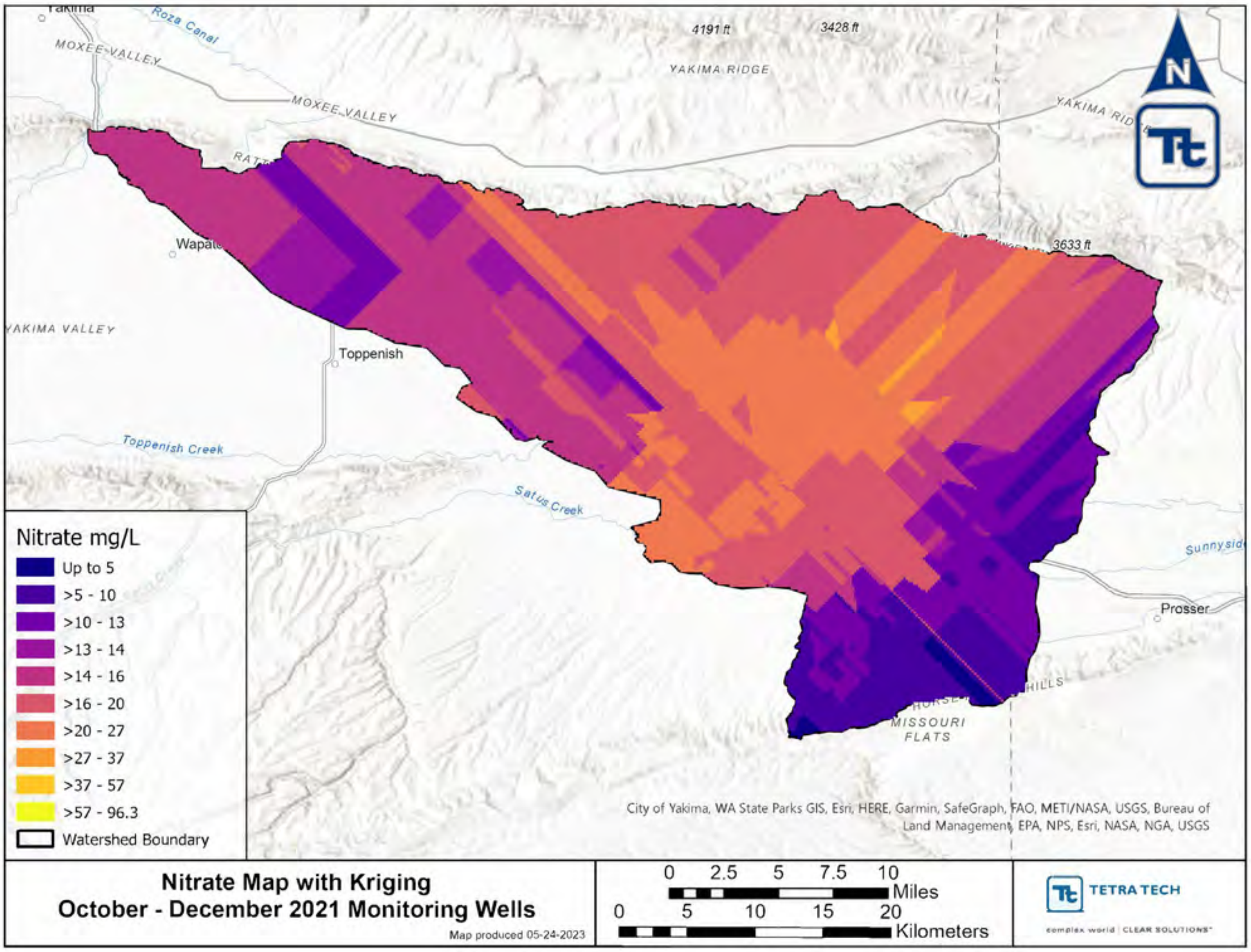

Figure 2. Nitrate Map with Kriging for the October-December 2021 Dataset for Monitoring Wells

Groundwater Level and Nitrate Map Generations

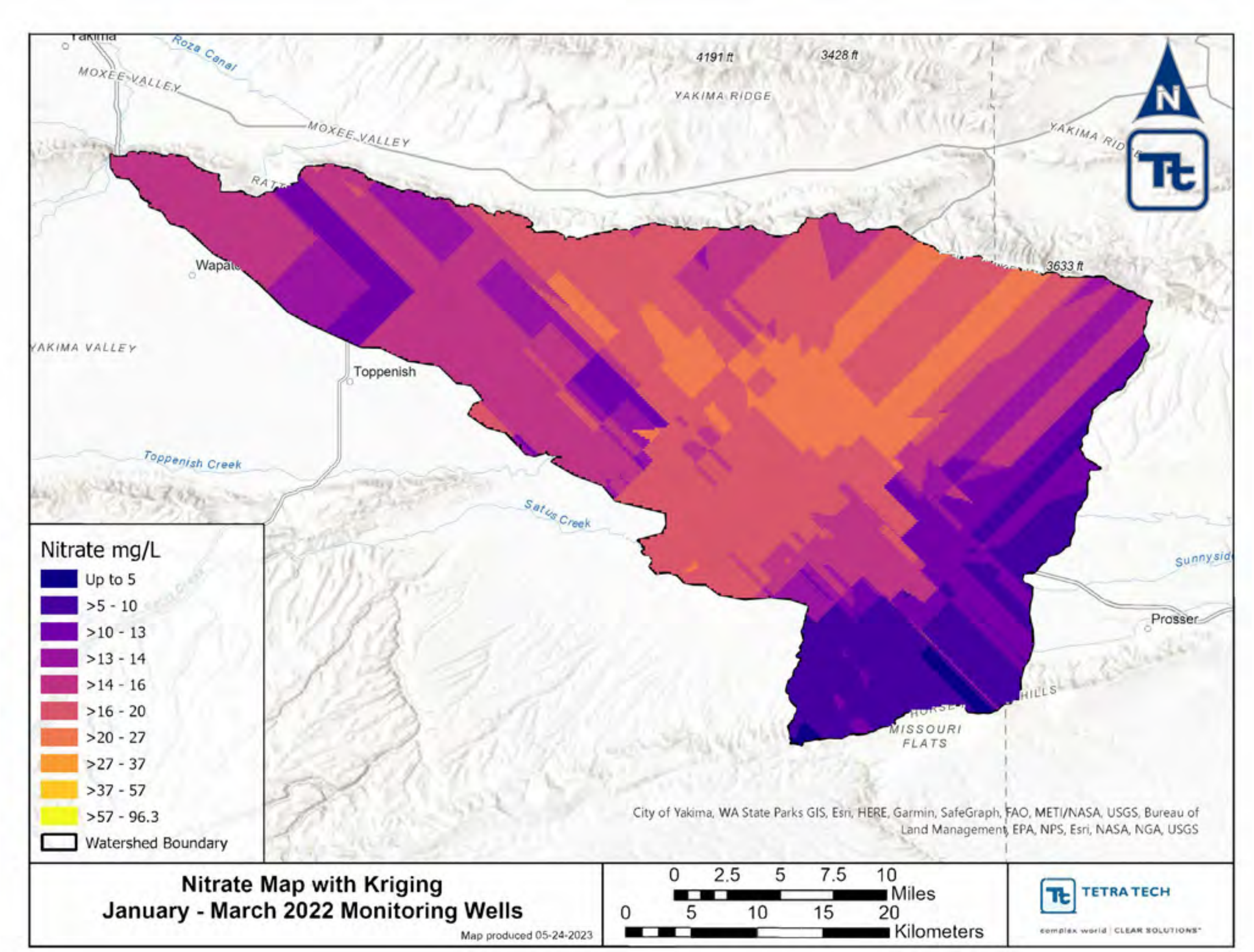

Figure 3. Nitrate Map with Kriging for the January-March 2022 Dataset for Monitoring Wells

Groundwater Level and Nitrate Map Generations

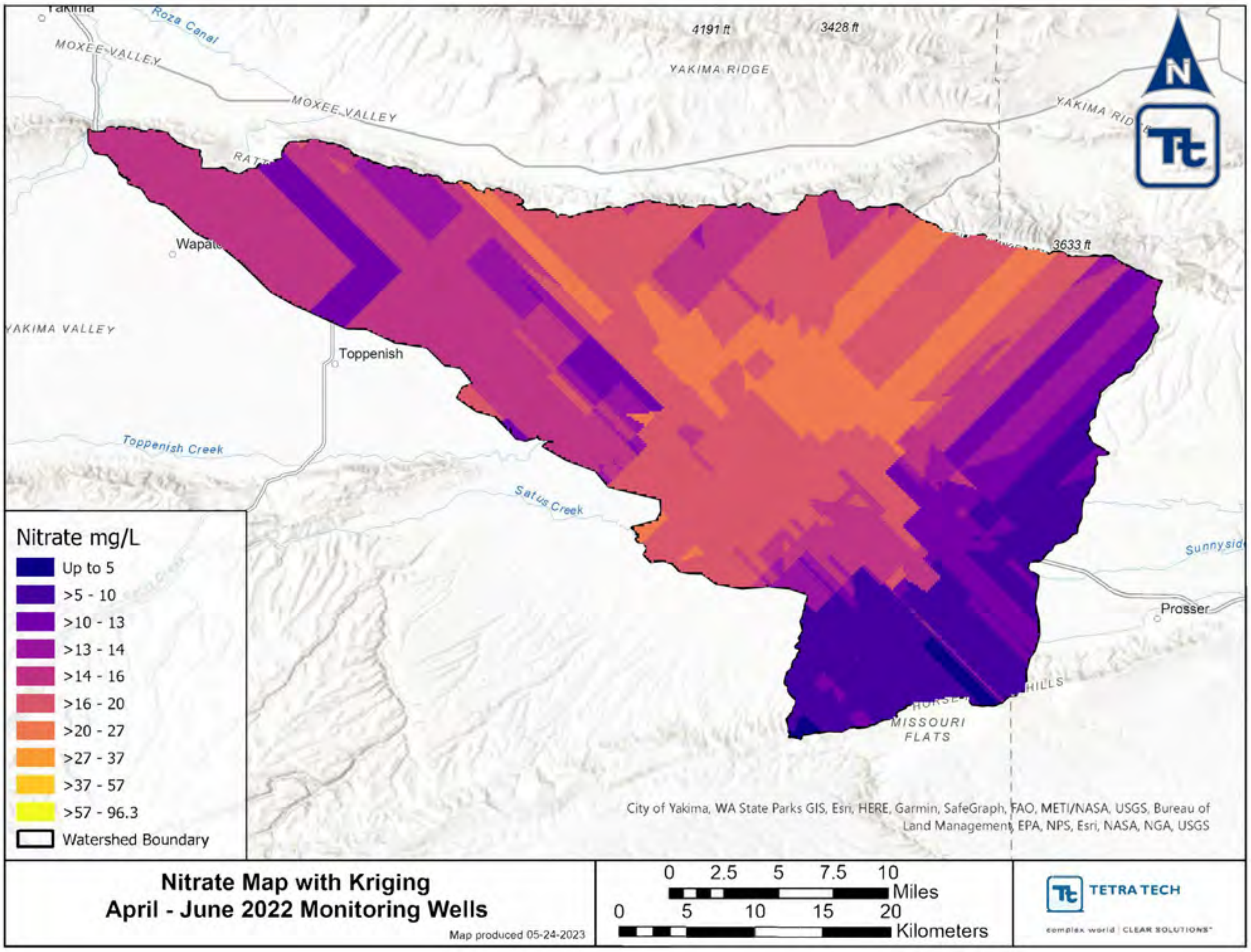

Figure 4. Nitrate Map with Kriging for the April-June 2022 Dataset for Monitoring Wells

Groundwater Level and Nitrate Map Generations

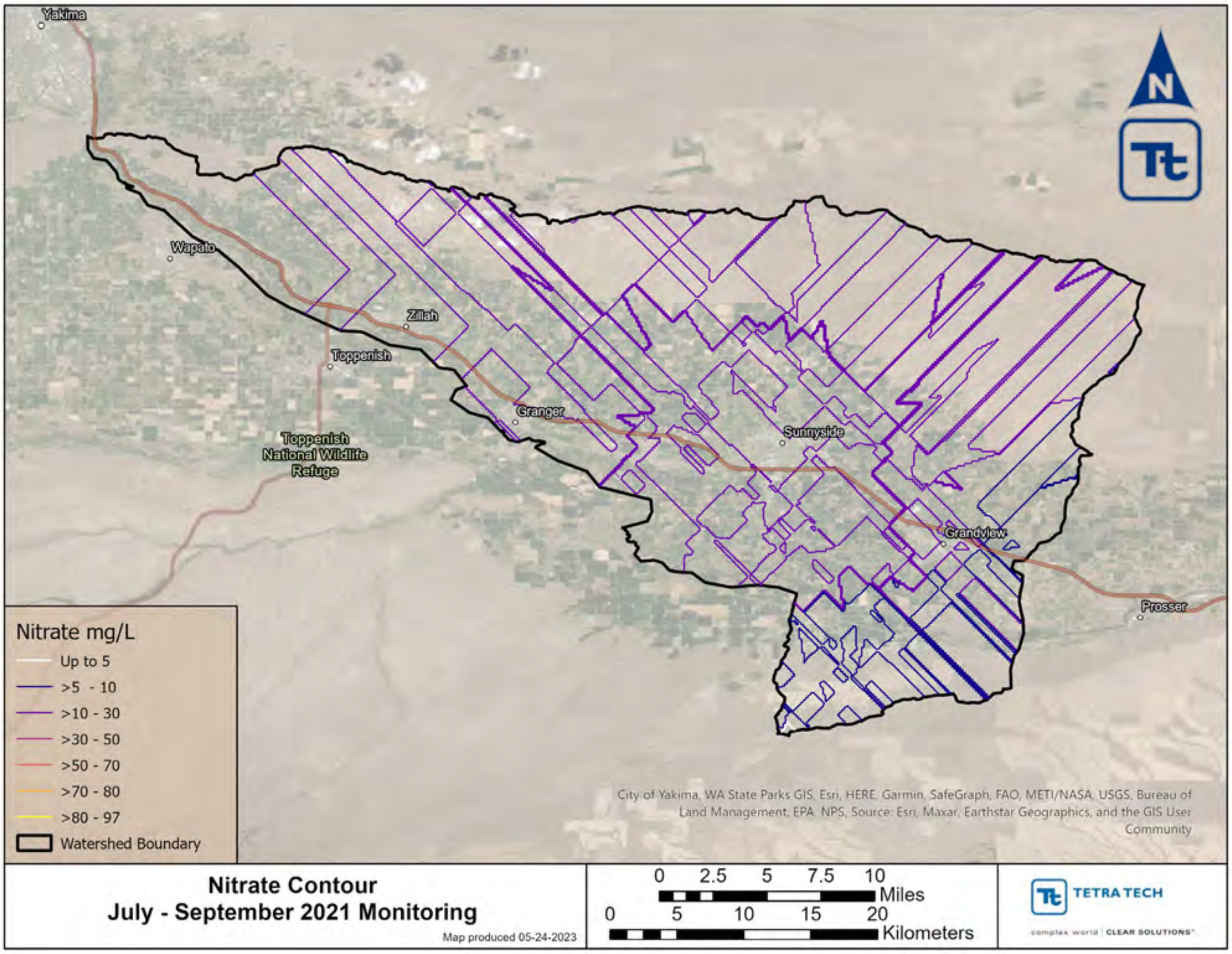

Figure 5. Nitrate Contour Map with Kriging for the July-September 2021 Dataset for Monitoring Wells

Groundwater Level and Nitrate Map Generations

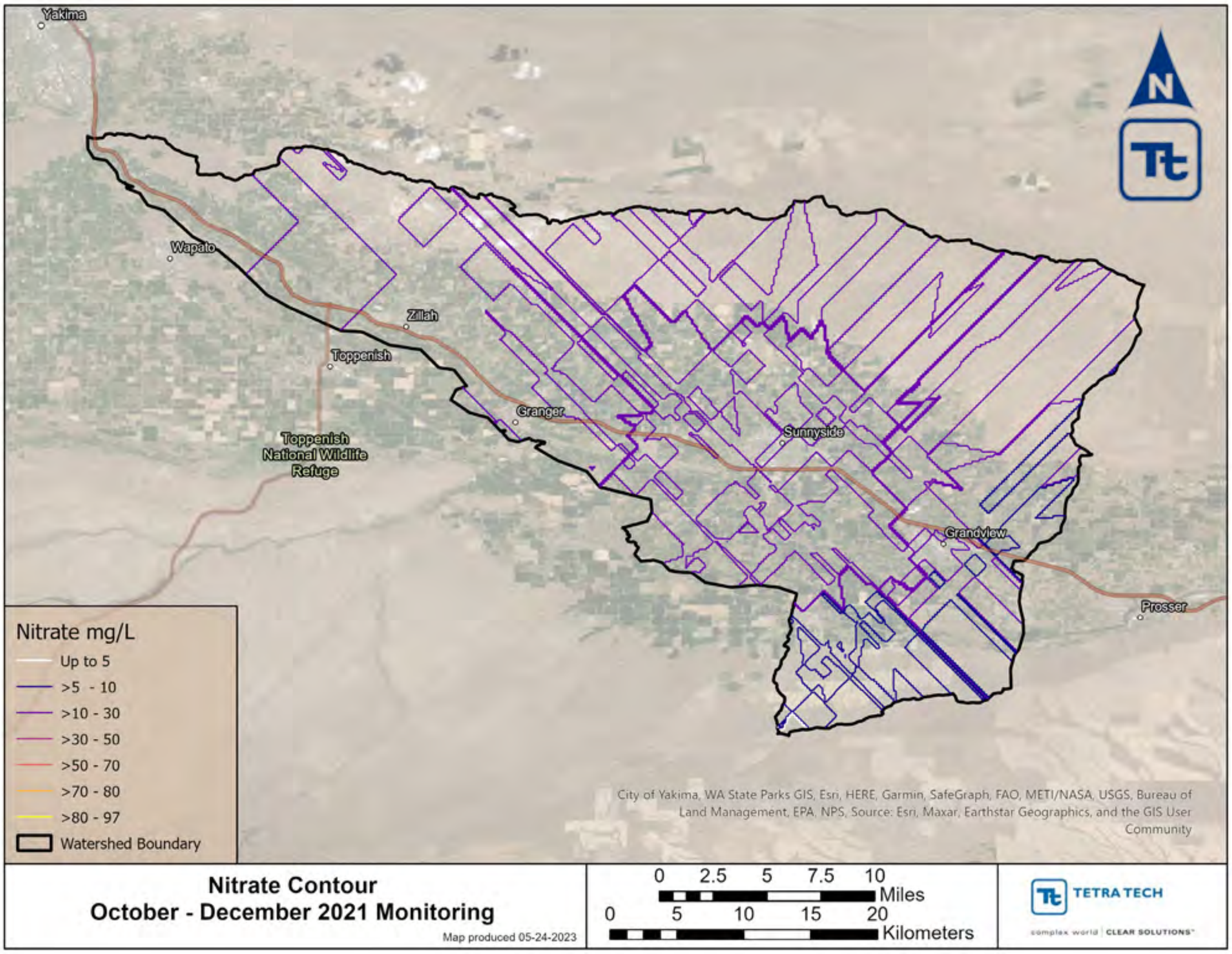

Figure 6. Nitrate Contour Map with Kriging for the October-December 2021 Dataset for Monitoring Wells

Groundwater Level and Nitrate Map Generations

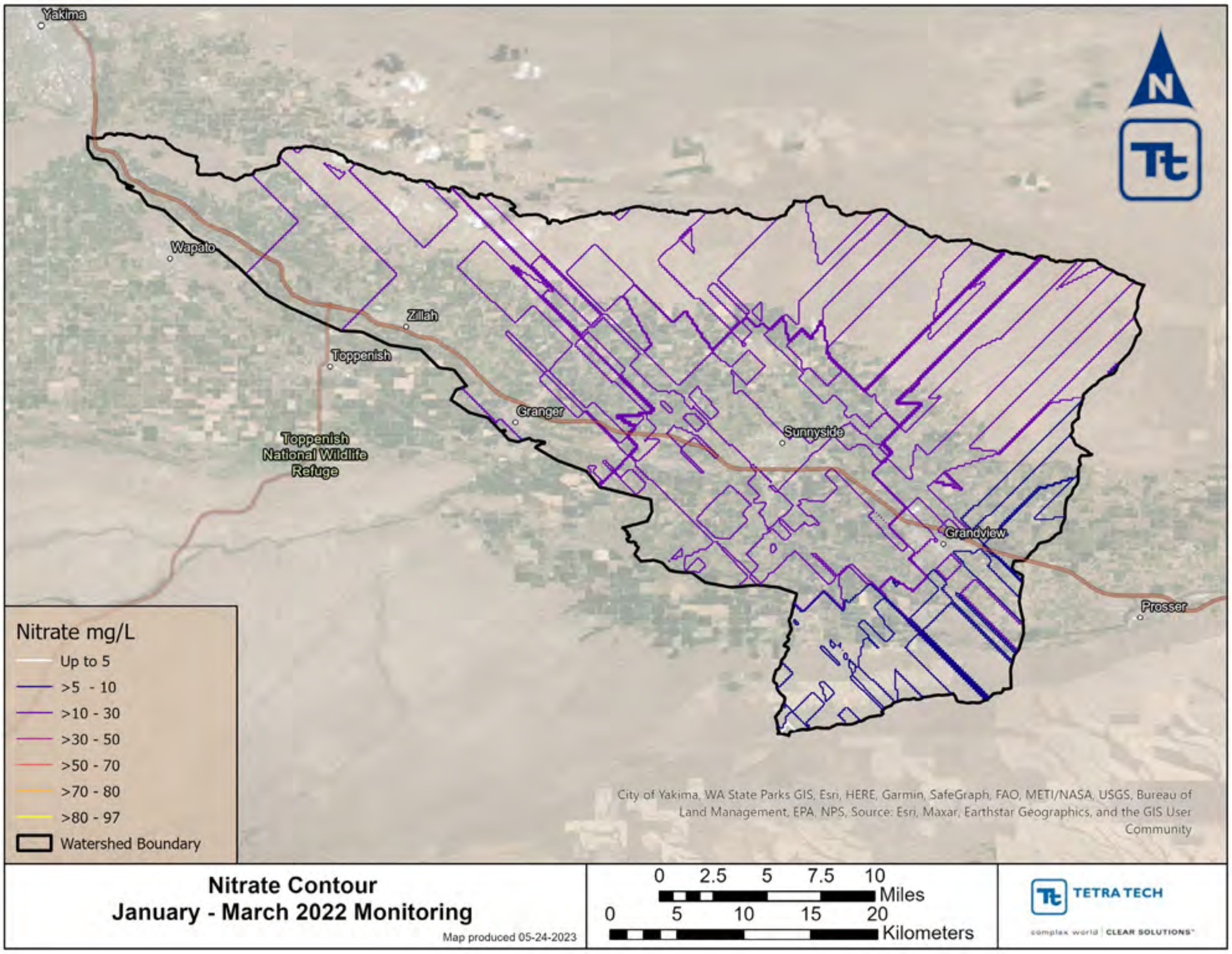

Figure 7. Nitrate Contour Map with Kriging for the January-March 2022 Dataset for Monitoring Wells

Groundwater Level and Nitrate Map Generations

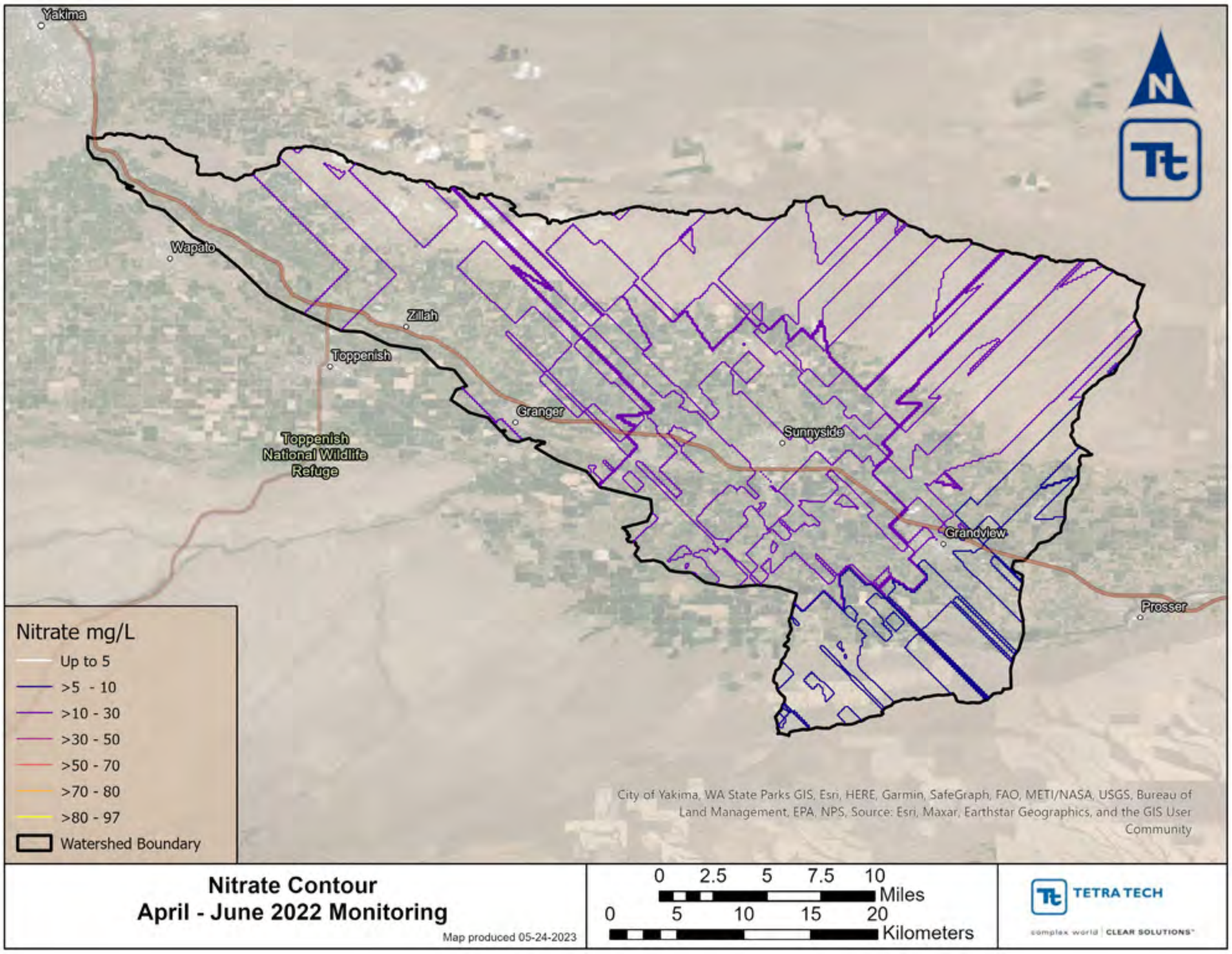

Figure 8. Nitrate Contour Map with Kriging for the April-June 2022 Dataset for Monitoring Wells